DOCTOR OF PHILOSOPHY

Impact of Electrocoagulation Parameters on Flocculation

Jones, John David

Award date:
2015

Awarding institution:
Bangor University

Impact of Electrocoagulation Parameters on Flocculation

Thesis Presented in Partial Fulfilment

for

Doctor of Philosophy

by

John David Jones

PRIFYSGOL
BANGOR
UNIVERSITY

Prifysgol Bangor • Bangor University

Abstract

Chemical coagulation and flocculation are conventional methods for the treatment of pollutant wastewater. Electrocoagulation (EC) is an experiential water treatment technology that presents an innovative and novel alternative in which sacrificial metal anodes dissolve controllably to dose wastewater electrochemically. Its principle advantage is its ability to provide active cations necessary for coagulation without chemical addition.

The technology however suffers from sporadic pollutant-centred studies scattered throughout the literature that focus only on optimising EC for the removal of a particular contaminant. The purpose of the work presented here is to provide a holistic study of EC for the benefit of understanding the effect of various parameters on the fate of floc particles and coagulation. It is hoped that this will aid in advancing the technology beyond the current pollutant-centred studies and allow future researchers to base operational parameters on the trends and patterns presented in this work.

In order to understand the impact of EC parameters on flocculation two wastewater sources were used. Trickling filter bed effluent from a sewage treatment plant containing 0.2 mmol/L phosphate pollution and a synthetic turbid system containing 1 g/L suspended colloids were used. This was due to their difference in pollutant nature, commonality in wastewater treatment applications, and their availability at the time of study.

The parameters investigated were; pollutant loading, inter-electrode distance, coagulant concentration, current density, agitation, electrolysis time, coagulant retention time, pH, and conductivity. Studies were also undertaken to compare EC to conventional chemical coagulation. Phosphate concentration, total suspended solids and turbidity pollutant removal efficiencies were used to infer the impact of the various chemical and process parameters on flocculation.

It was found that initial EC experiments could not compete similarly to chemical coagulation due to iron speciation differences between the two separate coagulant methods. It was found that non-EC parameters such as dissolved oxygen content and floc seeding played an important part in affecting flocculation along with coagulant concentration and

influent pH. Characterisation of floc aggregates formed revealed differences in floc sizes related to the various pollutant removal mechanisms of charge neutralisation and sweep-flocculation. Zeta potential measurements carried out delineated pH conditions in which either removal mechanism would prevail, whilst floc retention time studies provided information on the mechanisms involved in converting active iron hydroxide floc particles to deactivated magnetite particles. Ultimately, trends were delineated for all parameters studied revealing how changes to operational conditions affected; (i) coagulant removal mechanism, (ii) efficacy of produced flocculant, and (iii) size of floc particles.

Acknowledgements

This project was supported financially by Modern Water plc. Academic support is gratefully acknowledged from Dr Chris Gwenin at Bangor University and supervisory support is greatly appreciated from Dr Duarte Tito. An extended thank you also to the School of Chemistry for allowing this project to take place.

Thanks also to Miss Nicola Randles of Modern Water plc who enabled this project to come about, Dr Yanhua Hong of the School of Electronic Engineering for her assistance with the SEM work, and the Electrochemistry and Biosensors Research Group at Bangor University for their camaraderie. A final thank you to my family who have supported me throughout.

Table of Contents

Declaration and Consent ..... *i*
Abstract ..... *iv*
Acknowledgements ..... *vi*

1 Introduction **2**
1.1 Global Water Perspective 2
1.2 Water Legislation 2
1.2.1 Water Quality Guidelines 3
1.2.2 Drinking Water Standards 6
1.3 Water Management 8
1.4 Water Treatment 10
1.4.1 Coagulation 11
1.5 Electrocoagulation 13
1.5.1 Historical Background 13
1.5.2 Benefits and Drawbacks 14
1.5.3 Applications 16
1.5.4 Other Electrochemical Treatment Techniques 17
1.6 Other Wastewater Treatment Methods 18
1.6.1 Chemical and Physical Means of Water Recovery 19
1.7 Recent Improvements in Electrocoagulation 22
1.7.1 Improvement in EC Reactor Design 22
1.7.2 Improvement in Current Efficiency 22
1.8 Aim of Study 23
1.9 References 24

2 Fundamentals of Electrochemical Treatment **33**
2.1 Introduction 33
2.2 State of the Art 33
2.2.1 Overview 33
2.2.2 Theory 33
2.2.3 Methods of Coagulation 35
2.2.4 Electrode Reactions 36
2.2.5 Theoretical Estimates of Anodic Dissolution 39
2.3 Electrocoagulation Water Treatment 39
2.4 Electrochemical Factors Affecting Floc Generation 41
2.4.1 Process Parameters 42
2.4.2 Chemical Parameters 48
2.5 References 53

3 Materials and Methods **62**
3.1 Introduction 62
3.2 Electrocoagulation Design 62
3.2.1 Reactor Design 62
3.2.2 Electrode Design 63
3.3 Effluent 65

3.4 Experimental Set-Up 65
3.4.1 Chemical Coagulation Experiments 65
3.4.2 Electrocoagulation Experiments 66
3.5 Analysis 69
3.5.1 Atomic Absorption Spectrometry 69
3.5.2 Ultraviolet-visible Spectrometry 69
3.5.3 Inductively Coupled Plasma-Optical Emission Spectrometry 70
3.5.4 Turbidity 71
3.5.5 Total Suspended Solids 71
3.5.6 Dissolved Oxygen 71
3.6 Characterisation 72
3.6.1 Cyclic Voltammetry 72
3.6.2 Nano-arrayer 73
3.6.3 Scanning Electron Microscopy 74
3.6.4 X-Ray Diffraction 75
3.6.5 Transmission Electron Microscopy 75
3.6.6 Zeta Potential 76
3.7 Experimental Design 77
3.7.1 Experiment Set A 77
3.7.2 Experiment Set B 78
3.7.3 Experiment Set C 80
3.7.4 Electrochemical Parameter Study 80
3.8 References 84

4 Electrocoagulation 86
4.1 Introduction 86
4.2 Experiment Set A 86
4.2.1 Chemical Coagulation *vs.* Electrocoagulation 86
4.2.2 Section Conclusions 89
4.3 Experiment Set B 89
4.3.1 Mixing Regime I 90
4.3.2 Mixing Regime II 94
4.3.3 Section Conclusions 96
4.4 Experiment Set C 97
4.4.1 Coagulant Dilution 97
4.4.2 Greater Initial Dosing 106
4.4.3 Section Conclusions 110
4.5 References 110

5 Electrochemical Parameter Study 114
5.1 Introduction 114
5.2 Preliminary Test Work Parameters 114
5.2.1 Effect of Pollutant Loading on Flocculation 114
5.2.2 Effect of Inter-electrode Distance on Flocculation 115
5.2.3 Effect of Coagulant Dose on Flocculation 120
5.2.4 Section Conclusions 123
5.3 Process Parameters 124
5.3.1 Effect of Current Density on Flocculation 124
5.3.2 Effect of Agitation on Flocculation 126
5.3.3 Effect of Electrolysis Time on Flocculation 130

5.3.4 Effect of Coagulant Solution Retention Time on Flocculation 131
5.3.5 Section Conclusions 136
5.4 Chemical Parameters 137
5.4.1 Effect of pH on Flocculation 137
5.4.2 Effect of Conductivity on Flocculation 139
5.4.3 Section Conclusions 141
5.5 References 142

6 Characterisation 145
6.1 Introduction 145
6.2 Electrokinetic Studies 145
6.2.1 Zeta Potential *vs*. Coagulant Concentration 145
6.2.2 Zeta Potential *vs*. pH 146
6.3 Voltammetry Studies 148
6.4 Floc Imaging 150
6.5 Operational Costs 152
6.6 Sludge Production 153
6.7 References 154

7 Conclusions 156
7.1 Introduction 156
7.2 Conclusions Drawn from the Study 156
7.3 Future Work 159
7.4 Final Word 161

Appendix I 163
Appendix II 164

Impact of Electrocoagulation Parameters on Flocculation

Chapter 1

Introduction

1 Introduction

1.1 Global Water Perspective

Water and energy have been identified as the top two challenges for the 21st century.[1] Water quality and quantity are being compromised by increasing pollution from point and non-point sources such as agriculture and industry,[2] and an ever-increasing global population.[3] Cost-effective methods are necessary to treat a host of wastewater pollutants in a diverse range of situations.

The need for treated wastewater and clean drinking water is particularly critical in Third-World Countries as generally they have neither the capital nor the infrastructure to adequately address water problems.[4] Estuaries, canals, rivers and other water bodies have been polluted due to indiscriminate discharges of industrial effluents and other anthropogenic activities as well as natural processes.[5,6,7] Within twenty-five years an estimated sixty-four countries will have inadequate supplies of usable water for their incumbent populations.[8]

Highly developed countries in Western Europe, North America and Eastern Asia are also experiencing a critical need for wastewater cleaning as a result of an increasing population,[9] rapid urbanisation[10] and climatic changes.[11]

Access to suitable water supplies must thus be seen as a global challenge, the solution of which is dependent on the development and instigation of sustainable water management strategies.[12,13,14,15] New sustainable water management approaches will require fit-for-purpose use and the reuse of wastewater which is covered extensively by legislation.[16,17,18,19]

1.2 Water Legislation

The presence of water contaminants as a result of their use in modern society is a matter of growing concern to politicians, authorities and the public in the twenty-seven Member States of the European Union (EU). The strategy for minimisation of the effects that water

contaminants have in wastewater is to reduce present and future environmental and human exposure to wastewater pollutants.

Within the EU, the treatment of wastewater is regulated by a number of Directives established to control and enforce the water quality of its Member States. These Directives are designed to address all areas influenced by water management and Member States have a duty of responsibility to comply with the requirements set out in each Directive. It is however, entirely dependent on each individual EU State to design and enforce its own regulations and legislation to ensure that water quality is not compromised in regards to the parameters set out in the Directives.[20] The Directives listed below control the majority of water bodies that are associated with water management:[21]

- EC Directive on Integrated Pollution Prevention and Control (IPPC) (96/61/EC).
- EC Nitrates Directive (91/676/EC).
- EC Urban Waste Water Treatment Directive (91/271/EEC).
- EC Shellfish Waters Directive (79/923/EEC).
- EC Dangerous Substances Directive (2006/11/EC).
- EC Bathing Waters Directive (2006/7/EC).
- EC Water Framework Directive (2000/60/EC).

1.2.1 Water Quality Guidelines

Water quality guidelines and standards are used for the protection of the marine environment. Once substances of concern have been identified in relation to a particular discharge and some understanding of the fate, behaviour, and effects of the substance has been inferred, the appropriate standards can be identified.[22]

The standards listed are those used by the competent authorities in the management of water quality in the marine environment. These are the statutory standards that must be observed in receiving marine and estuarine waters and are used in setting discharge consents.

Environmental Quality Standards

Environmental quality standards (EQSs) have been derived under the requirements of the EC Dangerous Substances Directive (2006/11/EC) which classifies substances as List I and List II.[23,24] Standards for List I substances have been defined in daughter Directives to the EC Dangerous Substances Directive (2006/11/EC). The scientific justification for the standards is not available. Standards for List I substances are given in Table 1.1.

Table 1.1. Water quality standards for List I substances.

Parameter	Unit	Estuary water quality standard	Marine water quality standard
Mercury	µg/l	0.5 DAA	0.3 DAA
Cadmium	µg/l	5 DAA	2.5 DAA
Hexachlorocyclohexane HCH	µg/l	0.02 TAA	0.02 TAA
Carbon tetrachloride CCl_4	µg/l	12 TAA	12 TAA
Dichlorodiphenyltrichloroethane	µg/l	0.025 TAA	0.025 TAA
(Para, para-DDT)	µg/l	0.01 TAA	0.01 TAA
Pentachlorophenol (PCP)	µg/l	2 TAA	2 TAA
Aldrin	µg/l	0.01 TAA	0.01 TAA
Dieldrin	µg/l	0.01 TAA	0.01 TAA
Endrin	µg/l	0.005 TAA	0.005 TAA
Isodrin	µg/l	0.005 TAA	0.005 TAA
Hexachlorobenzene HCB	µg/l	0.03 TAA	0.03 TAA
Hexachlorobutadiene HCBD	µg/l	0.1 TAA	0.1 TAA
Chloroform	µg/l	12 TAA	12 TAA
1,2-Dichloroethane (ethylenedichloride)	µg/l	10 TAA	10 TAA
Perchloroethylene (tetrachloroethylene)	µg/l	10 TAA	10 TAA
Trichlorobenzene (all isomers)	µg/l	0.4 TAA	0.4 TAA
Trichloroethylene	µg/l	10 TAA	10 TAA

Key
D – Dissolved Concentration
T – Total Concentration
AA – Annual Average

The Dangerous Substances Directive (2006/11/EC) stated that standards for List II substances should be derived individually by respective Member States. The UK has set EQSs for List II substances as summarised in Table 1.2 on the following page.

Table 1.2. Water quality standards for List II substances.

Parameter	Unit	Water Quality Standard
Lead	µg/L	25 AD
Chromium	µg/L	15 AD
Zinc	µg/L	40 AD
Copper	µg/L	5 AD
Nickel	µg/L	30 AD
Arsenic	µg/L	25 AD
Boron	µg/L	7000 AT
Iron	µg/L	1000 AD
Vanadium	µg/L	100 AT
Tributyltin	µg/L	0.002 MT
Cyfluthrin	µg/L	0.001 PT
Sulcofuron	µg/L	25 PT
Flucofuron	µg/L	1.0 PT
Permethrin	µg/L	0.01 PT
Atrazine and Simazine	µg/L	2 AA; 10 MAC
Azinphos-methyl	µg/L	0.01AA; 0.04 MAC
Dichlorvos	µg/L	0.04 AA and 0.6 MAC
Endosulphan	µg/L	0.003 AA
Fenitrothion	µg/L	0.01 AA; 0.25 MAC
Malathion	µg/L	0.02AA; 0.5MAC
Trifluralin	µg/L	0.1AA; 20 MAC
4-chloro-3-methyl phenol	µg/L	40 AA; 200 MAC
2-chlorophenol	µg/L	50 AA; 250 MAC
2,4-dichlorophenol	µg/L	20 AA; 140 MAC
1,1,1-trichloroethane	µg/L	100 AA; 1000 MAC
1,1,2-trichloroethane	µg/L	300 AA; 3000 MAC
Bentazone	µg/L	500 AA; 5000 MAC
Benzene	µg/L	30 AA; 300 MAC
Biphenyl	µg/L	25 AA
Chloronitrotoluenes	µg/L	10 AA; 100 MAC
Demeton	µg/L	0.5 AA; 5 MAC
Dimethoate	µg/L	1 AA
Linuron	µg/L	2 AA
Mecoprop	µg/L	20 AA; 200 MAC
Naphthalene	µg/L	5 AA; 80 MAC
Toluene	µg/L	40 AA; 400 MAC
Triazophos	µg/L	0.005 AA; 0.5 MAC
Xylene	µg/L	30 AA; 300 MAC

Key
A – Annual,
D – Dissolved Concentration,
T – Total Concentration,
AA – Annual Average,
MAC – Maximum Allowable Concentration.

Other Directive Requirement Standards

Standards for a range of toxic and non-toxic contaminants have been set separately in order to meet specific Directive requirements. The standards for one of these, the EU Bathing Waters Directive (2006/7/EC), is likely to be frequently encountered by wastewater treatment works (WWTW) and operators discharging into marine waters. These standards are set to meet specific Directive requirements.

Bathing Waters Directive Standards

The standards in the EC Bathing Waters Directive (2006/7/EC) are only applicable in designated bathing waters during the bathing season and are designed to protect human health from the microbiological components of sewage and, to a lesser extent, the aesthetic appearance of the bathing waters.[25]

The standards shown in Table 1.3 were stipulated in the Directive and the reasoning behind their derivation is not known. The environment agencies are obliged to meet the imperative standards in designated bathing waters during the bathing season.

Table 1.3. Quality standards for fresh and saline waters stipulated in the EU Bathing Waters Directive (2006/7/EC).

Parameter	Unit	Guide value	Imperative value
INORGANIC SUBSTANCES AND GENERAL PHYSICO-CHEMICAL PARAMETERS			
Colour	–	–	–
Copper	mg/L	–	–
Dissolved oxygen	% saturation	80-120 T90	–
pH	–	–	6-9 T95
Turbidity	Secchi depth m	>2 T90	>1 T95
ORGANIC SUBSTANCES			
Hydrocarbons	µg/L	300 T90	–
Phenols	µg/L	5 T90	50 T95
Surfactants	µg/L (as lauryl sulphate)	300 T90	–
Tarry residues	–	–	–
MICROBIOLOGICAL PARAMETERS			
Faecal coliforms	per 100 mL	100 T80	2000 T95
Total coliforms	per 100 mL	500 T80	10000 T95
Faecal streptococci	per 100 mL	100 T90	–
Salmonella	per 1 L	–	0 T95
Enteroviruses	PFU/10 L	–	0 T95

Key
T – Total Concentration,
80 – 80 percentile,
90 – 90 percentile,
95 – 95 percentile.

1.2.2 Drinking Water Standards

The water quality parameters at customer taps are summarised in Table 1.4 on the following page and are set to protect human health.[26] Along with the contaminant of interest that should be controlled and its corresponding standard value, a description of why that standard has been set is also included.

Table 1.4. Water quality parameters at customers' taps.

Parameter	Standard	Justification
Colour	20 mg/L Pt/Co scale (Hazen Units)	Filtered colour caused by natural organic matter in water. The standard is set for aesthetic reasons and requires the water to be virtually colourless.
Turbidity	4 nephelometric turbidity units (NTU)	A standard of 1.0 NTU is applied to samples taken at water treatment works outlets.
Taste/Odour	Dilution Number 3 (at 25° C)	Water is examined by a taste panel, chlorine is acceptable.
pH (Hydrogen ion)	6.5 – 10.0 pH units	Alkaline conditions help to prevent corrosion of pipes.
Sulphate	250 mg/L	May be dissolved as water passes through rocks.
Sodium	200 mg/L	Standard is set well below the level that could affect human health.
Nitrate	50 mg/L	Excess may arise through fertiliser use although may be minimised through good agricultural practice.
Nitrite	0.5 mg/L	A standard of 0.1 mg/L is applied to samples taken at WWTW outlets as it can assist in reducing microbial activity.
Ammonium	0.5 mg/L	May be naturally present in some water sources.
Total Organic Carbon	No specific standard	Measures of the general organic content of the water and not indicative of any health hazard.
Aluminium/Iron	200 µL/200 µL	Occur naturally, used in some treatment plants to remove impurities but are themselves removed in the process. Iron may be associated with corrosion of unlined iron water mains.
Manganese	50 µL	Standard set for aesthetic reasons only as excess can lead to discolouration.
Copper	20 mg/L	Significant copper is likely to come from customers' pipes or fittings and can cause metallic taste or blue tint.
Fluoride	1.5 mg/L	Occurs naturally. Standard set to ensure no adverse health effects.
Antimony	5 µg/L	Very low levels of these substances may occur naturally.
Arsenic	10 µg/L	(Standards set with a large margin of safety for health reasons.)
Boron	1 µg/L	See above.
Cadmium	5 µg/L	See above.
Chromium	50 µg/L	See above.
Cyanide	50 µg/L	See above.
Mercury	1 µg/L	See above.
Nickel	20 µg/L	See above.
Selenium	10 µg/L	See above.
Lead	10 µg/L	See above.
Gross Alpha	0.1 Bq/L	Occur rarely at low levels, derived from rock strata.
Gross Beta	1.0 Bq/L	Occur rarely at low levels, derived from rock strata.
Pesticides	0.1 µg/L (individually) 0.5 µg/L (total)	Substances used by agriculture, industry, railways, local and highway authorities. Most individually are 0.1 µg/L but some are 0.3 µg/L.
Polycyclic Aromatic Hydrocarbons (PAH's)	0.1 µg/L	Associated with the deterioration of old coal-tar pipe linings which are no longer used and which are removed when identified as causing a problem.
Benzo 3,4-pyrene	0.01 µg/L	Standards set well below the levels of significance to health.
Conductivity	250 µS/cm	A measure of the total content of dissolved salts, generally naturally present, in the water. Levels above the standard could give rise to taste and contribute to corrosion.
Chloride	250 mg/L	Levels above the standard could give rise to taste.
Bromate	10 µg/L	Potentially present when ozone or hypochlorite are present in water treatment.
Total Hardness	No specific standard	Higher the hardness, the more soap that is required to form lather.
Tetrachloromethane	3 µg/L	Levels above the standard indicate the presence of solvents.
(Trichloroethane +)	3 µg/L	Levels above the standard indicate the presence of solvents.
Benzene	1 µg/L	Levels above the standard indicate the presence of solvents.
1,2-Dichloroethane	3 µg/L	Levels above the standard indicate the presence of solvents.
Trihalomethanes	100 µg/L	Formed when chlorine added to disinfect the water reacts with naturally occurring organic substances.
Chlorine Free/Total	No specific standard	Aim is to keep levels at customers' taps to a minimum – associated with taste and odour. *(Cont. on following page...)*

Parameter	Standard	Justification
Coliforms Total	0 per 100 mL	Very sensitive indicators of bacteria in the environment and are removed by treatment. Presence does not indicate direct risk to human health but detections are investigated as a matter of urgency.
Clostridium perfringens	0 per 100 mL	Coliforms in tap samples may be due to contamination of the tap.
Colonies 22° C & 37° C	No specific standard	Any high unusually levels of bacteria colonies prompts investigation.
E. coli/Enterococci	0 per 100 mL	Originate in the digestive system of warm blooded animals and their presence indicates contamination by faecal matter and therefore a higher risk that pathogens may be present.
Cryptosporidium	100 per 1000 L	Can cause cryptosporidiosis (diarrhoea) but other sources not just water can input the micro-organism into humans. Continuous sampling for cryptosporidium is done.

1.3 Water Management

The relationship between water consumption and water supply is becoming of ever greater global concern and effective water management will become even more imperative in solving water cleaning, supply and reuse problems in the future.[27,28,29]

Restoring vegetation and water flows to rivers in land will aid in lowering the water table. To increase water flow throughout the river network system, consumption of water must be reduced or, at least, stabilised. It is crucial therefore that correct management of the entire water cycle is addressed for a sustainable water supply and for future use. An integrated solution to clean used water and incorporate it back into the water cycle is required and any solutions formulated should account for all requirements and be able to meet global demand. The dynamics and interactions of water systems are complex; Figure 1.1 represents the interconnectedness of the water cycle.

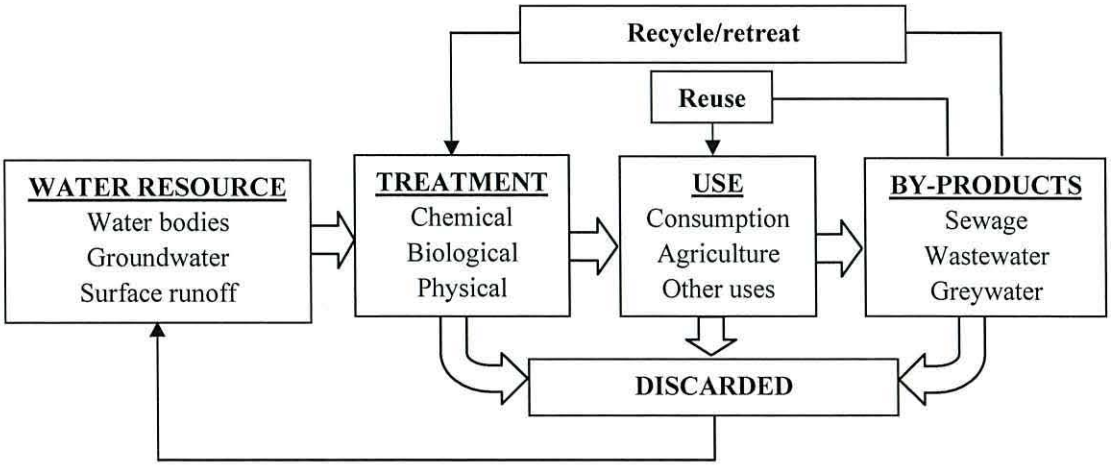

Figure 1.1. Water cycle relationship.

In order to prevent further environmental degradation, water extraction from the natural environment must be curtailed *via* minimising the demand or increasing the lifetime of usable water within the built environment. If water remains over an extended period in the built environment, this will lessen the overall consumption from the natural environment. This can be achieved through increasing water recycling and reuse, thus, regardless of water quality; any grade of water should be recognised as a valued resource.[30]

Sustainable water management systems relate water quality to appropriate usage, hence potable water is used for drinking water whereas lower grade water such as grey water is used for flushing lavatories. Figure 1.2 represents the relationship between water quality and use.

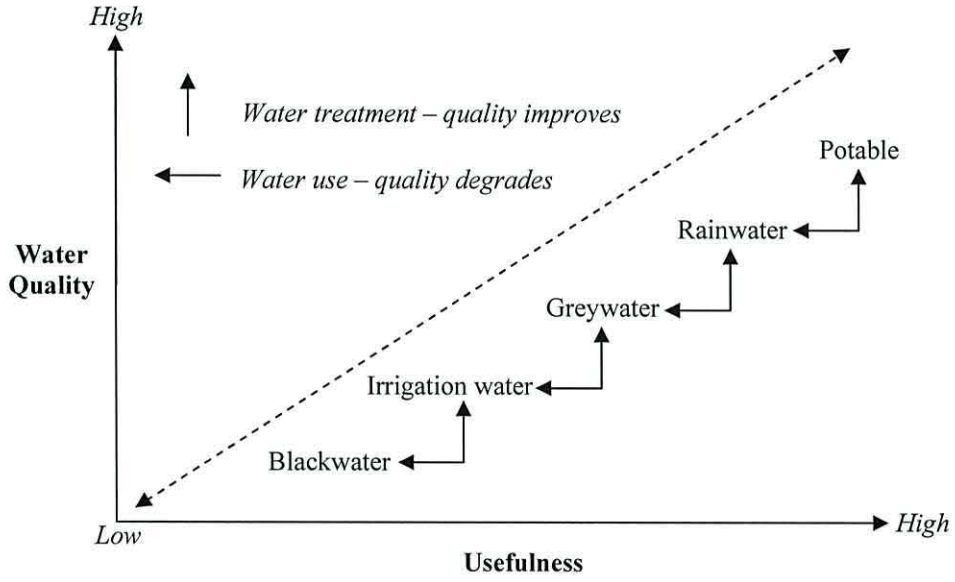

Figure 1.2. Cascade relationship between water quality and potential usefulness.

As the number of uses increases, so does the useable life of the water within the built environment. Water quality decreases as it is used thus it's potential for further usability becomes diminished. In order to reverse this, water quality must be improved and hence it must be treated to a standard equal to its intended reuse. Treated, high quality water can then have a greater residence time within the built environment but in order to achieve this, new science and technologies are needed, such as electrocoagulation.[31,32,33,34,35]

To increase water quality that is suitable for a particular purpose, whether for drinking water or toilet water, the technology used to enhance that water's quality must be able to operate over a wide pollutant spectrum. Consequently, smaller and localised treatment

technologies are preferential over centralised treatment systems. Centralised treatment requires transportation and infrastructure such as piping and pumping. Transporting water also requires energy and displaces a valuable commodity from its source, a potential usage point. Thus, small local water treatment technologies that extend the water's useable life and reduce consumption and transportation are increasingly becoming required.[36]

1.4 Water Treatment

The primary aim of water and wastewater treatment is the removal of particulate matter responsible for the degradation of a water body. Typically colloidal particles are accountable for this in raw waters and wastewaters and their stability in solution is due to their common distribution of charges on their surfaces that allows them to remain discrete through mutual repulsion. To remove them by gravitational sedimentation without any size enlargement pre-treatment is therefore difficult.

To overcome this and increase the size of colloidal particles so they may drop out of solution requires destabilisation of a suspension. This can be achieved through the neutralisation of the surface charge on particles by the addition of chemical coagulants or flocculants. Chemicals promote an increase in ionic strength of a colloidal containing medium and adsorb onto the surfaces of particles counterbalancing their original electrical charge. The net result is that charges are diminished and electrostatic repulsion is dampened allowing colloidal particles to interact and coagulate.

Chemical coagulation is the traditional method of purifying wastewater and involves destabilising colloidal particles through charge reversal, agglomerating them together and allowing them to settle out of solution. The overall product of coagulation is the formation of flocs that can destabilise colloidal particles through the following mechanisms:

- Adsorption. Occurs when oppositely charged ions adsorb onto the surfaces of particles thus reducing surface charge and the repulsive force between them.
- Inter-particle bridging. Typical with the use of polymerised metal coagulants that can form bridges between particles. This is common with long-chained, high molecular weight organic polymers whereby bridging occurs when a polymer chain adsorbs onto multiple particles through charge-charge interactions.

- Enmeshment. Where high concentration metal salts at neutral pH are used, the formation of insoluble hydrolysis products are generated that are capable of entrapping colloidal particles in large cloud-like structures referred to as sweep-flocs.

1.4.1 Coagulation

The process of water treatment and colloidal separation through coagulation can be considered in four steps. Initially, a metal salt is introduced into a wastewater volume. Secondly, fast mixing of the volume ensures that the coagulant is evenly dispersed throughout and that the volume is homogenous. After the completion of this dispersal phase, the solution is mixed again in the third step but at a slower rate where the induced velocity gradients provide particles the opportunity for contact and the formation and growth of precipitous solids; this phase is known as flocculation. Finally, through sedimentation or filtration, the coagulated solids are separated from the water and the filtrate or supernatant is siphoned off.

The most commonly used metals salts used in water and wastewater purification are aluminium and iron sulphates and chlorides due to their ability to form the multivalent ions Fe^{3+} and Al^{3+}. These can form mononuclear and polynuclear hydroxides in solution as well as neutral amorphous $Al(OH)_3$ and $Fe(OH)_3$ species that are poorly soluble. The distribution of iron and aluminium metal species in solution is presented in the solubility diagrams in Figure 1.3 on the following page.

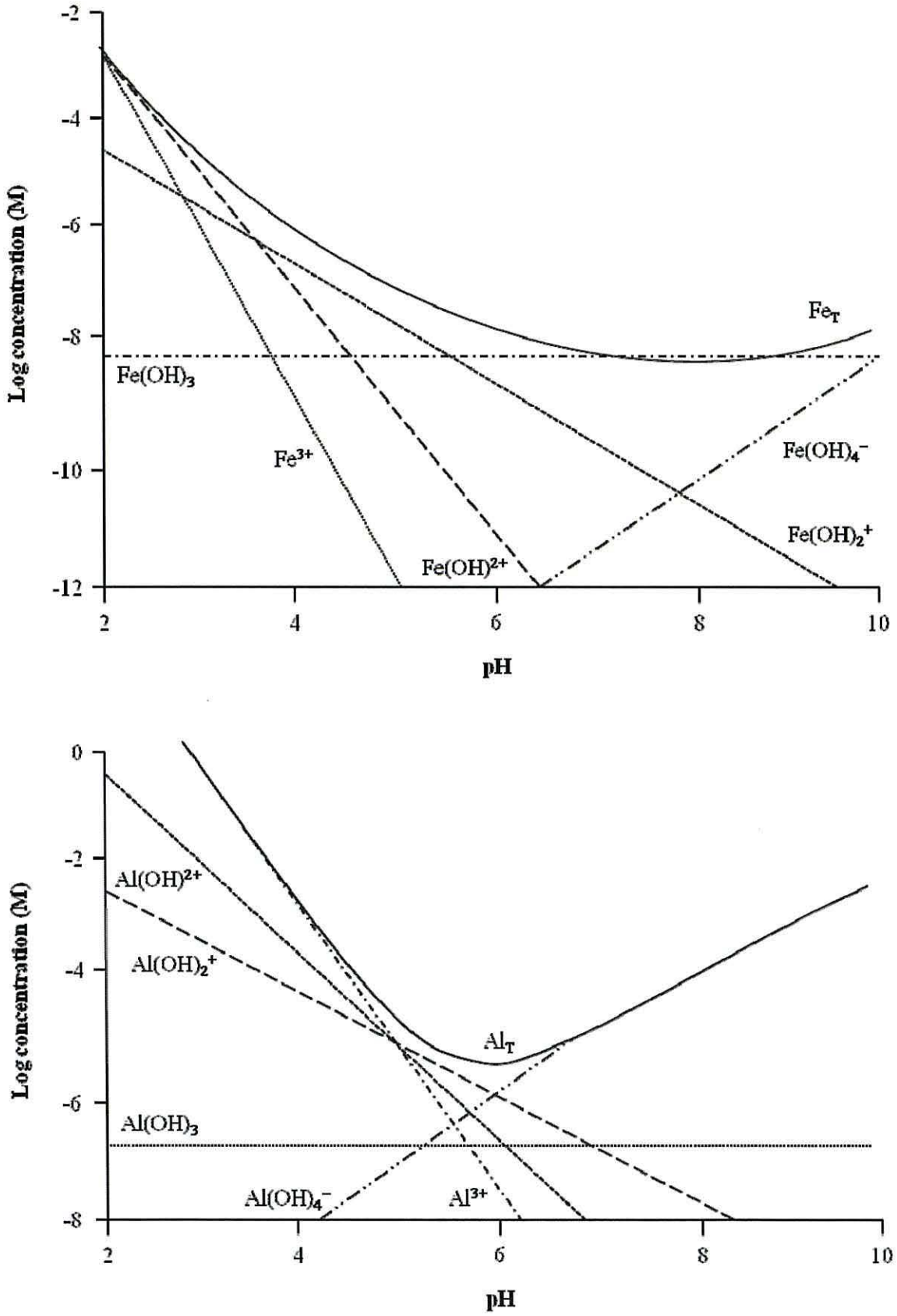

Figure 1.3. *Top.* Hydrolysis products of Fe^{3+}. *Bottom.* Hydrolysis products of Al^{3+}.[37]

An alternative to chemical coagulants however is the *in-situ* generation of flocculant, through electrochemical means, in which electrolytic oxidation of an appropriate anodic material is done. This method is called electrocoagulation (EC) and is a competitor process to the use of chemical coagulants.

1.5 Electrocoagulation

Electrocoagulation involves the elution of metallic electrodes (usually iron or aluminium) into a wastewater body and the subsequent floc formation of metal hydroxides that can perform the same removal tasks as chemical flocs. It is a viable technology to improve water quality and is an independent, transferrable treatment method with the ability to remove a host of pollutants.

However, opinions differ in the literature for explaining the key mechanisms that are in effect during EC. Presently, the technology's science is predominantly empirical and heuristic. These pragmatic studies consistently prove the feasibility of the technology, but due to a fundamental lack in understanding of the science behind the processes involved, the studies reported invariably fall short in exploiting the full potential of this technology. Consequently the accuracy in predicting performance of EC for varying contaminated water sources remains haphazard.

1.5.1 Historical Background

Electrocoagulation is not a new technology and literature indicates that it has been repeatedly discovered over the last one hundred years, both in continuous and batch applications. The concept of treating water electrochemically for purification using electrodes was first proposed since before the turn of the twentieth century when a treatment plant in London was built in 1889. Sewage water was treated by mixing it with seawater and electrolysing the liquor.[38] In 1909, in the United States, J. T. Harries received a patent for wastewater treatment by electrolysis with sacrificial aluminium and iron anodes.[39]

On a larger scale, a method for the purification of drinking water by EC was first applied in the United States in 1946.[40,41] This method utilised aluminium anodes to produce

aluminium hydroxide flocs by reaction at the electrode followed by hydrolysis. The electro-generated flocs sedimented rapidly, removing colour from the drinking water.

In 1956 treated river water in Britain was accomplished using iron electrodes with a similar type of system.[42] Both the investigations in 1946 and in 1956 showed promising results, e.g. high water quality as measured by turbidity and colour removal, but the methods were not widely adopted because of some expectations of high initial capital costs as compared to chemical dosing.

Recently however, there has been renewed interest in the use of EC due to the increase in environmental restrictions on effluent wastewater.[43] In 1972, EC was studied in the treatment of wastewater from a food industry.[44] This report compared EC to chemical dosing followed by dissolved air flotation (DAF). Floc formation was rapid in both cases but with the flocs formed from EC being compacted more quickly. The concept of EC was also applied to micro-organism harvesting from cultures and to the removal of protein and ether soluble substances from wastewater in the 1980's. [45,46,47,48]

In this decade, there was also significant work carried out utilising EC in a variety of ways in the treatment of wastewaters and in the removal of oil from oil-in-water emulsions.[49,50] Presently, EC is marketed by a small number of companies around the world. A variety of designs have been employed with no dominant construct. Often the EC units are used simply as a replacement for chemical dosing systems.

1.5.2 Benefits and Drawbacks

Electrocoagulation has the potential to be distinctly environmentally friendly, economical and the choice treatment for wastewater and other associated water management issues. As a stand-alone technology, EC avoids the use of chemical addition therefore eliminating the problem of neutralising excess chemicals and minimising the possibility of secondary pollution. It requires low current input and can be operated by green processes such as; windmills, solar energy and fuel cells.

Furthermore, it nullifies the costs associated with chemical use that has to be transported to site and thereafter stored in suitable vessels. Specialist training to site personnel is also needed for chemical dosing whilst handling and disposal of sludge stemming for chemical

coagulation is expensive and difficult. Most chemical precipitation sites have large caustic soda tanks to counter the decrease in pH normally associated with dosing chemical salts and generate large volumes of sludge that need to be collected and transported off site to specialist sludge disposal facilities.

Electrocoagulation is also efficient as adsorption of hydroxides on mineral surfaces is greater on *in-situ* rather than on pre-precipitated hydroxides when metal hydroxides are used as coagulant.[51] Electrocoagulation requires simple equipment and has sufficient operational latitude that it can be modified to operate and treat a variety of polluted waters with treated effluent containing less total dissolved solids (TDS) content compared to chemical treatment.[52] If water reuse is employed, the low TDS level contributes to a lower water recovery cost and sludge formed from EC is relatively easy to de-water as it is composed mainly of metallic oxides/hydroxides.

Flocs formed by EC are asymptotic to chemical floc with the only exception being that EC floc is larger in size, contains less water, is acid-resistant and is more stable thus lending itself more to separation and quicker filtration.[53] The gas bubbles produced during electrolysis can also aid in separation by carrying pollutant species to the top of water settler units where they can be concentrated, collected and removed.[54]

Electrocoagulation is easily operable with electrolytic processes in an EC reactor controlled electrically and with no moving parts thus limiting the maintenance required. In more rural areas where electrical supply maybe sporadic, EC can still be used as photovoltaic cells can provide enough power for sufficient treatment of local water bodies.[55]

Further benefits from using electrochemical techniques include: environmental compatibility, selectivity, versatility, amenability to automation safety, energy efficiency and cost effectiveness.[56] In addition to these, the following advantages can be added: electrochemical based systems allow controlled and rapid reactions,[57] smaller systems become practical and, instead of using chemicals and micro-organisms,[58,59] the systems employ only electrons to facilitate water treatment. In this regard, EC can be ruminated as a clean science procedure since the treatment of contaminated effluent relies upon the electron being utilised as a reagent.[60]

Although EC has numerous advantages, it has some drawbacks as discussed below. The sacrificial electrodes are dissolved into wastewater streams as a result of oxidation and therefore regular replacement of the worn electrodes is required. A minimum conductivity of the wastewater suspension is required for operation limiting its use with low TDS containing waters.

With regard to organic compounds removal, some toxic chlorinated organic compounds may be formed *in-situ* where chlorides may be present in the wastewater.[61] Waters with high fulvic and humic acid content may also be amenable to the formation of tri-halomethanes.[62]

An impermeable oxide layer may form on the cathode that can interfere with performance and lead to a reduction in efficiency of EC. The initial capital cost of EC may be inflated in areas where electrical supply is sporadic or cost of electricity is high.

1.5.3 Applications

There has been a great deal of interest reported in the literature in using EC for treatment of wastewater containing; suspended particles,[63,64,65] heavy metals,[66,67,68] oil wastes,[69,70] landfill leachate derived organic matter,[71] foodstuffs,[72] textile dyes,[73,74,75,76,77] arsenic,[78] phenolic waste,[79] aqueous suspensions of ultrafine particles and refractory organic pollutants including lignin and ethylenediamine-N, N, N, N-tetra-acetic acid (EDTA).[80] The electrochemical treatment of various wastewaters has been reported in depth,[81] but only a small number of authors[82,83] have focused on the variables that are crucial to the enhancement of the performance of EC.

Other cited studies in the literature point to work carried out on the electrochemical treatment of waters containing boron,[84] alcohol distillery wastewater[85] and poultry slaughterhouse wastewater.[86] Table 1.5 on the following page presents pollutants removed by EC in laboratory studies. The physicochemical nature of the pollutant influences its interaction within an electrocoagulating reactor thus determining its removal mechanism. Heavy metals and other ions are predominantly electroprecipitated out of aqueous media, whereas suspended solids become adsorbed onto coagulant species.

Table 1.5. Summary of pollutants removed by EC in water and wastewater sources.

Reference	Pollutant	Current density	Electrode material	Removal path	Reactor
FATS, OILS GREASES (FOG's)					
Sangal *et al.*[87]	Soluble oil	6.5-139 A/m^2	Al electrodes	Settled	Batch
Ahmadi *et al.*[88]	Oil	10-12.5 mA/cm^2	Fe electrodes	Settled	Batch
Mostefa and Tir[89]	Oil	6-14 mA/cm^2	Flat sheets of steel/stainless steel	Flotation in separate cell	Batch
COLOUR					
Un *et al.*[90]	Dye, COD	20-30 mA/cm^2	Fe wire netting sheet & Fe cathode plates	Settled	Batch
Yavuz *et al.*[91]	Dye, COD	2-20 mA/cm^2	Fe/Al electrode pair	Settled	Batch
Bhatnagar *et al.*[92]	Dye, COD	30-140 A/m^2	Graphite electrode	Settled	Batch
HEAVY METALS					
de Mello Ferreira *et al.*[93]	Cu, Zn, Ni	7-42 A/m^2	Fe & Al electrodes	Settled	Batch
Hernández *et al.*[94]	Ni, Cr in drinking water	0.2-1.6 mA/cm^2	Al electrodes	Settled & filtered	Batch
Aji *et al.*[95]	Mn, Zn, Ni, Cu	2-25 mA/cm^2	Fe; monopolar	Filtered	Batch
URBAN & INDUSTRIAL WASTEWATERS					
Larue *et al.*[96]	Latex particles	11-88 mA/cm^2	Fe/Fe	Settled & filtered	Batch
Hutnan *et al.*[97]	COD	3-8 mA/cm^2	Fe/Al; monopolar	Floated and settled	Continuous
Kliaugaite *et al.*[98]	Humic substances	1-4.6 mA/cm^2	Fe/Fe	Settled & filtered	Continuous
IONS					
Lakshmi *et al.*[99]	Nitrate	0.1-0.75 A/dm^2	Al/Al	Floated	Batch
Emamjomeh *et al.*[100]	Fluoride	18.75 A/m^2	Al; monopolar	Floated and settled	Batch
Alfafara *et al.*[101]	P, Algae from eutrophied lake water	mA/cm^2	Al/titanium alloy or carbon anode	Electroflocculation and electroflotation	Batch and continuous

1.5.4 Other Electrochemical Treatment Techniques

The following sub-paragraphs briefly highlight other EC related water clean-up technologies that have been reported within the literature.

Electrochemical Precipitation

Several historical EC treatment methods are based on the electrochemical precipitation (EP) of heavy metal ions as hydroxide species and these treatments have been used for the removal of ions such as Cd(II), Cu(II), Ni(II), Fe(II), Cr(III) and Al(III).[102]

In a reported application, groundwater from a SuperFund site in the United States, an area deemed extremely toxic by the USEPA (United States Environmental Protection Agency) due to industrial contamination, was treated *via* EP. The mercury, cadmium, lead, arsenic, selenium, and copper contaminants were removed to below their consent levels.[103]

However, it is difficult to bring any specificity into the system and metals exit from the system as solids with complex compositions. Consequently, the precipitated metals are in their least valuable form and in most applications, as recycling of these metal forms cannot be accomplished, after filtration they are sent to disposal.

Electrodialysis

This electrochemical procedure has been used with anodising bath solutions. When anodising aluminium, regular replacement and disposal of the solution in the bath is required when aluminium concentrations exceed 80 g/L due to the spent bath solution containing high levels of aluminium and sulphuric acid. As a result, neutralisation and metal removal prior to disposal is necessary. By adding an electrodialysis (ED) unit to an anodising bath system, the longevity of the system is increased as the unit maintains a low metal ion concentration in the anodising bath solution by transporting aluminium ions from the bath, through a membrane, into a sister bath that captures the ions.[104]

Electrochemical Ion Exchange

This process is well-established and used throughout industry in the removal of metal containing effluent solutions. The technology is very efficient in treating low concentrations of contaminants as the process utilises high surface area resins. The main advantage of this process is the high selectivity that can be adopted depending on which heavy metal species are required for removal, e.g. nickel or aluminium.[105,106]

1.6 Other Wastewater Treatment Methods

A wide range of non-EC derived wastewater treatment technologies are also found within the literature and mention should be made of these as they are accepted wastewater treatment methods in direct competition with EC. The competing technologies include; evaporation, reverse osmosis, ultra filtration, precipitation, solvent extraction and ion exchange,[107] some of which are discussed next.

1.6.1 Chemical and Physical Means of Water Recovery

Precipitation Recovery

Chemical precipitation of sparingly soluble metal compounds with lime, sulphide and caustic soda are the most commonly used and economical methods for metal removal. Equation 1 illustrates the reaction involved when iron sulphate and caustic soda are reacted together to form the corresponding iron hydroxide species:

$$2NaOH_{(aq)} + FeSO_{4(aq)} \rightarrow Fe(OH)_{2(s)} + Na_2SO_{4(aq)} \qquad \textbf{Equation 1}$$

Aside from the cost effectiveness of the treatment process, its appropriateness as a first step of a hybrid separation process already makes the precipitation method widely used.

However, heavy metals cannot be removed efficiently by hydroxide precipitation alone. Higher degrees of removal can be achieved by sulphide precipitation, but consequently, high volumes of toxic sludge are produced leading to difficulties in disposal.[108] A more sustainable, effective and economic method could be rectified for heavy metal removal and recovery if a process scheme which can achieve selective separation of metals, and produce reusable pure metal sludge's, could be developed.

This was achieved in a study in which a hybrid precipitation-polymer enhanced ultrafiltration based separation scheme was developed for the removal and recovery of cadmium, aluminium, copper and iron in a cadmium electroplating bath. The precipitation scheme, comprising of three consecutive steps, involved: (i) acidic treatment with nitric acid, (ii) alkali precipitation by sodium hydroxide, and (iii) sulphide precipitation by sodium sulphide. A result of this process was the decomposition of cyano-metal complexes, the removal of the entirety of the iron content and approximately half the content of the nickel during the acidification step, and through the addition of sodium hydroxide, the remaining heavy metals were precipitated with pure $Cd(OH)_2$ being obtained. A valuable product used in the electroplating industry.

In sulphide precipitation, the addition of sodium sulphide in an alkali pH range led to cadmium precipitation whereas copper was totally precipitated in the acidic pH range. After the precipitation experiments, polymer enhanced ultra-filtration (PEUF) was then applied.[109] Polymer enhanced ultra-filtration is one of the complexation enhanced ultra-

filtration processes based on the complexation between a water-soluble polymeric binding agent and the target component which is to be separated from the aqueous solution.[110]

Metal removal and recovery therefore, achieved by such a process involving selective separation of the metals combined with micro or ultra-filtration, has produced re-usable pure metal sludge's. This process has shown to be a more sustainable, effective, suitable and an economical hybrid operation for the removal and recovery of metals from streams.

Other studies involving chemical precipitation have demonstrated near total removal of iron and aluminium precipitate from acid mine drainage (AMD) with purities of 93.4% and 92.1% having been achieved in the resultant metal sludge's.[111,112]

Sorption

Calcium phosphate minerals, referred to as apatite's, have been used as sorbents for different metals. Adsorption of heavy metals including; barium, cadmium, magnesium, aluminium, nickel, lead, and zinc from solutions by apatite's have been demonstrated by several authors.[113,114] Magnetite's (Fe_3O_4) ability to remove metals from aqueous solutions has also been highlighted in the literature as well as the use of alumina (Al_2O_3) as an absorbent.[115,116,117]

Activated Carbon

Activated carbon has shown promising results in decontaminating heavy metal polluted wastewaters.[118] The application of magnetic particle technology to solve contamination problems has received considerable attention in the last ten years. Magnetic particles have been used to adsorb contaminants from aqueous or gaseous effluents and, after adsorption, can be separated from solution by a simple magnetic procedure. Such works carried out are scattered sparsely throughout the literature but does mark the beginning of research being undertaken in this field.[119,120,121]

Consequently, work has been limited and due to the small surface area of the magnetic materials used; this has impacted on their adsorption capacity and hence restricted their application. Furthermore, the preparation of those magnetic materials requires several steps and specialist chemicals and procedures.

However, activated carbon is more favourable in that it offers an attractive and inexpensive option for the removal of organic and inorganic contaminants from effluent wastewaters. Due to its high surface area and porous structure it can efficiently absorb gases and compounds dispersed or dissolved in liquids.[122] The adsorption of several organic contaminants in water, such as pesticides, phenols and chorophenols, has also been reported.[123]

Reverse Osmosis

Studies involving reverse osmosis (RO) have shown 75 – 95% recovery of water and near total removal of metals in the permeates of metal finishing effluents.[124] As such, RO technology has been used to recover plating chemicals from rinse waters and even to purify mixed wastewaters for reuse. In industry, RO units separate valuable metal ions from rinse solutions that can be recycled to plating baths thus generating an economically worthwhile procedure.

Conversely, RO membranes are expensive and certain effluents may require pre-treatment to remove fouling materials such as carbonates and oils. Other problems associated with RO concern the membranes that are used as they are extremely heat sensitive and deteriorate at higher temperatures. Some membranes also deteriorate at pH values below 3.

Bioremediation

Micro-organisms have been used to remove metal ions from solution. An example is *Zoogloea ramigera* which can be immobilised to *Ca-alginate* to obtain higher adsorption capacity levels and yields when packed into a column and operated in continuous mode.[125] However, aluminium adsorption in the immobilised-cell column is limited due to diffusion of the solute through the pores.

Bioleaching

A simple and effective technology for metal extraction from low-grade ores and mineral concentrates. *Thiobacillus ferrooxidans* and *T. thiooxidans* are bacteria which are able to convert insoluble metal sulphides into soluble metal sulphates.[126] This process is used essentially for recovering copper, uranium and gold.

Roasting

Roasting is a method that has been used in the recovery of copper on an industrial scale. Extraction is done *via* roasting the metal slag with $FeSO_4$ and then leaching with water to bring the metal ion into solution.[127]

1.7 Recent Improvements in Electrocoagulation

Despite EC being known as an electrochemical wastewater treatment technique for the last century, there is very little discussion to be found within the literature regarding the improvement of design and performance of the technology. Furthermore, there are very limited sources found that discuss improvements made towards a better understanding in delineating the chemical and process variables that can improve EC floc formation processes. Those that have been published have been highlighted in the following sections.

1.7.1 Improvement in EC Reactor Design

In a published article, EC treatment of wastewater using Al electrodes was trialled in two different reactor configurations. It was found that the reactor designed to enable water to travel vertically up through the cell interacting with the electrodes as it flowed upwards, outperformed the reactor configured horizontally where the water was directed to flow linearly along electrode surfaces. The former reactor design also outperformed conventional chemical coagulation treatment that it was compared to.[128]

1.7.2 Improvement in Current Efficiency

Current efficiency is partially dependant on minimising the IR-drop across anode electrodes. Oxygen evolution, as a consequence of Equation 2 (section 2.3.4), represents an unwanted leakage of current that impacts on overall current efficiency. This can be minimised however through choice of anodic material by selecting materials that present a high overpotential for the evolution of oxygen from occurring.

A number of authors have experimented with binary and ternary alloys as well as combining carbon electrodes and titanium sheets coated with active oxides.[129,130,131] These anodes have been used for the electrochemical treatment of wastewater containing phenols, organic dyes, chloro-substituted phenols and tannery wastes.

1.8 Aim of Study

It is among the objects of embodiment of this work to provide an understanding of the fate of floc particles generated as a function of various electrochemical parameters with a view of delineating trends and patterns in floc formation and development in relation to pollutant removal. Parameters such as pollutant loading; inter-electrode distance; coagulant concentration; current density; agitation; electrolysis time; coagulant retention time; pH; and conductivity, divided into process and chemical classifications, will be investigated. It is also among the objects of embodiment to provide a comparison of EC to the standardised practice of chemical coagulation *via* ferric chloride ($FeCl_3.6H_2O$) dosing.

It is hoped that by developing an understanding of the fate and behaviour of electrochemically generated floc, this knowledge can be transferred and used to develop a holistic study to EC treatment of any wastewaters and move away from solely pollutant centred studies. The overall ambition of this work is to provide a better scientific foundation to facilitate an improvement in the development of the technology. The remainder of this report is set out as follows and contains seven chapters.

This first chapter covered an introduction to the problems associated with global water supplies and detailed the need for effective, cheap and green technology to shift towards a more prominent role in wastewater clean-up.

Chapter 2 discusses the background of EC and introduces the fundamental principles that lie behind the technology. Electrochemical equations and reaction mechanisms at work during operation are also presented. Details on operational parameters affecting performance and treatment of wastewater are also provided.

Chapter 3 is devoted to the materials and methods used in this study.

Chapter 4 presents results and analyses of the initial trials detailing the comparative experiments between EC and chemical coagulation. The ranging of coagulant dosage, both chemically and electrochemically was also experimentally determined. These studies were designed to provide the reader with a foundation onto which Chapter 5 follows.

Chapter 5 concentrates on the electrochemical study of EC generated floc and demonstrates trends and patterns in floc development as a function of operational parameters, divided into 3 categories: (i) preliminary test work – pollutant loading; inter-electrode distance; coagulant concentration, (ii) process parameters – current density; agitation; electrolysis time; coagulant retention time, and (iii) chemical parameters – pH; and conductivity.

Chapter 6 characterises the flocculant complexes generated during the experiments, whilst Chapter 7 is dedicated to the conclusions drawn from this study.

1.9 References

1. UNESCO. The United Nations World Water Development Report: Water and Energy. UNESCO Publishing, 2014.
2. Hill, M. K. Understanding Environmental Pollution, 3rd edition. Cambridge University Press, 2010.
3. Olsson, G. Water and Energy. IWA Publishing, 2012
4. Jacobs, I. M. The Politics of Water in Africa: Norms, Environmental Regions and Transboundary Cooperation in the Orange-Senqu and Nile Rivers. Continuum International Publishing Group, 2012.
5. Ahuja, S. Comprehensive Water Quality and Purification. Elsevier, 2013.
6. Reyes, J. A., Sawyer, W. C. Latin American Economic Development. Routledge, 2011.
7. McKinney, M. L., Schoch, R. M., Yonavjak, L. Environmental Science: Systems and Solutions, 5th Edition. Jones and Bartlett, 2013.
8. Commonwealth Knowledge Network. Summary of Discussion on Desalination, 14th -30th October and 1-7 November 2000. Wiley, 2000.
9. Chamie, J. World Population Prospects, Volume III: Analytical Report. United Nations Publications, 2002.
10. Dept. of Economic and Social Affairs. World Urbanization Patterns. United Nations Publications, 2002.
11. Kiem, A. S. Climate Variability and Change. In Shrestha, S., Babel, M. S., Pandey, V. P. (Eds.) Climate Change and Water Resources, p31-69. CRC Press, 2014.
12. Kadi, M. A. Integrated Water Resources Management (IWRM): The International Experience. In Martinez-Santos, P., Aldaya, M. M., Llamas, M. R. (Eds.) Integrated Water Resources Management in the 21st Century: Revisiting the paradigm, p3-17. CRC Press, 2014.
13. Stålnacke, P., Nagothu, S., Quevauviller, P. Developing the Science – Policy Interface to Integrate Water Research and Management. In Sessa, C. (Ed.) Sustainable Water Ecosystems Management in Europe: Bridging the Knowledge of Citizens, Scientists and Policy Makers, p7-15. IWA Publishing, 2012.
14. Knowles, G. J. Funding Sustainable Water Infrastructure Solutions: A Uniform Approach. In Brebbia, C. A., Popov, V. (Eds.) Water Resources Management VI, p15-27. WIT Press, 2011.

15. Heal, K. V. Constructed Wetlands for Wastewater Management. In Booth, C. A., Charlesworth, S. M. (Eds.) Water Resources in the Built Environment: Management Issues and Solutions, p336-350. John Wiley & Sons, 2014.
16. European Commission. Regulation (EC) No 648/2004 of the European Parliament and of the Council of 31 March 2004 on Detergents. Official Journal of the European Union, 2004.
17. European Commission. Directive 2004/35/CE of the European Parliament and of the Council of 21 April 2004 on environmental liability with regard to the prevention and remedying of environmental damage. Official Journal of the European Union, 2004.
18. European Commission. Regulation (EC) No 1907/2006 of the European Parliament and of the Council of 18 December 2006 concerning the Registration, Evaluation, Authorisation and Restriction of Chemicals (REACH), establishing a European Chemicals Agency, amending Directive 1999/45/EC/ and repealing Council Regulation (EEC) No 793/93 and Commission Regulation (EC) No 1488/94 as well as Council Directive 76/769/EEC and Commission Directives 91/155/EEC, 93/67/EEC, 93/105/EC and 2000/21/EC. Official Journal of the European Union, 2006.
19. European Commission. Proposal for a Directive of the European Parliament and of the Council on waste electrical and electronic equipment (WEEE) Recast. Official Journal of the European Union, 2008.
20. Department for Environment, Food and Rural Affairs and the Environment Agency. Contaminants in Soil: Collation of Toxicological Data and Intake Values for Humans. DEFRA, 2002.
21. European Commission. Heavy Metals in Waste. DG ENV. E3, EEC, 2002.
22. SAC Scientific. Survey of Potentially Dangerous Substances in UK Waters. 7/7/201, DoE PECD, 1987.
23. Grimwood, M. J., Dixon E. Assessment Of Risks Posed By List II Metals To Sensitive Marine Areas (SMAs) And Adequacy Of Existing Environmental Quality Standards (EQSs) For SMA Protection. Report to English Nature, 1997.
24. European Commission. DIRECTIVE 2006/118/EC OF THE EUROPEAN PARLIAMENT AND OF THE COUNCIL of 12 December 2006 On The Protection Of Groundwater Against Pollution And Deterioration. Official Journal of the European Union, 2006.
25. European Commission. Directive 2006/7/EC Of The European Parliament And Of The Council Of 15 February 2006 Concerning The Management Of Bathing Water Quality And Repealing Directive 76/160/EEC. Official Journal of the European Union, 2006.
26. World Health Organization. Guidelines for Drinking Water Quality: Surveillance and Control of Community Supplies, Second Ed., Vol III. WHO Publication, 1997.
27. Clark, R. M., Hakim, S. Securing Water and Wastewater Systems: Global Experiences. Springer, 2013.
28. White, R. Water Management: The Decision Making Process. AuthorHouse, 2014.
29. Gleick, P. H. The World's Water Volume 7: The Biennial Report on Freshwater Resources. Island Press, 2012.
30. Keraita, B., Drechsel, P., Klutse, A., Cofie, O. On-farm Treatment Options for Wastewater, Greywater and Fecal Sludge with Special Reference to West Africa, Volume 1 of Resource and Reuse Series. IWMI, 2014.

31. Whipple, D. Electrocoagulation: A Technology for Water Recycle and Wastewater Treatment. Technology and Research Initiative 2006/2007. University of Arizona, 2007.
32. Jahed, E., Khodaparast, M. H. H., Lotfian, F., Khaneghah, A. M. Performance Investigation of Electrochemical Treatment Process on Wastewater of Applicable Decolourisation Resins in Sugar Factories. Sugar Tech 2014; 16 (3): 311-318.
33. Denton M. S., Bostick W. D. New Innovative Electrocoagulation (EC) Treatment Technology for BWR Colloidal Iron Utilizing the Seeding and Filtration Electronically (SAFE™) System. Conference Information: 11th International Conference on Environmental Remediation and Radioactive Waste Management. Proceedings Of The 11th International Conference On Environmental Remediation And Radioactive Waste Management 2009; Part's A and B: 1153-1172.
34. Removal of arsenic, phosphates and ammonia from well water using electrochemical/chemical methods and advanced oxidation: A pilot plant approach. Journal of Environmental Science and Health Part A-Toxic/Hazardous Substances & Environmental Engineering 2014; 49 (9):1007-1014.
35. Rodriguez J., Stopic S., Krause G. Feasibility assessment of electrocoagulation towards a new sustainable wastewater treatment. Environmental Science and Pollution Research 2007; 14 (7): 477-482.
36. Beagles, A. Global Environmental Technology: Electrocoagulation – Science and Applications. ECO International, 2004.
37. Duan, J., Gregory, J. Coagulation by hydrolysing metal salts. Advances in Colloid and Interface Science 2003; 100-102: 475-502.
38. Perng, Y. S., Wang, I. C., Yu, S. T., Chang, A. Y., Shih, C. Y. Pilot treatment of OCC-based paper mill wastewater using pulsed electrocoagulation. Water Quality Research Journal of Canada 2007; 42 (1): 63-71.
39. Vik, E. A., Carlson, D. A., Eikun, A. S., Gjessing, E. T. Electrocoagulation of potable water. Water Research 1984; 18 (11): 1355-1360.
40. Stuart, F. E. Electronic water purification; Progress report on the electronic coagulator – a new device which gives promise of unusually speedy and effective results. Water and Sewage 1946; 84: 24-26.
41. Bonilla, C. F. Possibilities of the electronic coagulator for water treatment. Water and Sewage 1947; 85: 21-45.
42. Holden, W. S. Electrolytic dosing of chemicals. Proceeding of the Society for Water Treatment and Examination 1956; 5: 120.
43. Organisation for Economic Co-operation and Development. Environmental Performance Reviews. OECD Publishing, 2013.
44. Kuhn, A. T. Electrochemistry of Cleaner Environments. Plenam, 1972.
45. Contreras, S., Preber, M., del Rio, A., Soto, M. A., Toha, J., Veloz, A. A highly efficient electrolytic method for micro-organism flocculation from aqueous cultures. Biotechnology and Bioengineering 1981; 23: 1165.
46. Contreras, S., Preber, M., Toha, J. Purification of wastewater by electrolysis. Biotechnology and Bioengineering 1981; 23: 1881.
47. Volkova, A. N., Ivanova, L. V., Yakovlev, V. I. Zhurnal prikladnoi khimii. 1981; 5: 970.
48. Matveenko, A. P., Strizhev, E. F., Volkova, A. N., Ivanova, L. V., Yakovlov, V. I. Electrocoagulation of bio-organic impurities in wastewaters from biochemical processes. Journal of Applied Chemistry USSR 1981; 54: 2258.
49. Kornilov, V. M., Svetlitsky, A. S., Smirnov, O.V. Journal of Applied Chemistry USSR 1980; 53: 401.

50. Pazenko, T. Y., Khalturina, T. I., Kolova, A. F., Rubailo, I. S. Electrocoagulation treatment of oil-containing wastewaters. Journal of Applied Chemistry USSR 1985; 58: 2383.
51. Vasudevan, S., Jayaraj, J., Lakshmi, J., Sozhan, G. Removal of iron from drinking water by electrocoagulation: Adsorption and kinetics studies. Korean Journal of Chemical Engineering 2009; 26 (4): 1058-1064.
52. Harif, T., Khai, M., Adin, A. Electrocoagulation versus chemical coagulation: Coagulation/flocculation mechanisms and resulting floc characteristics. Water Research 2012; 46 (10): 3177-3188.
53. Woytowich D. L., Dalrymple C. W., Britton M. G. Electrocoagulation (CURE) treatment of ship bilgewater for the U. S. Coast Guard in Alaska. Marine Technology Society Journal 1993; 27 (1): 62-67.
54. Moayedi, H., Kazemian, S., Vakili, A. H., Ghareh, S., Nazir, R. Coagulation of the suspended organic colloids using the electroflocculation technique. Journal of Dispersion Science and Technology 2014; 35 (2): 273-282.
55. Zhang, S., Zhang, J, Fong, W., Li, F., Cheng, X. Removal of phosphate from landscape water using an electrocoagulation process powered directly by photovoltaic solar modules. Solar Energy Materials and Solar Cells 2013; 117: 73-80.
56. Rajeshwar, K., Ibanez, J., Swain, G. M. Electrochemistry and the environment. Journal of Applied Electrochemistry 1994; 24: 1077-1090.
57. Fisher, A. C. Electrode Dynamics. Oxford Chemistry Primer, 1996.
58. Haydar, S., Aziz, J. A. Coagulation-flocculation studies of tannery wastewater using combination of alum with cationic and anionic polymers. Journal of Hazardous Materials 2009; 168 (2-3): 1035-1040.
59. Yan, H.-Y., Xiao, M., Zhang, Z.-Z., Li, J.-Q., Shi, B.-Q. Remediation of oilfield wastewater produced from alkaline/surfactant/polymer flooding by using a combination of coagulation and bioaugmentation. Petroleum Science and Technology 2014; 32 (13): 1521-1528.
60. Parga, J. R., Vazquez, V., Gonzalez, G., Cisneros, M. M. Thermodynamic studies of chromium adsorption on iron species generated by electrocoagulation. Chemical Engineering and Technology 2010; 33 (10): 1582-1590.
61. Zaroual, Z., Chaair, H., Essadki, A. H., El Ass, K., Azzi, M. Optimizing the removal of trivalent chromium by electrocoagulation using experimental design. Chemical Engineering Journal 2009; 148 (2 – 3): 488-495.
62. Koparal, A. S., Yildiz, Y. Ş., Keskinler, B., Demircioğlu, N. Effect of initial pH on the removal of humic substances from wastewater by electrocoagulation. Separation and Purification Technology 2008; 59 (2): 175-182.
63. Varank, G., Erkan, H., Yazycy, S., Demir, A., Engin, C. Electrocoagulation of tannery wastewater using monopolar electrodes: process optimization by response surface methodology. International Journal of Environmental Research 2014; 8 (1): 165-180.
64. Ibrahim, D. S., Lathalakshmi, M., Muthukrishnaraj, A., Balasubramanian, N. An alternative treatment process for upgrade of petroleum refinery wastewater using electrocoagulation. Petroleum Science 2013; 10 (3): 421-430.
65. Sadeddin, K., Naser, A., Firas, A. Removal of turbidity an suspended solids by electro-coagulation to improve feed water quality of reverse osmosis plant. Desalination 2011; 268 (1-3): 204-207.

66. Nouri, J., Mahvi, A. H., Bazrafshan, E. Application of electrocoagulation process in removal of zinc and copper from aqueous solutions by aluminium electrodes. International Journal of Environmental Research 2010; 4: 201-208.
67. Keerthi, V. V., Balasubramanian, N. Removal of heavy metals by hybrid electrocoagulation and microfiltration processes. Environmental Technology 2013; 34 (20): 2901-2906.
68. Kabuk, H. A., Avsar, Y., Ilhan, F., Ulucan, K. Comparison of pH adjustment and electrocoagulation processes on treatability of metal plating wastewater. Separation Science and Technology 2014; 49 (4): 613-618.
69. Karhu, M., Kuokkanen, V., Kuokkanen, T., Rämö, J. Bench scale electrocoagulation studies of bio oil-in-water and synthetic oil-in-water emulsions. Separation and Purification Technology 2012; 96: 296-305.
70. Saeedi, M., Khalvati-Fahlyani, A. Treatment of oily wastewater of a gas refinery by electrocoagulation using aluminium electrodes. Water Environment Research 2011; 83 (3): 256-264.
71. Tsai, T., Lin, S. T., Shue, Y. C., Su, P. L. Electrolysis of soluble organic matter in leachate from landfills. Water Research 1997; 31: 3073-3081.
72. Beck, E. C., Giannini, A. P., Ramirez, E. R. Electrocoagulation clarifies food wastewater. Food Technology 1974; 22: 18-19.
73. Khandegar, V., Saroha, A. K. Electrocoagulation for the treatment of textile industry effluent – A review. Journal of Environmental Management 2013; 128: 949-963.
74. Tünay, O., Şimşeker, M., Kabdaşlı, I., Ölmez-Hancı, T. Abatements of reduced sulphur compounds, colour and organic matter from indigo dyeing effluents by electrocoagulation. Environmental Technology 2014; 35 (13): 1577-1588.
75. Tyagi, N., Mathur, S., Dinesh, K. Electrocoagulation process for textile wastewater treatment in continuous upflow reactor. Journal of Scientific & Industrial Research 2014; 73 (3): 195-198.
76. Bansal, S., Kushwaha, J. P., Sangal, V. K. Electrochemical treatment of reactive Black 5 textile wastewater: optimization, kinetics, and disposal study. Water Environment Research 2013; 85 (12) 2294-2306.
77. Phalakornkule, C., Polgumhang, S., Tongdaung, W., Karakat, B., Nuyut, T. Electrocoagulation of blue reactive, red disperse and mixed dyes, and application in treating textile effluent. Journal of Environmental Management 2010; 91 (4): 918-926.
78. Balasubramanian, N., Kojima, T., Srinivasakannan, C. Arsenic removal through electrocoagulation: kinetic and statistical modelling. Chemical Engineering Journal 2009; 155 (1-2): 76-82.
79. Treatment of petrochemical wastewater containing phenolic compounds by electrocoagulation using a fixed bed electrochemical reactor. International Journal of Electrochemical Science 2013; 8 (1): 1534-1550.
80. Chiang, L. C., Chang, J. E., Tseng, S. C. Electrochemical oxidation pre-treatment of refractory organic pollutants. Water Science Technology 1997; 36 (2 – 3): 123-130.
81. Sahu, O., Mazumdar, B., Chaudhari, P. K. Treatment of wastewater by electrocoagulation: a review. Environmental Science and Pollution Research 2014; 21 (4): 2397-2413.
82. Dubrawski, K. L., Du, C., Mohseni, M. General potential-current model and validation for electrocoagulation. Electrochimica Acta 2014; 129: 187-195.
83. Dubrawski, K., Mohseni, M. Standardizing electrocoagulation reactor design: iron electrodes for NOM removal. Chemosphere 2013; 91 (1): 55-60.

84. Isa, M. H., Ezechi, E. H., Ahmed, Z., Magram, S. F., Kutty, S. R. M. Boron removal by electrocoagulation and recover. Water Research 2014; 51: 113-123.
85. Kara, S., Gürbulak, E., Eyvaz, M., Yüksel, E. Treatment of winery wastewater by electrocoagulation process. Desalination and Water Treatment 2013; 51 (28-30): 5421-5429.
86. Bayar S., Tildiz, Y., Yilmaz, A., Koparal, A. S. The effect of initial pH on treatment of poultry slaughterhouse wastewater by electrocoagulation. Desalination and Water Treatment 2014; 52 (16-18): 3027-3053.
87. Sangal, V. K., Mishra, I. M., Kushwaha, J. P. Electrocoagulation of soluble oil wastewater: parametric and kinetic study. Separation Science and Technology 2013; 48 (7): 1062-1072.
88. Ahmadi, S., Sardari, E., Javadian, H. R., Katal, R., Sefti, M. V. Removal of oil form biodiesel wastewater by electrocoagulation method. Korean Journal of Chemical Engineering 2013; 30 (3): 634-641.
89. Mostefa, N. M., Tir, M. Coupling flocculation with electroflotation for waste oil/water emulsion treatment: optimisation of the operating conditions. Desalination 2004; 161: 115-121.
90. Un, U. T., Aytac, E. Electrocoagulation in a packed bed reactor – complete treatment of colour and COD from real textile wastewater. Journal of Environmental Management 2013; 123: 113-119.
91. Yavuz, Y., Shahbazi, R., Koparal, A. S., Öğütveren, Ü. B. Treatment of Basic Red 29 dye solution using iron-alunimium electrode pairs by electrocoagulation and electro-Fenton methods. Environmental Science and Pollution Research 2014; 21 (14): 860-8609.
92. Bhatnagar, R., Joshi, H., Mall, I. D., Srivastava, V. C. Electrocoagulation oxidation of textile industry wastewater by graphite electrodes. Toxic/Hazardous Substances and Environmental Engineering 2014; 49 (8): 955-966.
93. de Mello Ferreira, A., Marchesiello, M., Thivel, P.-X. Removal of copper, zinc and nickel present in natural water containing Ca2+ and HC03– ions in electrocoagulation. Separation and Purification Technology 2013; 107: 109-117.
94. Hernández, M. C., Barletta, L., Dogliotti, M. B., Russo, N., Fino, D., Spinelli, P. Heavy metal removal by means of electrocoagulation using aluminum electrodes for drinking water purification. Journal of Applied Electrochemistry 2012; 42 (9): 809-817.
95. Aji, B. A., Yavuz, Y., Koparal, A. S. Electrocoagulation of heavy metals containing model wastewater using monopolar iron electrodes. Separation and Purification Technology 2012; 86: 248-254.
96. Larue, O., Vorobiev, E., Vu, C., Durand, B. Electrocoagulation and coagulation by iron of latex particles in aqueous suspensions. Separation and Purification Technology 2003; 31 (2): 177-192.
97. Hutnan, M., Drtil, M., Kalina, A. Anaerobic stabilisation of sludge produced during municipal wastewater treatment by electrocoagulation. Journal of Hazardous Materials 2005; 131 (1-3): 163-169.
98. Kliaugaite, D., Yasadi, K., Euverink, G., Bijmans, M. F. M., Racys, V. Electrochemical removal and recovery of humic-like substances from wastewater. Separation and Purification Technology 2013; 108: 37-44.
99. Lakshmi, J., Sozhan, G., Subramanyan, V. Recovery of hydrogen and removal of nitrate from water by electrocoagulation process. Environmental Science and Pollution Research 2013: 20 (4); 2184-2192.

100. Emamjomeh, M. M. Sivakumar, M., Varyani, A. S. Analysis and the understanding of fluoride removal mechanisms by an electrocoagulation/flocation (ECF) process. Desalination 2011; 275 (1-3): 102-106.
101. Alfafara, C. G., Nakano, K., Nomura, N., Igarashi, T., Matsumura, M. Operating and scale-up factors for the electrolytic removal of algae from eutrophied lake water. Journal of Chemical Technology and Biotechnology 2002; 77: 871-876.
102. Bancroft, J., Dalrymple, I. M. Environmental Protection Bulletin 1996; (45): 24-34.
103. Pletcher, D. Metal ion removal from effluents. Watts New 1996; 2 (3).
104. Joint Service Pollution Opportunity Handbook. Electrodialysis Technology for Anodizing Bath Solutions. Joint Servie P2 Technical Library, 2006.
105. Malpass, G. The removal of Ni(II) from model waste solutions by electrochemical methods. MSc. Thesis, University of Wales, Bangor, 1999.
106. Jiang, T., Chollier-Brym, M. J., Dubé, G., Lasia, A., Brisard, G. M. Electrodeposition of aluminium from ionic liquids: Part I electrodeposition and surface morphology of aluminium from aluminium chloride ($AlCl_3$)–1-ethyl-3-methylimidazolium chloride ([EMIm]Cl) ionic liquids Surfaces and Coatings Technology 2006; 201: 1-9.
107. Cecille, L., Casarci, M., Pietrelli, L. New separation chemistry techniques for radioactive waste and other specific applications. Cambridge University Press, 1991.
108. Peters, R. W., Ku, Y. AIChE Symposium Series: Separation of heavy metals and other trace contaminants, 1985.
109. Ýslamoglu, S., Yýlmaz, L. Removal and recovery of heavy metals from industrial waste streams by means of a hybrid-precipitation and polymer enhanced ultrafiltration. Institute of Chemical Engineers Technical Program, 2006.
110. Mulder, M. Basic Principles of Membrane Technology, 1st Ed. Kluwer Academic Publishers, 1991.
111. Xinchao, W., Viadero Jr, R. C., Buzby, K. M.. Recovery of iron and aluminum from acid mine drainage by selective precipitation. Environmental Engineering Science 2005; 22 (6): 745-755.
112. Jenke, D. R., Diebold, F. E. Recovery of valuable metals from acid mine drainage by selective titration. Water Research 1983; 17 (11): 1585-1590.
113. Meehan, J., Simon, H., Admassu, W., Crawford, R. Study on apatite usage in remediation of Rocky Flats heavy metal contaminated pond sludge. PhD Thesis, University of Idaho, 1995,
114. Ma, Q. Y., Logan, T. J., Traina, S. J., Ryan, J. A. Effects of NO^{3-}, Cl^-, F^-, SO_4^{2-}, and CO_3^{2-} on Pb^{2+} immobilization by hydroxyapatite. Environmental Science Technology 1994; 28 (3): 408-418.
115. Jeanjean, J., Rouchard, J. C., Tran, L., Federoff, M. Sorption of uranium and other heavy metals on hydroxyapatite. Journal of Radioanalytical and Nuclear Chemistry 1995; 201 (6): 529-539.
116. Navratil, J. D. Metal recovery and waste processing using ferrites. EPD Congress '90, D.R. Gaskell (Ed.) The Minerals, Metals and Materials Society, Kensington, NSW, Australia, 125-128, 1990.
117. Santos-Yabe, M. J., de Oliveira, E. Heavy metals removal in industrial effluents by sequential adsorbent treatment. Advances in Environmental Research 2003; 7 (2): 263-272.
118. Luiz, C. A., Oliveira, R. V., Rios, R. A., Fabris, J. D., Garg, V., Sapag, K., Lago, R. M. Activated carbon/iron oxide magnetic composites for the adsorption of contaminants in water. Carbon 2002; 40: 2177-2183.

119. Booker, N. A., Priestley, K. D., Ritchie, C. D., Sudarmana, D. L., Woods, M. A. Sewage clarification with magnetic particles. Water Science and Technology 1991; 23 (7-9): 1703-1712.
120. Sing, K. S. Technology Profile: Ground Water Monitor 1994: 60-76.
121. Safarik, I., Safarikova, M., Buricova, V. Magnetic separations in biosciences and biotechnology. Collection of Czechoslovak Chemical Communications 1995; 60: 1448-1456.
122. Matson, P. and Mark, H. B. Activated carbon: surface chemistry and adsorption from solution. Dekker, 1971.
123. Martin-Gullon, I., Font, R. Dynamic pesticide removal with activated carbon fibres. Water Research 2001; 35 (2): 516-520.
124. Benito, Y., Ruiz, M. L. Reverse osmosis applied to metal finishing wastewater. Desalination 2002; 142: 229-234.
125. Sağ, Y., Nourbakhsh, M., Aksu, Z., Kutsal, T. Comparison of Ca-alginate and immobilized *Z. ramigera* as sorbents for copper(II) removal. Process Biochemistry 1995; 30 (2): 175-181.
126. Torres, F. The bioleaching of different sulphide concentrates using thermophilic bacteria. Metallurgical and Materials Transactions B – Process Metallurgy and Materials Processing Science 1995; 26 (3): 455-465.
127. Altundogan H. S., Tumen, F. Metal recovery from copper converter slag by roasting with ferric sulphate. Hydrometallurgy 1997; 44 (1-2): 261-267.
128. Jiang, J. – Q., Graham, N., André, C., Kelsall, G. H., Brandon, N. Laboratory study of electro-coagulation flotation for water treatment. Water Research 2002; 36: 4064-4078.
129. Vlyssides, A. G., Israilides, C. J. Electrochemical oxidation of a textile dye and finishing wastewater using a Pt/Ti electrode. Journal of Environmental Science and Health 1998; 33 (5): 847-862.
130. Szpyrkowicz, L., Naumczyk, J., Zilio-Grandi, F. Electrochemical treatment of tannery wastewater using Ti/Pt and Ti/Pt/Ir electrodes. Water Research 1995; 29 (2): 517-524.
131. Cossu, R., Polcaro, A. M., Lavagnolo, M. C., Mascia, M., Palmas, S., Renoldi, F. Electrochemical treatment of landfill leachate: oxidation at Ti/PbO_2 and Ti/SnO_2 anodes. Environmental Science and Technology 1998; 32: 3570-3573.

Chapter 2

Fundamentals of Electrochemical Treatment

2 Fundamentals of Electrochemical Treatment

2.1 Introduction

To fully exploit the potential of EC as a wastewater treatment technology, a quantitative understanding of the interactions occurring between the fundamental electrochemical process mechanisms is required. However, in depth research aimed at providing such a quantitative understanding of EC's pollutant removal mechanisms has only begun recently.[132,133,134,135,136,137,138] There has been minimal effort to better understand the processes that could provide design parameters to optimise the performance of EC systems. Thus, this chapter will begin by reviewing the available literature on EC and its applications, as well as introducing a structured approach to highlight commonalities and differences between the works reported.

2.2 State of the Art

2.2.1 Overview

Electrocoagulation is a process consisting of creating metallic hydroxide flocs within the wastewater by electrodissolution of soluble anodes, primarily fabricated from iron or aluminium.[139] With traditional chemical coagulation, metal salts such as ferric chloride or Alum ($Al_2(SO_4)_3.18H_2O$), polymers or poly-electrolytes are added to wastewater which induces precipitation of pollutants.[140,141] In EC, coagulation and precipitation are not conducted by delivering chemicals to the system but *via* electrodes in an electrochemical cell (reactor).[142]

2.2.2 Theory

Electrocoagulation is a complex process involving many chemical and physical phenomena operating simultaneously that use consumable electrodes to supply metal ions into a wastewater stream. In an EC process the coagulating ions are produced in situ *via* three successive stages;[143] (i) coagulant formation by electrolytic oxidation of the sacrificial anode(s), (ii) destabilisation of the pollutants, particulate suspension and breaking of emulsions, and (iii) aggregation of the destabilised phases to form flocs.

The destabilisation mechanism of the pollutants, particulates and breaking of emulsions can be described as follows:

- Compression of the diffuse double layer around the charged species by the interactions of ions generated by oxidation of the sacrificial anode.
- Charge neutralisation of the ionic species present in wastewater by counter-ions produced by the electrochemical dissolution of the sacrificial anode. These counter-ions reduce the electrostatic inter-particle repulsion to the extent that van der Waal's forces attraction predominates, thus causing coagulation. A zero net charge results in the process.
- Floc formation; the floc formed as a result of coagulation creates a sludge blanket that entraps and bridges colloidal particles still remaining in the aqueous medium.

A floc can be described as a highly porous and loosely-connected aggregate made up of many primary particles. Floc size and structure are the main parameters that influence removal efficiency rates.[144]

The solid oxides, hydroxides and oxyhydroxides of floc complexes have strong adsorptive capacities and provide active surfaces for the adsorption of the polluting species. Electrocoagulation has been successfully employed in removing a host of pollutants from a variety of industrial effluents and is the reason for both its on-going industrial attraction, and its inherent complexity (due to the wide range of possible pollutant removal mechanisms).

In an EC experiment, the electrode assemblies are connected to an external direct current (DC) power supply source and a potential is applied to the electrodes. This causes two separate reactions.

At the anodes in an EC reactor, metallic ions are released into solution through the electrolytic oxidation of the sacrificial electrodes.[145] The produced ions immediately hydrolyse to form monomeric hydroxide ions and polymeric hydroxide complexes, the latter being excellent coagulating agents, depending on pH of the solution.[146] These highly charged cationic polymeric hydroxides destabilise the negatively charged colloidal particles carried towards the anodes by electrophoretic motion allowing for their

aggregation and formation of floc.[147,148] The consumable anodes are used to continuously produce polymeric hydroxides in the vicinity of the anode.

In a parallel reaction, water is also subjected to electrolysis producing oxygen bubbles at the anode and hydrogen bubbles at the cathode.[149] Accompanying electrochemical reactions are dependent on species present in the water and usually evolve electrolytic gases. The coagulant's delivery and its nature influence the coagulation and separation processes by its speciation, removal path and associated electrolytic gases.

2.2.3 Methods of Coagulation

The objective of coagulation is to destabilise the suspension by coating the negatively charged surface of colloidal particles with positively charged species. Thus, the coagulant is used to reduce any repulsive forces thereby lowering the energy barrier and enabling particles to agglomerate.

Pollutant ions are often electroprecipitated out of solution whilst charged suspended solids are adsorbed onto the charged coagulant. As such, pollutants present in wastewater are therefore treated either by chemical reactions and precipitation, or by physical and chemical attachment to colloidal materials generated by the anode erosion. Two mechanisms of charge neutralisation and sweep-floc coagulation are important in electrochemical water treatment.[150,151,152]

Charge Neutralisation

Positively charged polymeric hydroxides formed through the electrodissolution of the anode adsorb onto the surfaces of colloidal particles that are typically negative in charge.[153] A resultant reduction of the net charge of the newly formed complex occurs as the cationic polymeric hydroxide decreases the repulsive potential of the electrical double layer of the pollutant species.[154,155,156] As such, any inter-particle electrostatic repulsion is reduced to a point whereby van der Waal's forces can predominate, in particular induced dipole-dipole forces (London Forces).[157]

The Deryaguin, Landau and Verwey, Overbeek (DLVO) theory describes the interactions between these forces of attraction and repulsion.[158,159] It combines the effects of van der Waal's attraction and the electrostatic repulsion due to the double layer of counter-ions.

In this new reduced charged state, the newly formed non-polar complexes are attracted to each other due to quantum mechanical theory of dispersion forces.[160,161,162] The electron densities surrounding the molecules probabilistically travel about the molecule leaving certain areas less charged than other areas momentarily producing a multipole. This multipole can interact and cause other multipoles to be created in fellow non-polar molecules resulting in induced polarity. This induced polarity between the neutralised pollutant particles binds them together forming floc.[163]

Sweep-floc Coagulation

At sufficiently high coagulant dosage, and dependent upon the solubility of the metal hydroxide, when the amount of ions added to wastewater exceeds the solubility of the metal hydroxide, formation of the amorphous metal hydroxide precipitate takes place.[164] These precipitates can physically sweep the colloidal particles from suspension by enmeshment. This mechanism is called sweep-floc coagulation and since it does not involve charge reversal, it is more popularly used in water treatment.[165]

2.2.4 Electrode Reactions

A simple electrocoagulation reactor can consist of one anode and one cathode as illustrated in Figure 2.1 on the following page. The electrodes are connected to a DC power supply and a potential is applied across the electrodes. As current passes through the metal electrodes, the anode material undergoes oxidation, while the cathode is subjected to reduction or reductive electrodeposition of elemental metals.[166,167,168,169,170]

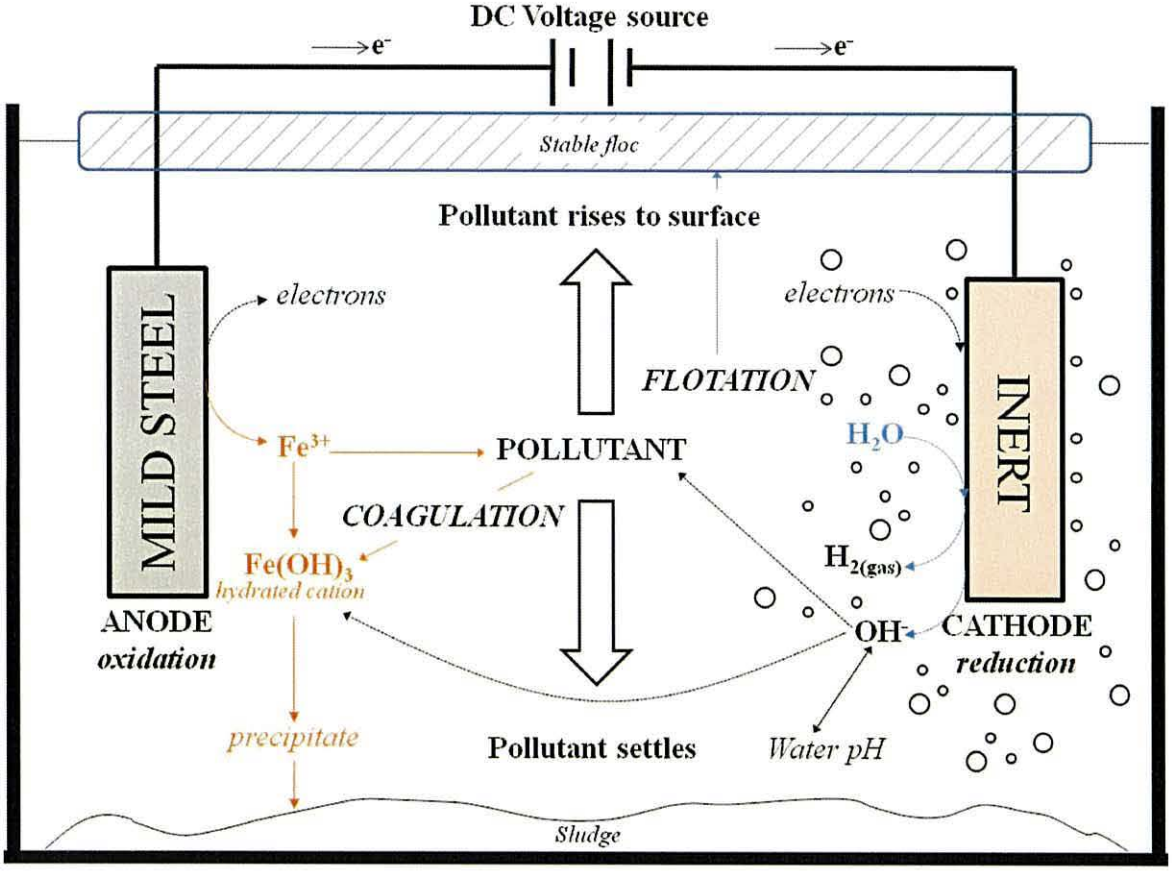

Figure 2.1. Schema of a bench-scale two-electrode electrocoagulation cell and associated processes.

The electrochemical reactions occurring in an EC cell are shown in Equation's 2 – 8 below.[171] Iron, a commonly used anode material is used as the exemplar. Equations illustrating the electrodissolution of aluminium are shown in Appendix I. Equation 2 represents the anodic electrodissolution of iron.

$$Fe_{(s)} \rightarrow Fe^{2+}_{(aq)} + 2e^{-} \qquad \textbf{Equation 2}$$

Equation 3 shows how oxygen evolution occurs at the anode:

$$2H_2O_{(l)} \rightarrow 4H^{+}_{(aq)} + O_{2(g)} + 4e^{-} \qquad \textbf{Equation 3}$$

At the cathode, elemental electrodeposition can occur as shown in Equation 4:

$$Fe^{2+}_{(aq)} + 2e^{-} \rightarrow Fe_{(s)} \qquad \textbf{Equation 4}$$

Simultaneously, hydrogen gas is also generated at the cathode. Under alkaline or neutral pH conditions, hydrogen is best produced *via* Equation 5 on the following page:

$$2H_2O_{(l)} + 2e^- \rightarrow 2OH^-_{(aq)} + H_{2(g)}$$ **Equation 5**

Under acidic pH conditions, Equation 6 shows best the evolution of hydrogen at the cathode:

$$2H^+_{(aq)} + 2e^- \rightarrow H_{2(g)}$$ **Equation 6**

Following on from this, there are two mechanisms for the production of metal hydroxides that have been proposed within the literature.[172] Equation's 7 and 8 show how, once the ferrous ions are in solution (*via* Equation 2), they complex with hydroxide ions produced at the cathode as the by-product of Equation 5:

Mechanism I.

$$Fe^{2+}_{(aq)} + 2H_2O_{(l)} \rightarrow Fe(OH)_{2(s)} + H_{2(g)}$$ **Equation 7**

Mechanism II. (In the presence of O_2, dissolved Fe^{2+} can further oxidise to insoluble $Fe(OH)_3$)

$$2Fe^{2+}_{(aq)} + 5H_2O_{(l)} + \tfrac{1}{2}O_{2(g)} \rightarrow 2Fe(OH)_{3(s)} + 4H^+_{(aq)}$$ **Equation 8**

Consequently, with Mechanism II, the protons can be directly reduced to H_2 gas at the cathode as shown by Equation 9:

$$8H^+_{(aq)} + 8e^- \rightarrow 4H_{2(g)}$$ **Equation 9**

From Equation's 7 and 8, it is clear that iron ions can exist in either a ferrous state, where the iron carries two positive charges, or in a ferric state, whereby each ion carries three positive charges. This is due to ferrous iron undergoing further hydrolysis.

The overall state of iron in water depends on pH and the redox potential. By increasing the pH, iron in solution in the form Fe^{2+} or Fe^{3+} will hydrolyse to form precipitates.[173] As such, ferrous ions generated by the electrochemical oxidation of the anodic electrode will therefore form monomeric ions, $Fe(OH)^+$, $Fe(OH)_2$ and $Fe(OH)_4^{2-}$ between pH 7 – 14.[174] Some ferrous ions will oxidise to ferric ions and these will hydrolyse to form monomeric $Fe(OH)_3$ (referred to as bernalite) and polymeric hydroxyl complexes, principally $Fe(H_2O)_6^{3+}$, $Fe(H_2O)_5(OH)^{2+}$, $Fe(H_2O)_4(OH)_2^+$, $Fe(H_2O)_8(OH)_2^{4+}$ and $Fe(2(H_2O)_6(OH)_4^{4+}$

depending on pH of the effluent solution.[175,176,177,178,179,180,181] These nascent Fe^{+} hydroxides, polyhydroxides and polyhydroxymetallic complexes have very strong affinity for suspended colloids and oppositely charged ions resulting in very good coagulation.

2.2.5 Theoretical Estimates of Anodic Dissolution

A derivation of Faraday's law may be used to calculate the amount of iron released into solution following electrolytic oxidation of the anode material. The amount of iron dissolved is dependent on operating current passing through the electrolyte and the operational run time.

Faraday's law (Equation 10) relates the mass of iron electrolytically generated going into solution, with current input and total run time of the operation:

$$w = \frac{itM}{zF} \qquad \textbf{Equation 10}$$

Where w is the iron dissolved (g of M/cm^2); i is the current input (A); t is the contact time (s); M is the molecular mass of iron (M= 55.85); z is the number of electrons involved in the redox reaction (z = 2); and F is Faraday's constant (96,486 C/mol).

Using this equation, the amount of iron coagulant inputted into solution may theoretically be calculated and generally there is agreement between the calculated amount of electro-oxidised material going into solution as a result of a defined quantum of current passing through the solution, and the experimental amount determined through photometric or other analysis.

2.3 Electrocoagulation Water Treatment

Electrochemical methods are uniquely capable of removing an array of pollutants from a variety of industrial effluents and wastewaters. From the literature, EC has been demonstrated to show its capability in removing pollutants ranging from: heavy metals[182] and suspended solids;[183] to petroleum products[184] and colour from dye-containing solutions.[185,186] Although electrochemical technology has been practiced for most of the twentieth century, in recent years, it has ascended in importance with progress made into

the understanding of the electrochemical processes at work at electrode interfaces, and due to the increase in environmental restrictions on effluent wastewater.

Electrochemical techniques such as; electrocoagulation, electrochemical ion exchange,[187] electrodecantation,[188,189,190] electrodialysis,[191,192,193,194] electrokinetic remediation[195,196,197,198] and electroflotation,[199,200,201,202] offer the possibility of treating wastewater without the need for voluminous amounts of chemicals, if any. Compact and robust instrumentation development has also meant that the above mentioned electrochemical techniques have the potential to replace existing, sophisticated processes that require: (i) large volumes and/or number of chemicals, and (ii) massive containers that are typical of wastewater treatment sites. Figure 2.2 demonstrates the substitution of EC equipment for conventional wastewater treatment plants.

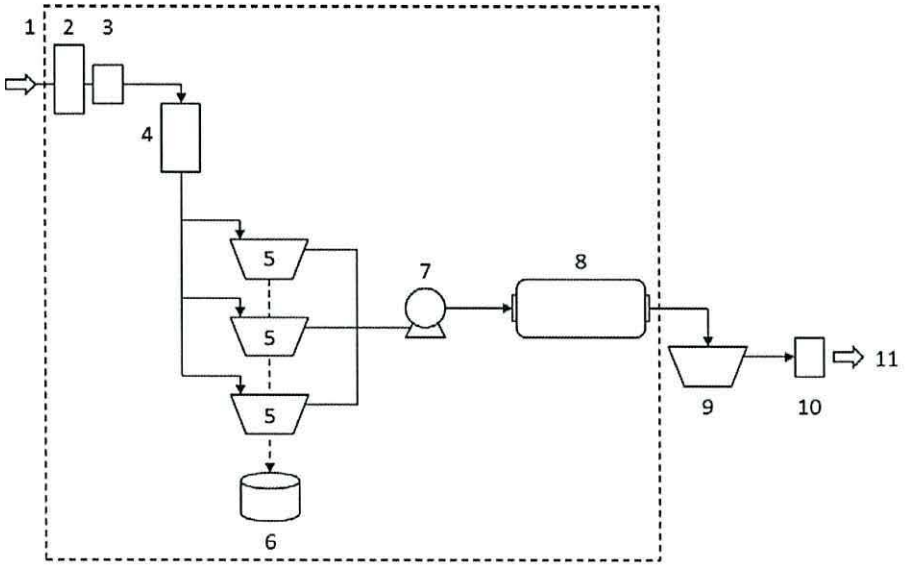

Figure 2.2. Schematic flow-diagram of a typical wastewater treatment plant and its processes that can be replaced by EC (shown in the dashed line box): 1 – raw water inlet; 2 – drum screen; 3 – grit removal; 4 – flow distribution; 5 – primary settlers; 6 – sludge treatment; 7 – pump; 8 – oxidation ditch; 9 – clarifier; 10– chlorination; 11 – final effluent outlet.

As a consequence, a very simple replacement with EC technology could prevent economically unfeasible capital costs. Moreover, the electrochemical technology available today is based on several different concepts in the electrochemistry field. The three basic sciences of electrochemistry, flotation and coagulation can be identified from the literature that interrelate with each other.[203] These independent scientific disciplines can be conceptualised in Figure 2.3 on the following page in which the amalgamation of all three sciences results in electrochemical technology formulated and developed for wastewater treatment.

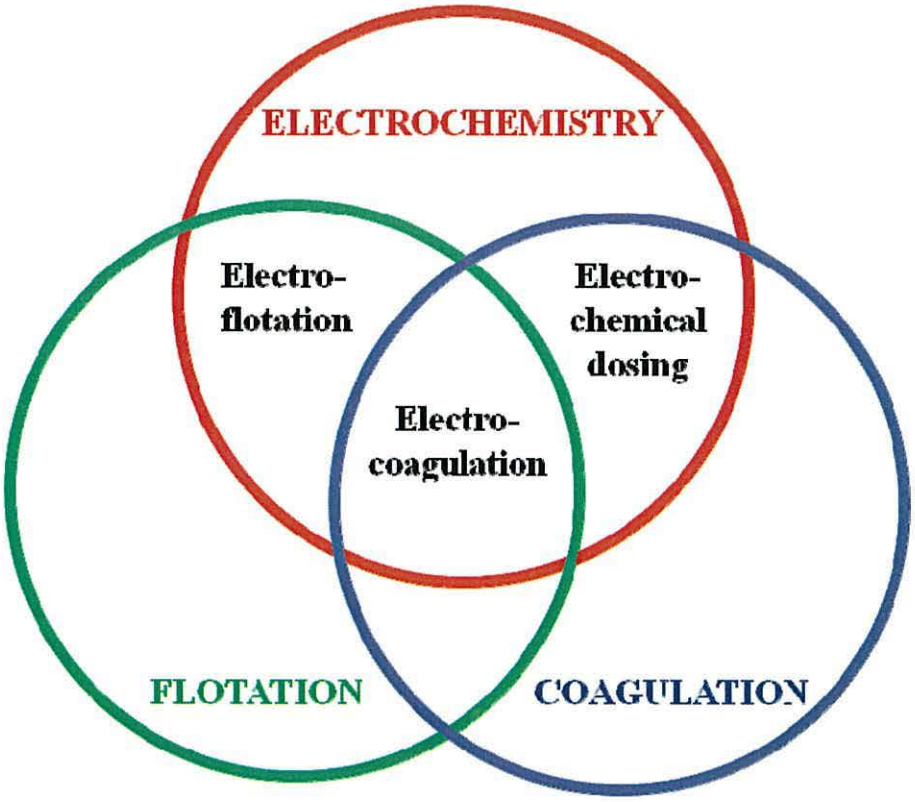

Figure 2.3. Venn diagram of the main scientific fields underlining electrochemical based wastewater treatment techniques.

2.4 Electrochemical Factors Affecting Floc Generation

Electrocoagulation can be considered as an accelerated corrosion process.[204] Its mechanisms are yet to be clearly understood as there appears to be a dearth in the fundamental understanding of the electrochemical factors, that influence EC and that can lead to improved floc generation and effective removal of ionic species and compounds from wastewater.

Despite EC technology having been used extensively in the last decade, the available literature reveals only a limited, systematic approach to quantifying the various electrochemical factors that inter-react with each other. Very little work has been done on developing a holistic approach.[205] This may be due to a lack of sufficient quantitative understanding of the many interactions that occur during EC and the ability to predict the relative importance of these interactions for a given polluted water body. The pollutant-centred studies populating the literature very often prove the feasibility of EC as an effective wastewater treatment provider, but inexorably fail to further exploit its potential by exploring the fundamental mechanism at work and being incorporated within a broader-based understanding of the technology.[206]

As such, the focus of this chapter is to summarise the variables that have been identified within the literature as influential in contributing to EC floc generation. The key parameters listed also serve a dual purpose as they are recognised factors that have a significant impact on EC performance overall as a wastewater treatment application. The variables have been divided into chemical and process parameter sub-sections.

2.4.1 Process Parameters

There has been a range of laboratory, pilot and industrial scale EC unit's produced.[207] Electrocoagulation technology has often been integrated with secondary wastewater treatment equipment such as dissolved air flotation (DAF) units[208], filtration[209] and reverse osmosis (RO).[210]

Although discussing the intricacies of the different designs of EC reactors that are reported within the literature is of some importance, to do so would go beyond the scope of this chapter and the reader is directed to Holt *et al.*, 2004[211] for a more comprehensive review of reactor design.

Suffice to say, for this report; the design of EC reactors influences its operation and efficiency to a degree. Thus, included in the following sub-paragraphs are the main process parameters related to EC configuration that are of utmost importance in floc generation.

Current Density

Current density is a function of applied cell current and effective surface area of anodic electrodes. Reactor operation and process parameters cited in the literature vary enormously and anodic current densities have been reported anywhere from 0.001 – 200 mA/cm^2.[203] Current density has been identified by many authors as the key operational parameter influencing the amount of anodic material electro-dissolved into a wastewater stream. Thus, its impact on the amount of coagulum formed is directly related to the removal efficiency of pollutant species.[153] Other authors however, have reported that it has no significant role on pollutant removal.[212]

Current Density and Pollutant Removal Path

Operational current density is critical in batch EC (treatment of a fixed wastewater volume per treatment cycle) as it is the only electrochemical parameter that is controlled directly. It determines both the rate of electrochemical coagulant dosage supplied and electrolytic bubble density production. The latter determines whether flocculated particles either rise to the surface of a treated water column, or sink to the bottom as a consequence of bubble attachment to the flocs produced. Current density also impacts secondarily on solution mixing and mass transfer at electrodes.

Work reported has revealed that aggregated pollutant settlement is favoured at low current densities (below 0.3 mA/cm^2) where fewer bubbles are produced at the cathode as the by-product of equation 4. Consequently, due to the limitation in bubble generation, there is a decrease in solution mixing and material uplift. As such, the favoured pollutant removal path is electroprecipitation (EP). Conversely, at higher current densities (greater than 2.7 mA/cm^2) flotation is favoured due to a higher bubble density rate and coagulant dosage. This forces precipitated floc to rise to the surface as bubbles attach themselves to the agglomerated particles.[211] At this point electroflotation (EF) is predominantly the favoured removal path of the pollutant.

Electrode Material

An EC reactor is an electrochemical cell and thus its performance is directly related to the operational state of its electrodes. As a result, choice of electrode material has been highlighted as another process parameter influencing EC floc generation. The material chosen will affect cell voltage; as different oxidation potentials exist for different materials and can, in turn, affect the separation achieved.[213] More fundamentally, the choice of anode material also determines the cation introduced into solution.

Electrodes used vary in material, design and mode of operation ranging from simple plate electrodes through to raschig rings and the use of pellets in a packed bed style EC reactor.[214] Inert (non-sacrificial) electrodes such as platinum, dimensionally stable alloys (DSAs) and titanium have all been observed in removing contaminants from solution and initiating coagulation.[215]

Direct and indirect oxidation of organics present in wastewater[216] and the removal of FOGs, suspended solids and chemical oxygen demand (COD) from restaurant wastewater have also been documented using various metal/metal oxide-coated titanium electrodes.[135] However, the high cost of these materials and the large consumption of the electrodes has limited their use to small applications only.[217]

Moreover, the majority of work undertaken within the literature has been carried out using aluminium and iron derived electrodes; primarily mild and stainless steel. A host of authors have reported excellent floc formation and associated pollutant removal efficiencies using either material as the corrodible anode, with material selection predominantly based on the pollutant of interest to be removed from the aqueous media, cost of materials, low oxidation potential and inertness towards the system.[154,218] Other authors have trialled both aluminium and iron plate electrodes independently to assess which material enhances pollutant removal.[219] In work carried out in removing colour from dye-containing solutions, three factors were determined to influence the choice of using either iron or aluminium electrodes; (i) initial pollutant concentration, (ii) pollutant type, (iii) stirring rate.[185]

Work has also been reported in investigating the relationship between size of cations introduced into solution and removal efficiency of organic waste. The size of the cation produced, 10 – 30 μm for Fe^{3+} compared to 0.05 – 1 μm for Al^{3+}, was suggested to contribute to the higher efficiency of iron electrodes.[220] However, this assumption was purely based on a single experiment using chemical absorption of oxygen as the only measurement. Furthermore, other authors have rebutted this observing that EC processes at aluminium surfaces are greatly enhanced compared to steel surfaces.[221]

However, it has been noted that iron electrodes introduce a green colour into treated water which then turns yellow and turbid. This effect is due to the presence of ferrous ions which oxidise to ferric in acidic or neutral conditions. The formation of ferric hydroxide ($Fe(OH)_3$) derived floc, as a result of the reaction of Fe^{3+} with OH^- ions, gives a yellow colour to EC treated water and increases turbidity. This phenomenon is the reason for choosing aluminium electrodes for drinking water EC treatment as floc consisting of aluminium hydroxide ($Al(OH)_3$) is white and does not dramatically impact on turbidity.[222] Yet, in the case of arsenic removal and coloured wastewater; iron electrodes are much

more effective than aluminium. The reason for this special case is that the adsorption capacity of hydrous aluminium oxide for arsenic is lower than for ferric oxides.[223]

Only a very few reports within the literature on the combined use of both aluminium and iron electrodes in the same EC reactor have been published. Aluminium has been used as the sacrificial anode and stainless steel or iron as the cathode for the removal of carbon black, clay and suspended solids without changing polarity of electrodes.[224,225,226,227] The use of combination electrodes of dissimilar metals and the frequent change of their polarity has not yet been studied. This may provide interesting results on alternative floc formation and removal mechanisms for the removal of both organic materials and heavy metals from water.

Within the last six years, arsenic removal efficiency of an aluminium-iron combination electrode EC system has been described.[228] Yet, the use of combined aluminium and iron anodes in the same electrolytic cell for industrial wastewater applications has not yet been reported.

Inter-electrode Distance

The gap-spacing of electrodes plays an integral part in the efficiency of cation delivery into solution that is responsible for generating floc. Work cited in the literature has demonstrated that with an increase in inter-electrode distance, pollutant removal decreases.[229]

During EC, once a potential is applied to electrodes, anodic oxidation is initiated. As operational time proceeds, the formation of an oxide layer on the surfaces of the anodes develops.[230] This anodic plating increases resistance between cathode-anode that is amplified as inter-electrode distance increases. Consequently, after sufficient time, current is dramatically reduced unless applied potential is increased to overcome the rise in resistance.

As resistance increases, the ohmic loss (IR-drop) increases which subsequently inhibits the rate of anodic oxidation. As the rate of anodic oxidation slows; the number of cations introduced at the anode as a function of Equation 2 (section 2.2.4 Electrode Reactions) decreases. Accordingly, floc production thus deteriorates and coalescence of pollutants

diminishes. This observable fact is exacerbated as inter-electrode distance increases when working in potentiostatic mode.

At a minimum inter-electrode distance, the resistance for current flow in solution is low such that it facilitates the electrolytic processes involved in adequate floc generation and pollutant removal. The variation in IR-drop is governed by the following (Equation 11);[231]

$$\eta_{IR} = I \frac{d}{A\kappa} \qquad \textbf{Equation 11}$$

where I is the current (A); d is distance between the electrodes (cm); A is active anode surface (cm^2) and κ is specific conductivity (μS/cm). The above equation infers that three different factors influence IR-drop and they are:[232]

- Solution conductivity;
- Electrode surface area;
- Inter-electrode distance.

Therefore, at constant solution conductivity and anodic surface area, IR-drop increases with increasing inter-electrode distance. Any increase in IR-drop is not beneficial during EC and in order to minimize this, apart for the immediate effect of reducing the gap-spacing between consecutive cathode and anode electrodes, other remedies reported include; (i) the use of a highly conductive solution, (ii) increasing the cross-sectional area of the electrodes, (iii) the inclusion of a potentiostat in order to compensate for IR-drop.[143]

As well as the minimisation of any IR-drop, other reported work has demonstrated the importance of mass transfer and turbulence kinetics at the electrode-electrolyte interfacial region as a function of inter-electrode distance.

At minimum electrode spacing, turbulence at the base and at the top of the electrodes is enhanced. Hence, for larger electrode spacing's the movement of the cationic metals, hydroxides and anionic pollutant participant species is slower, the thickness of the concentration boundary layer in the inter-electrode gaps is larger and thus the reaction rate decreases.[233] This behaviour indicates the relative importance of water motion and turbulence on floc generation and their dependence on inter-electrode distance.

Electrolysis Time

Residence time[234,235] in environmental engineering refers to the amount of time that wastewater spends in a reactor for flocculation to occur before transferring to secondary treatment phases such as sedimentation basins.[236,237]

However, this term can be considered ambiguous for EC as it is the *in situ* formation of the electrochemically generated coagulum, through the anodic oxidation and subsequent release of metallic cations, which initiate the processes of coagulation and flocculation. It is therefore important to differentiate between residence time, whereby the complete system is taken into consideration and includes coagulation and flocculation, and the time taken for coagulation alone. Since the primary factor in determining the amount and removal efficiency of EC floc generated starts with the input of cations into raw wastewater, the time taken for a volume of water to pass over active anodic plate surfaces is more definitive.

A more appropriate term therefore is electrolysis time and refers to the time taken for water to pass through the electrode compartment of an EC system only and come into contact with electrochemical reactions and processes. It is characterised by the time taken for a pollutant particle to spend within an electrode containing chamber. Therefore, by this definition electrolysis time begins from the moment a particle enters an electrode gap and ends the moment said particle leaves the confines of an electrode gap. Essentially, it is the time taken for wastewater to come into contact with anodic plate surfaces. Consequently, all cell voidage within the electrode containing chamber must be taken into consideration and accounted for in determining the actual free volume for wastewater to flow through. Contact time (τ) can therefore be defined by the following (Equation 12):

$$\tau = \frac{V-(\sigma+\rho)}{q} \qquad \textbf{Equation 12}$$

Where V is total volume of the electrode containing compartment (m^3); σ is the occupying volume of electrodes (m^3); ρ is cell voidage volume (m^3) and q is flow rate (m^3/hr).

However, within the literature the majority of authors have chosen the former phrase of residence time but have applied it to the definition of electrolysis time (minus the consideration of cell voidage). Subsequently, whereas residence times have been reported

in published works, strictly speaking the authors have been discussing the time period over which untreated solutions have come into contact with anodes. Thus, in this work electrolysis time has replaced the phrase residence time for ease of clarity.

2.4.2 Chemical Parameters

The operation, control and chemical interactions of an EC system affect floc generation, performance and reliability. The chemical interactions of the pollutant (type and concentration) and the association of iron speciation with pH, electrode passivation and the chemical characteristics of the water body to be treated, can also affect the outcome of EC generated floc.

pH

Solution pH determines the speciation of metal ions released through cationic dissolution of the anode. The pH influences the state of other species in solution and the solubility of floc formed. Thus, solution pH influences the overall efficacy of EC floc. The predominance of particular ions can be predicted using Pourbaix (Eh-pH) diagrams as represented in Figure 2.4 for both iron and aluminium on the following page.

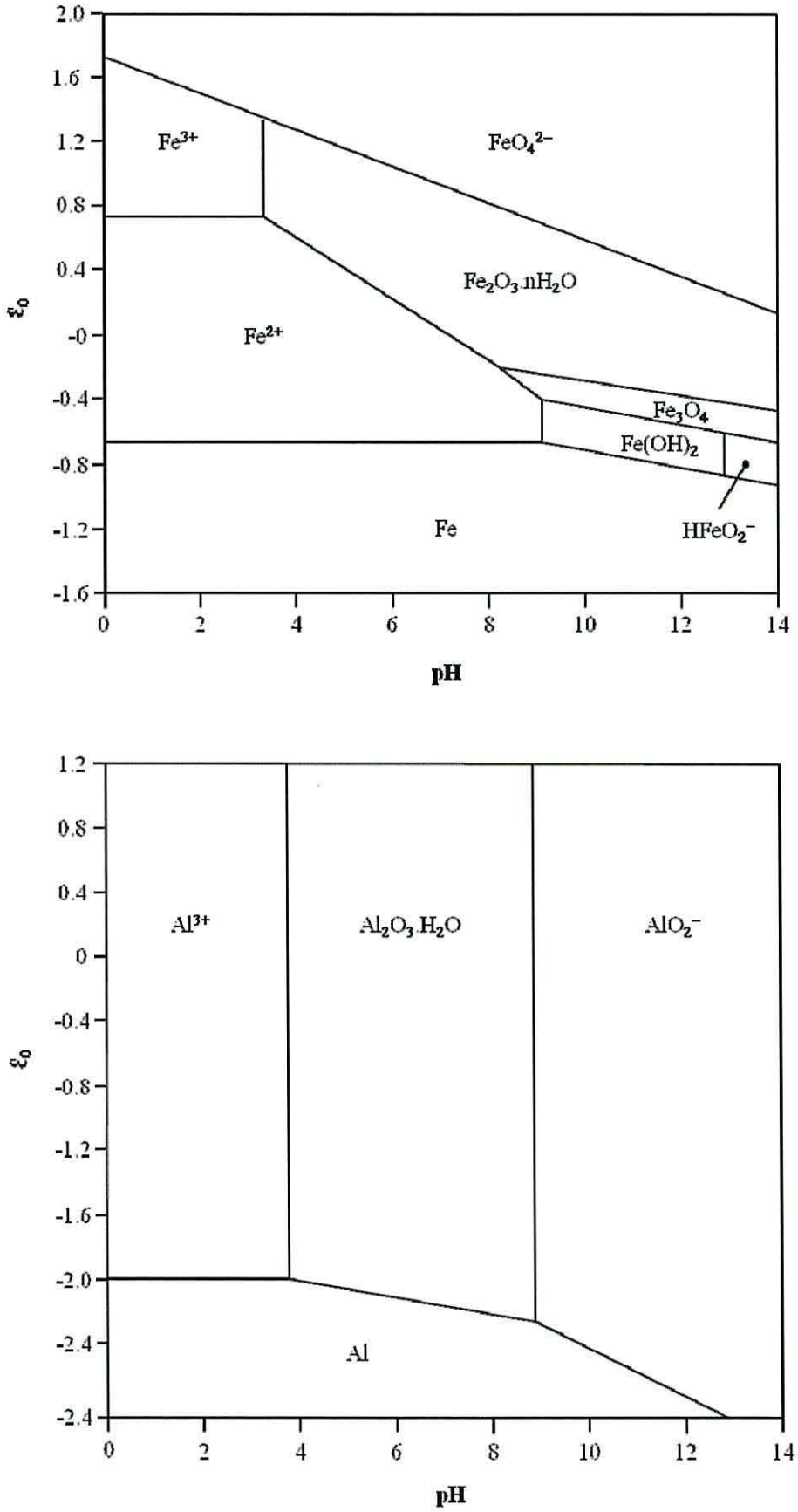

Figure 2.4. ***Top.*** **Pourbaix diagram for iron.** ***Bottom.*** **Pourbaix diagram for aluminium.**[238]

Pourbaix diagrams thermodynamically depict the form of an element as a function of potential and pH. The Pourbaix diagram is a type of predominance diagram in that it shows the prevalent form of an element's existence under a given set of conditions. These diagrams give a visual representation of the oxidising and reducing abilities of the major stable compounds of an element and are used frequently in geochemical, environmental and corrosion applications. For this work, whereby the metal of interest is iron, a Pourbaix diagram is useful in that it can indicate the dominant iron form (Fe^{2+}/Fe^{3+}) that will be anodically released through electro-oxidation as a factor of the prevailing pH of the solution.

In Figure 2.4, predominant ion boundaries are represented by intersecting lines. As such a Pourbaix diagram can be read much like a standard phase diagram but with a different set of axes. The vertical axis is labelled E*h* (denoted as ε_0) for the voltage potential with respect to the standard hydrogen electrode (SHE) as calculated by the Nernst equation. The '*h*' stands for hydrogen, although other standards may be used.[239]

As a tool for initially postulating iron species versus pH, the Pourbaix diagram can adequately predict changes in metal species with changes in pH but fails in addressing changes between metal oxidation states during EC. An important change as different oxidation states released into solution affect the type of floc produced and the resultant pollutant removal mechanism.

With respect to this work and specifically to iron, authors have reported a pH increase during batch EC operation as the result of hydroxide ion production (Equation 4) *via* hydrolysis on the cathode.[240,241,242] However, literature reports are conflicting with regard to the production of Fe^{2+} or Fe^{3+} at the anode and subsequent interaction with hydroxide molecules.

Most EC studies have been pollutant centred and the solids $Fe(OH)_2$ or $Fe(OH)_3$ have been reported to be formed in these studies based on supposition rather than experimental fact. What follows is a summary of the ambiguity in anodic reactions reported within the literature surrounding the evolution and release of different iron oxidation states.

It is important to clarify this point in order to understand the implications of the rise in pH during EC operation on the type of iron ion released into solution and its impact on the generation of floc produced:

1. Some studies have reported that electrolytic oxidation of iron produces Fe^{2+} which hydrolyses to form insoluble $Fe(OH)_2$ (Equation 7).[243] Other authors have reported the formation of $Fe(OH)_2$ without providing details of its formation.[244]
2. Some studies have reported the generation of Fe^{2+} at the anode with subsequent oxidation by dissolved oxygen and hydrolysis to form $Fe(OH)_3$ precipitate.[173]
3. Lastly, some studies have reported an altogether different mechanism involving a one-step electrolytic oxidation of an iron anode to Fe^{3+} followed by hydrolysis to form insoluble $Fe(OH)_3$, Equations 13 – 14 below:[245]

$$Fe_{(s)} \rightarrow Fe^{3+}_{(aq)} + 3e^- \qquad \textbf{Equation 13}$$

$$Fe^{3+}_{(aq)} + 3OH^-_{(aq)} \rightarrow Fe(OH)_{3(s)} \qquad \textbf{Equation 14}$$

These changes in the variety of purported ways that either Fe^{2+} or Fe^{3+} is electrolytically dissolved into solution plays a fundamental effect on floc formation. Work carried out recently has revealed that Fe^{2+}, not Fe^{3+} is the dominant iron ion produced at the anode as the by-product of Equation 2.[168] Thermodynamically, the production of Fe^{2+} is also favoured and as such for the remainder of this review, it will be impressed upon that within an EC cell, iron is electro-oxidised at the anode from the insoluble metallic form to Fe^{2+}.

The dependency however on whether the iron ions in solution remain as Fe^{2+} or whether external factors change their oxidation state to Fe^{3+}, is where pH can have an influence. During batch EC, pH increases near the diffusion layer of the anode due to hydroxide generation at the cathode. This localised increase in pH hastens Fe^{2+} oxidation to Fe^{3+} and thus the formation of $Fe(OH)_3$ coagulant. However, initial pH of solution or if pH is controlled within the EC cell, can alter the speed at which initially generated Fe^{2+} oxidises to form Fe^{3+} and subsequent $Fe(OH)_3$. Consequently, the ratio of Fe^{2+}/Fe^{3+} is pH dependant.

The amount of Fe^{2+} remaining after generation and mixing decreases with increasing pH due to the escalation of oxidation rate to Fe^{3+}. At pH 6.5, oxidation of Fe^{2+} is slow and the

hydroxides produced at the cathode are not used up. Charge neutralisation coagulation dominates and the floc produced is fine and its strength is derived from van der Waal's bonding forces. At pH 8.5, Fe^{2+} is completely oxidised and results in the generation of floc containing $Fe(OH)_3$. Sweep-floc coagulation dominates which produces stronger floc as the primary binding forces are particle bridging. However, at pH $\geq$ 8.5, as $Fe(OH)_3$ is amphoteric, some $Fe(OH)_4^-$ formation may occur leading to a loss in floc efficacy. At pH 7.5, incomplete oxidation occurs and there exists a mixture of soluble Fe^{2+} and insoluble $Fe(OH)_3$[246,247]. The likely end products are summarised in Table 2.1.

Table 2.1. Likely end products of EC as a function of pH.

pH	Rate of Fe^{2+} oxidation	Time frame	End product
6.5	Extremely slow	Hours	Fe^{2+}
7.5	Fast	Minutes	$Fe^{2+}/Fe(OH)_3$
8.5	Rapid	Seconds	$Fe(OH)_3$

From the literature, the factors of extreme pH sensitivity of Fe^{2+} oxidation and pH variation inside an EC cell during operation can combine to yield highly variable floc formation and pollutant removal mechanisms.

Conductivity

Work carried out to investigate the effect of conductivity on restaurant wastewater showed there to be no change in treatment efficiencies when altered from 443 to 2,850 μS/cm.[248] This is in contrast to the findings of other authors who have reported significant loss in dye removal efficiency from textile wastewater as a consequence of reducing conductivity.[249]

This inconsistency however may be due to the difference in pollutant removal mechanisms that occurred between the two studies. Commonly, EC is used in an electrochemical oxidative capacity for the removal of dyes and colours from textile effluents.[250] Conversely, the removal of pollutants from restaurant wastewater is purely through coagulation and flocculation alone.[251]

Alkalinity

There are scarce references within the literature relating to alkalinity and its effect on EC efficacy. Work carried out investigating the removal of copper (Cu^{2+} in lithium bromide (LiBr)) in refrigerant cooling solutions, (as a consequence of its corrosion of copper parts

inside the refrigeration unit), showed there to be no adverse effect upon EC performance with an increase in alkalinity.[252]

The lowest Cu^{2+} and residual Fe^{2+} ion concentrations were found to be prevalent in the refrigerant solution that had the highest of the tested alkalinity levels, adjusted at 134 meq/L. This could be explained by the fact that the higher hydroxide concentration allowed Cu^{2+} and Fe^{2+}/Fe^{3+} ions to precipitate out more easily. Measurements reported within the work demonstrated no appreciable refrigerant alkalinity change throughout the EC treatment. This could be a consequence of Fe^{2+} and OH^- being produced at identical stoichiometric amounts during the electrolysis process. Therefore, both ions left the LiBr solution in the form $Fe(OH)_2$. Only a small fraction of Fe^{2+} was left to oxidise so H^+ production as the by-product of Fe^{2+} oxidation did not alter the refrigerant alkalinity. Overall, in the only specific piece of work directly investigating changes in alkalinity found within the literature, it was reported that alkalinity did not show a significant impact on metal ion removal.

2.5 References

132. Barkley, N. P., Farrell, C. W., Gardner-Clayson, T. W. Alternating current electrocoagulation for Superfund site remediation. Air and Waste 1993; 43 (5): 784-789.
133. Bissen, M., Frimmel, F. H. Arsenic - a review. Part II: Oxidation of arsenic and its removal in water treatment. Acta Hydrochimica et Hydrobiologica 2003; 31 (2): 97-107.
134. Blais, J. F., Dufresne, S., Mercier, G. State of the art of technologies for metal removal from industrial effluents. Revue des Sciences de l'Eau 1999; 12 (4): 687-711.
135. Chen, G. H., Chen, X. M., Yue, P. L. Electrocoagulation and electroflotation of restaurant wastewater. Journal of Environmental Engineering 2000; 126 (9): 858-891.
136. Feng, C., Sugiura, N., Shimada, S. Development of a high performance electrochemical wastewater treatment system. Journal of Hazardous Materials 2003; 103 (1-2): 65-78.
137. Bojic, A. L., Bojic, D., Andjelkovic, T. Removal of Cu^{2+} and Zn^{2+} from model wastewaters by spontaneous reduction-coagulation process in flow conditions. Journal of Hazardous Materials 2009; 168 (2-3): 813-819.
138. Mouedhen, G., Feki, M., De Petris-Wery, M. Electrochemical removal of Cr(VI) from aqueous media using iron and aluminium as electrode materials: Towards a better understanding of the involved phenomena. Journal of Hazardous Materials 2009; 168 (2-3): 983-991.

139. Koparal, A. S., Öğütveren, Ü. B. Removal of nitrate from aqueous solutions by electrodialysis. International Journal of Environmental Studies 2002; 59 (3); 323-329.
140. Donnini, J. C., Kan, J., Szynkarczuk, J., Hassan, T. A, Kar, K. L. The operating cost of electrocoagulation. Canadian Journal of Chemical Engineering 1994; 72: 1007-1012.
141. Diemert, S., Wang, W., Andrews, R. C., Li, X. F. Removal of halo-benzoquinone (emerging disinfection by-product) precursor material from three surface waters using coagulation. Water Research 2013; 47 (5): 1773-1782.
142. Koparal, A. S. The removal of salinity from produced formation by conventional and electrochemical methods. Fresenius Environmental Bulletin 2002; 11 (12a): 1071-1077.
143. Mollah, M. Y. A., Morkovsky, P., Gomes, J. A. G., Kesmez, M., Parga, J., Cocke, D. L. Fundamentals, present and future perspective of electrocoagulation. Journal of Hazardous Materials 2004; B114: 199-210.
144. Larue, O., Vorobiev, E. Floc size estimation in iron induced electrocoagulation and coagulation using sedimentation data. International Journal of Mineral Processing 2003; 71 (1-4): 1-15.
145. Bukhari, A. A. Investigation of the electro-coagulation treatment process for the removal of total suspended solids and turbidity from municipal wastewater. Bioresource Technology 2008; 99: 914-921.
146. Kara, S. Treatment of transport container washing wastewater by electrocoagulation. Environmental Progress and Sustainable Energy 2013; 32 (2): 249-256.
147. Ai, Y., Joo S. W., Jiang Y. T. Transient electrophoretic motion of a charged particle through a converging-diverging microchannel: Effect of direct current-dielectrophoretic force. Electrophoresis 2009; 30 (14): 2499-2506.
148. Xiao, F., Zhang, X. R., Ma, J. Indecisiveness of electrophoretic mobility determination in evaluating Fe(III) coagulation performance. Separation and Purification Technology 2009; 68 (2): 273-278.
149. Paul, A. B. Proceedings of the 22nd WEDC Conference on Water Quality and Supply, New Delhi, India, 1996.
150. Kim, S. H., Moon, B. H., Lee, H. I. Effects of pH and dosage on pollutant removal and floc structure during coagulation. Microchemical Journal 2001; 68: 197-203.
151. Thomas, D. N., Judd, S. J. and Fawcett, N. Flocculation modelling: a review. Water Research 1999; 33 (7): 1579-1592.
152. Letterman, R. D., Amirtharajah, A. and O'Melia, C. R. Coagulation and Flocculation. Water Quality and Treatment, a Handbook of Community Water Supplies. McGraw-Hill, 1999.
153. Pouet, W. A., Grasmick, A. Urban wastewater treatment by electrocoagulation and flotation. Water Science and Technology 1995; 31: 275-283.
154. Mameri, N., Yeddou, A. R., Lounici, H., Belhocine, D., Grib, H., Bariou, B. Deflourination of septentrional Sahara water of North Africa by electrocoagulation process using bipolar aluminium electrodes. Water Research 1998; 32: 1604-1612.
155. Lyklema, J. The Scientific Basis of Flocculation. Sijthoff and Noordhoff International Publishers, 1978.
156. Hunter, R. J. Introduction to Modern Colloid Science. Oxford University Press, 1993.
157. Bytautas, L., Ruedenberg, K. Ab initio potential energy curve of F-2. IV. Transition from the covalent to the van der Waals region: Competition between multipolar and

correlation forces. Journal of Chemical Physics 2009; 130 (20) Article Number: 204101.
158. Deryaguin, B. V. and Landau, L. D. A theory of the stability of strongly charged lyophobic sols and so the adhesion of strongly charged particles in solutions of electrolytes. Acta Physicochim USSR 1941; 14: 633.
159. Verwey, E. J. W., Overbeek, J. T. G. Theory of the stability of lyphobic colloids. Elsevier, 1948.
160. Tamulis, A., Tamulis, V. Quantum mechanical design of molecular electronics OR gate for regulation of minimal cell functions. Journal of Computational and Theoretical Nanoscience 2008; 5 (4): 545-553.
161. Dickhoff, W. H., Van Neck, D. Many Body Theory Exposed: Propagator description of quantum mechanics in many-body systems. World Scientific, 2005.
162. Fetter, A. L., Walecka, J. D. Quantum Theory of Many-particle Systems. Dover Publications, 2003.
163. Kornboonraksa, T., Lee, S. On-line monitoring of floc formation in various flocculants for piggery wastewater treatment. Desalination and Water Treatment – Science and Engineering 2009; 1 (1-3): 248-258.
164. Eldan, M., Shoham, T., Erel, Y., Mandler, D. Monitoring Heavy Metals in Seawater by Their Electrochemically Induced Deposition as Hydroxides. Electroanalysis 2009; 21 (3-5): 368-378.
165. Sethu, V. S., Aziz, A. R., Aroua, M. K. Recovery and reutilisation of copper from metal hydroxide sludges. Clean Technologies and Environmental Policy 2008; 10 (2): 131-136.
166. Canizares, P., Martinez, F., Carmona, M., Lobato, J., Rodrigo, M. A. Continuous electrocoagulation of synthetic colloid-polluted wastes. Industrial and Engineering Chemistry Research 2005; 44 (22): 8171-8177.
167. Aouni, A., Fersi, C., Sik Ali, M. B., Dhahbi, M. Treatment of textile wastewater by a hybrid electrocoagulation/nanofiltration process. Journal of Hazardous Materials 2009; 168 (2-3): 868-874.
168. Lakshmanan, D., Clifford, D. A., Samanta, G. Ferrous and ferric ion generation during iron electrocoagulation. Environmental Science and Technology 2009; 43 (10): 3853-3859.
169. Linares-Hernandez, I., Barrera-Diaz, C., Roa-Morales, G., Bilyeu, B., Ureña-Núñez, F. Influence of the anodic material on electrocoagulation performance. Chemical Engineering Journal 2009; 148 (1): 97-105.
170. Zongo, I., Leclerc, J. P. Maïga, H. M., Wéthé, J., Lapicque, F. Removal of hexavalent chromium from industrial wastewater by electrocoagulation: A comprehensive comparison of aluminium and iron electrodes. Separation and Purification Technology 2009; 66: 159-166.
171. Moreno, H. A., Cocke, D. L., Jewel, A. G. G., Morkovsky, P., Parga, J. R., Peterson, E., Garcia, C. Electrochemical reactions for electrocoagulation using iron electrodes. Industrial and Engineering Chemistry Research 2009; 48 (4): 2275-2282.
172. Den, W. Huang, C. Electrocoagulation for removal of silica nano-particles from chemical-mechanical-planarization wastewater. Colloids and Surfaces A: Physicochemical Engineering Aspects 2005; 254: 81-89.
173. Hansen, H. K., Núñez, P., Grandon, R. Electrocoagulation as a Remediation Tool for Wastewaters Containing Arsenic. Minerals Engineering 2006; 19 (5): 521-524.
174. Hem, J. D. Stability field diagrams as aids in iron chemistry studies. Journal of American Water Works Association 1961; 53: 211.

175. Önder, E., Koparal, A. S., Öğütveren, Ü. B. An alternative method for the removal of surfactants from water: Electrochemical coagulation. Separation and Purification Technology 2007; 52 (3): 527-532.
176. Johnson, P. N., Amirtharajah, A. Ferric chloride and alum as single and dual coagulants. Journal of American Water Works Association 1983; 5: 232-239.
177. Baes, C. F., Mesner, R. E. The Hydrolysis of Cations. Krieger Publishing, 1976.
178. Stumm, W., Lee, G. F. Oxygenation of ferrous iron. Industrial Engineering and Chemical Research 1961; 53: 143-146.
179. Sundstrom, D. W., Klei, H. E. Wastewater Treatment. Prentice-Hall, 1979.
180. Tamura, H., Goto, K., Nagayama, M. The effect of ferric hydroxide on the oxygenation of ferrous ions in neutral solution. Corrosion Science 1976; 16: 197-207.
181. Daneshwar, N., Oladegarazope, A., Djafarzadeh, N. Decolourisation of basic dye solutions by electrocoagulation: An investigation of the effect of operational parameters. Journal of Hazardous Materials 2006; B129: 116-122.
182. Osipenko, V. D., Pogorelyi, P. I. Electrocoagulation neutralization of chromium containing effluent. Metallurgist 1977; 21 (9): 44-45.
183. Sadeddin, K., Naser, A., Firas, A. Removal of turbidity and suspended solids by electro-coagulation to improve feed water quality of reverse osmosis plant. Desalination 2011; 268 (1-3): 204-207.
184. Amosov, V. V., Zil'brtman, A. G. Experience in local treatment of wastewaters from petrochemical production. Chemistry and Technology of Fuels and Oils 1976; 12 (11): 850-852.
185. Do, J. S., Chen, M. L. Decolourisation of dye-containing solutions by electrocoagulation. Journal of Applied Electrochemistry 1994; 24 (8): 785-790.
186. Xiong, Y., Strunk, P. K., Xia, H., Zhu, X., Karlsson, H. T. Treatment of dye wastewater containing acid orange II using a cell with three-phase three-dimensional electrode. Water Research 2001; 35 (17): 4226-4230.
187. Neville, M. Ninth International Forum on Electrolysis in the Chemical Industry - Applied Electrochemical Technologies. USA, 1995.
188. Belongia, B. M., Haworth, P. D., Baygents, J. C. Treatment of alumina and silica chemical mechanical polishing waste by electrodecantation and electrocoagulation Journal of the Electrochemical Society 1999; 146 (11): 4124-4130.
189. Winchester, B. G., Caffrey, M., Robinson, D. Enzyme purification by electrodecantation. Biochemical Journal 1971; 121 (2): 161-168.
190. Kranz, T., Lappe, F. Electrodecantation of serum proteins. Hoppe Seylers Z Physiological Chemistry 1975; 356 (10): 1545-1554.
191. Drouiche, N., Grib, H., Abdi, N., Electrodialysis with bipolar membrane for regeneration of a spent activated carbon. Journal of Hazardous Materials 2009; 170 (1): 197-202.
192. Kirkelund, G. M., Ottosen, L. M., Villumsen, A. Electrodialytic remediation of harbour sediment in suspension – Evaluation of effects induced by changes in stirring velocity and current density on heavy metal removal and pH. Journal of Hazardous Materials 2009; 169 (1-3): 685-690.
193. Wang, Q. S. Ying, T. J., Jiang, T. J. Demineralization of soybean oligosaccharides extract from sweet slurry by conventional electrodialysis. Journal of Food Engineering 2009; 3: 410-415.
194. Zabolotsky, V. I., Nikonenko, V. V., Pismenskaya, N. D., Istoshin, A. G. Electrodialysis Technology for Deep Demineralization of Surface and Ground Water. Desalination 1996; 108 (1-3): 179-181.

195. Xiu, F. R., Zhang, F. S. Electrokinetic recovery of Cd, Cr, As, Ni, Zn and Mn from waste printed circuit boards: Effect of assisting agents. Journal of Hazardous Materials 2009; 170 (1): 191-196.
196. Mishchuk, N. A. Soil electroremediation features in potentiostatic and galvanostatic modes. Journal of Water Chemistry and Technology 2009; 31 (4): 205-212.
197. Park, S. W., Lee, J. Y., Yang, J. S. Electrokinetic remediation of contaminated soil with waste-lubricant oils and zinc. Journal of Hazardous Materials 2009; 169 (1-3): 1168-1172.
198. Hanay, O., Hasar, H., Kocer, N. N. Effect of EDTA as washing solution on removing of heavy metals from sewage sludge by electrokinetic. Journal of Hazardous Materials Volume 2009; 169 (1-3): 703-710.
199. Essadki, A. H., Gourich, B., Vial, C. Defluoridation of drinking water by electrocoagulation/electroflotation in a stirred tank reactor with a comparative performance to an external-loop airlift reactor. Journal of Hazardous Materials 2009; 168 (2-3): 1325-1333.
200. Wang, C. T., Chou, W. L., Kuo, Y. M. Removal of COD from laundry wastewater by electrocoagulation/electroflotation. Journal of Hazardous Materials 2009; 164 (1): 81-86.
201. Balla, W., Essadki, A. H., Gourich, B., Dassaa, A., Chenik, H., Azzi, M. Electrocoagulation/electroflotation of reactive, disperse and mixture dyes in an external-loop airlift reactor. Journal of Hazardous Materials 2010; 184 (1-3): 710-716.
202. Mahvi, A. H., Ebrahimi, S. J. A., Mesdaghinia, A., Gharibi, H., Sowlat, M. H. Performance evaluation of a continuous bipolar electrocoagulation/electrooxidation-electroflotation (ECEO-EF) reactor designed for simultaneous removal of ammonia and phosphate from wastewater effluent. Journal of Hazardous Materials 2011; 192 (3): 1267-1274
203. Holt, P. K. Electrocoagulation: Unravelling and Synthesizing the Mechanisms Behind a Water Treatment Process. PhD thesis, Faculty of Engineering, The University of Sydney, 2003.
204. Ozyonar, F., Karagozoglu, B. Systematic assessment of electrocoagulation for the treatment of marble processing wastewater. International Journal of Environmental Science and Technology 2012; 9 (4): 637-646.
205. Mollah, M. Y. A., Schennach, R., Parga, J. R., Cocke, D. L. Electrocoagulation – Science and applications. Journal of Hazardous Materials 2001; 84 (1): 29-35.
206. Parga, J. R., Cocke, D. L., Valenzuela, J. L., Kesmez, M., Gomes, J. A. G., Valverde, V. As removal by EC technology in the Comarca Lagunera Mexico. Journal of Hazardous Materials 2005; 124 (1-3): 247-255.
207. Jiang, J. Q., Graham J. J. D., André, C. M., Kelsall, G. H., Brandon, N. P., Chipps, M. J. Comparative performance of an electrocoagulation/flotation system with chemical coagulation/dissolved air flotation: a pilot-scale trial. Water Science and Technology 2002; 2 (1): 289-297.
208. Yu, Z., Fan, Y. H. Study on Integrated Multifunctional Reactor of Vortex-electrocoagulation in conjunction with Dissolved Air Flotation and Contact Filtration Process. Proceedings of Information Technology and Environmental System 2008; 2: 339-348.
209. Timmes, T. C., Kim, H. C. Dempsey, B. A. Electrocoagulation pre-treatment of seawater prior to ultrafiltration: Bench-scale applications for military water purification systems. Desalinisation 2009; 249 (3): 895-901.

210. Den, W., Wang, C. J. Removal of silica from brackish water by electrocoagulation pre-treatment to prevent fouling of reverse osmosis membranes. Separation and Purification Technology 2008; 59 (3): 318-325.
211. Holt, P. K., Barton, G. W., Mitchell, C. A. The future for electrocoagulation as a localised water treatment technology. Chemosphere 2004; 127.
212. Chen, X., Chen, G. Yue, P. L. Separation of pollutants from restaurant wastewater by electrocoagulation. Separation and Purification Technology 2000; 19: 65-76.
213. Ghosh, D. Solanki, H., Purkait, M. K. Removal of Fe(II) from tap water by electrocoagulation technique. Journal of Hazardous Materials 2008; 155: 135-143.
214. Ogutveren, U. B., Goenen, N., Koparal, S. Removal of dye stuffs from wastewater: Electrocoagulation of Acilan Blau using soluble anode. Journal of Environmental Science and Health, Part A: Environmental Science and Engineering A27 1992; 5: 1237-1247.
215. Chen, X., Deng, H. Removal of humic acids from water by hybrid titanium-based electrocoagulation with ultrafiltration membrane processes. Desalination 2012; 300: 51-57.
216. Naumczyk, J., Szypyrokowicz, L., Zilio-Grandi, F. Electrochemical treatment of textile wastewater. Water Science and Technology 1996; 34 (11): 17-24.
217. Chen, G. Electrochemical technologies in wastewater treatment. Separation and Purification Technology 2004; 38 (1): 11-41.
218. Abuzaid, N .S., Bukhari, A. A., Al-Hamouz, Z. M. Ground water coagulation using soluble stainless steel electrodes. Advances in Environmental Research 2002; 6: 325-333.
219. İrdemez, Ş., Demircioğlu, N., Yildiz, Y. Ş., Bingül, Z. The effects of current density and phosphate concentration on phosphate removal from wastewater by electrocoagulation using aluminium and iron plate electrodes. Separation and Purification Technology 2006; 52: 218-227.
220. Baklan, V. Y., Kolesnikova, I. P. Influence of electrode material on electrocoagulation. Journal of Aerosol Science 1996; 27 (1): S209-S210.
221. Hulser, P., Kruger, U. A., Beck, F. The cathodic corrosion of aluminium during the electrdeposition of paint: electrochemical measurements. Corrosion Science 1996; 38 (1): 47-57.
222. Barrera-Díaz, C., Ureña-Núñez, F., Campos, E., Palomar-Pardavé, M., Romero-Romo, M. A combined electrochemical-irradiation treatment of highly coloured and polluted industrial wastewater, Radiation Physics and Chemistry 2003; 67: 657-663.
223. Ratna, P., Kumar, S. Chaudhari, K. C., Khilar, S. Majan, P. Removal of arsenic from water by electrocoagulation, Chemosphere 2004; 55: 1245-1252.
224. Avetisyan, D. P., Tarkhanyan, A. S., Safaryan, L. N. Electroflotation coagulation removal of carbon black from acetylene production wastewaters, Soviet Journal of Water Chemistry and Technology 1984; 6: 345-346
225. Holt, P. K., Barton, G. W., Wark, M., Mitchell, C. A. A quantitative comparison between chemical dosing and electrocoagulation, Colloids and Surfaces 2002; A211: 233-248.
226. Ivanishvili, A. I., Przhegorlinskii, V. I., Kalinichenko, T. D. Comparative evaluation of the efficiency of electrocoagulation and reagent methods of clarifying wastewater, Soviet Journal of Water Chemistry and Technology 1987; 9: 468-469.
227. Syrbu, V. K., Drondina, R. V., Romanov, A. M., Ershov, A. I. Combined electroflotocoagulation apparatus for water purification. Elektronnaya Obrabotka Materialov 1986; 57-59.

228. Jewel, A.G., Gomesa, A., Daida, P., Kesmez, M., Weir, A. M., Moreno, H., Jose, R., Parga, B., Irwin, C. G., Hylton-McWhinney, D., Grady, T., Peterson, A. E., Cocke, L. D. Arsenic removal by electrocoagulation using combined Al – Fe electrode system and characterization of products. Journal of Hazardous Material 2007; B139: 220-231.
229. Modirshahla, N., Behnajady, M. A., Mohammadi-Aghdam, S. Investigation of the effect of different electrodes and their connections on the removal efficiency of 4-nitrophenol from aqueous solution by electrocoagulation. Journal of Hazardous Materials 2008; 154 (1-3); 778-786
230. Avsar, Y., Kurt, U., Gonullu, T. Comparison of classical chemical and electrochemical processes for treating rose processing wastewater. Journal of Hazardous Materials 2007; B148: 340-345.
231. Strokach, P. P. The prospects of using anodic dissolution of metal for water purification. Electrochemical Industrial Processes Biology 1975; 55: 375.
232. Martínez-Villafañe, J. F., Montero-Ocampo, C., García-Lara, A. M. Energy and electrode consumption analysis of electrocoagulation for the removal of arsenic from underground water. Journal of Hazardous Materials 2009; 172: 1617-1622.
233. Basha, C. A., Soloman, P. A., Velan, M., Balasubramanian, N., Kareem, L. R. Participation of electrochemical steps in treating tannery wastewater. Industrial and Engineering Chemistry Research 2009; 48 (22): 9786-9796.
234. Essadki, A. H., Bennajah, M., Gourich, B., Vial, Ch., Azzi, M., Delmas, H. Electrocoagulation/electroflotation in an external-loop airlift reactor – Application to the decolorization of textile dye wastewater: A case study. Chemical Engineering and Processing: Process Intensification 2008; 47 (8): 1211-1223.
235. Wolf, D., Resnik, W. Residence time distribution in real systems. Industrial and Engineering Chemistry 1963; 2 (4): 1-9.
236. Davis, M., Masten, S. Principles of environmental engineering and science. McGraw Hill, 2004.
237. Bo, L., Federico, G. Transport equation for local residence time of a fluid. Science Direct 2004; 59 (3): 513-523.
238. Pourbaix, M. Atlas of Electrochemical Equilibria in Aqueous Solutions. Pergamon, 1966.
239. Garrels, R. M., Christ, C. L. Solutions, Minerals, and Equilibria. Harper and Row, 1965.
240. Parga, R., Cocke, D. L., Valverde, V. Characterisation of electrocoagulation for removal of chromium and arsenic. Chemical Engineering Technology 2005; 28 (5): 605-612.
241. Zhu, B., Clifford, D. A., Chellam, S. Comparison of electrocoagulation and chemical coagulation pretreatment for enhanced virus removal using microfiltration membranes. Water Research 2005; 39 (13): 3098-3108.
242. Kobya, M., Senturk, E., Bayramoglu, M. Treatment of poultry slaughterhouse wastewaters by electrocoagulation. Journal of Hazardous Materials 2006; 133 (1): 172-176.
243. Ghernaouta, D., Badisa, A., Kellila, A. Ghernaoutb, B. Application of electrocoagulation in *Escherichia coli* culture and two surface waters. Desalination 2008; 219 (1-3): 118-125.
244. Balasubramanian, N., Madhavan, K. Arsenic removal from industrial effluent through electrocoagulation. Chemical Engineering and Technology 2001; 24: 519-521.

245. Jarvis, P., Jefferson, B., Gregory, J., Parsons, S. A. A review of floc strength and breakage. Water Research 2005; 39: 3121-3137.
246. Wolf, R. H. H., Ester, K., Deželić, N., Šipalo-žuljevi, J. The influence of amphoteric polyelectrolyte gelatin on the formation of cobalt(II), nickel(II), magnesium(II), manganese(II), iron(III) and aluminium(III) hydroxide. Colloid and Polymer Science 1974; 252 (7- 8): 570-573.
247. Lin, S. H., Peng, C. F. Treatment of textile wastewater by electrochemical method. Water Research 1996; 30: 587-592.
248. Vlyssides, A. G., Loizidou, M., Karlis, P. K., Zorpas, A. A., Papaioannou, D. Electrochemical oxidation of a textile dye wastewater using a Pt/Ti electrode Journal of Hazardous Materials 1999; B70: 41-52.
249. Szpyrkowicz, L., Juzzolino, C., Kaul, S. N., Daniele, S., De Faveri, M. D. Electrochemical oxidation of dyeing baths bearing disperse dyes. Industrial and Engineering Chemical Research 2000; 39 (9): 3241-3248.
250. Cañizares, A., Gadri, J., Lobato, B., Nasr, R., Paz, M., Rodrigo, A., Saez, C. Electrochemical oxidation of azoic dyes with conductive-diamond anodes. Industrial and Engineering Chemical Research 2006; 45 (10): 3468-3473.
251. Murthy, Z. V. P., Nancy, C., Kant, A. Separation of pollutants from restaurant wastewater by electrocoagulation. Separation Science and Technology 2007; 42 (4): 819-833.
252. Chang, H. The presence of Cu(II) in lithium bromide refrigerant resulting from corrosion of copper parts. Separation and Purification Technology 2006; 52 (1): 191-195.

Chapter 3

Materials and Methods

3 Materials and Methods

3.1 Introduction

A general description of techniques and procedures used throughout the project for the study of floc behaviour is given here. The design and construction of an instrumental laboratory scale EC reactor is also provided and investigates the effects on floc of different electrochemical parameters. Variations to any particular experimental procedures are given where appropriate.

3.2 Electrocoagulation Design

3.2.1 Reactor Design

The experimental EC reactor used for all experiments was developed from deciding between the three dominant hierarchical questions listed below:

1. Batch or continuous mode?
2. Coagulation only, or coagulation and flotation?
3. Additional separation processes post-EC?

The way in which these three questions were answered, decided how best to design the reactor. As the predominance of work encountered in industry is dependent upon operating in continuous mode, with the goal of generating coagulation only without flotation, and the expectance of having additional separation processes such as decanter tanks/lamella tanks present post-EC, it was decided to use a single pass hermetically sealed EC reactor (cell) as shown in Figure 3.1 on the following page.

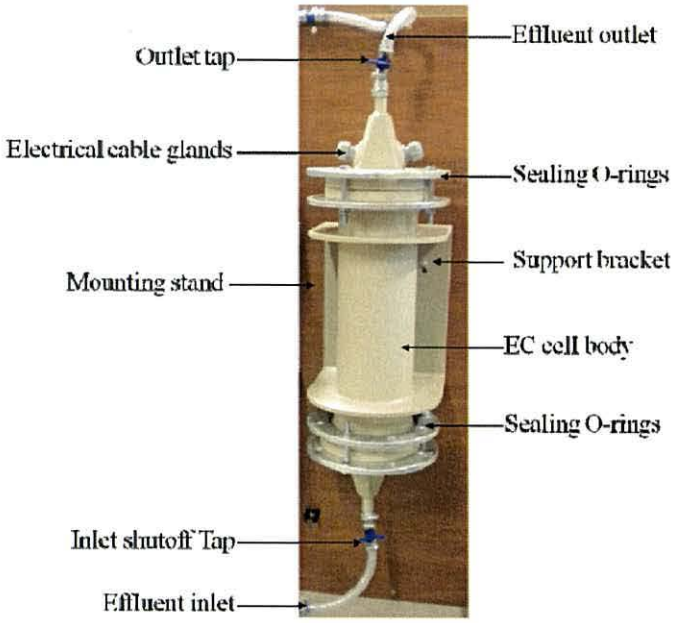

Figure 3.1. Electrocoagulation reactor (cell) used.

The continuous mode EC cell was constructed of polypropylene material with overall dimensions 900 × 250 × 280 mm and was mounted vertically onto a support stand that could sit atop a work bench.

3.2.2 Electrode Design

The design of the electrodes used was entirely dependent on the type of coagulant to be released. Iron cations and their hydrolysed derivatives were the desired coagulant in this study and hence mild steel electrodes (material grade code CR4) were used for both the anode and cathode. Figure 3.2 on the following page illustrates the assembly of the electrode pack used.

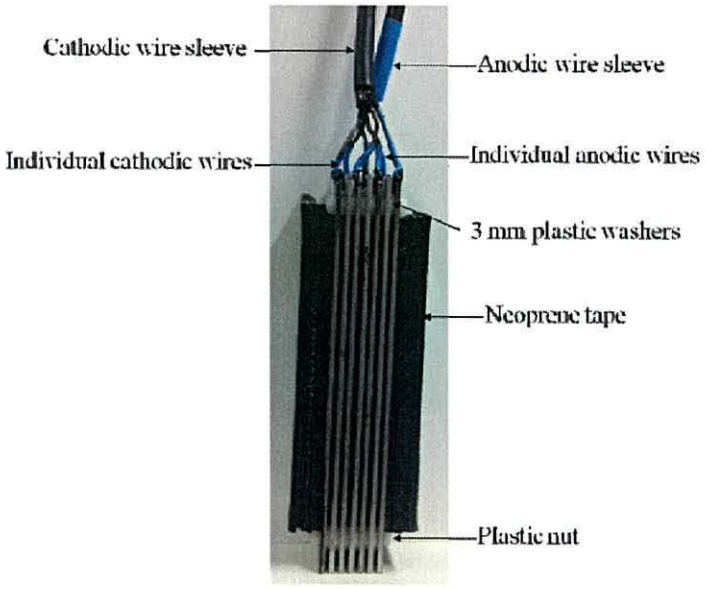

Figure 3.2. Mild steel electrode pack designed to deliver iron coagulant into solution.

The electrode arrangement consisted of three anodes and four cathodes with dimensions 250 × 55 × 3 mm. Inter-electrode distance was set at 3 mm using plastic washers (3 mm width) that were placed in between electrodes at the bottom and top corners of each electrode. The washers were held in placed *via* plastic studding that ran through the electrode assembly and were held in place with plastic securing nuts. The electrode pack was connected in mono-polar mode as depicted in Figure 3.3.

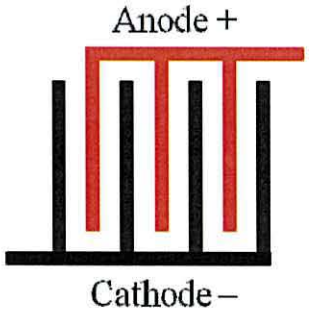

Figure 3.3. Monopolar electrode connections in the EC reactor.

Electrical connections were made by welding and hermetically sealing individual electrical wires to separate electrodes and gathering them in anodic and cathodic groupings. The grouped wires were then encased in separate insulating plastic sleeves that were directed towards the power supply. The electrode pack was fitted inside the EC cell with non-conducting, water resistant neoprene tape to fill the void at either side of the electrodes with the cell walls and thus prevent effluent from travelling up the cell wall sides bypassing the electrode pack.

3.3 Effluent

Coagulation experiments were conducted using two different effluent sources. Initial trials were carried out on effluent containing 0.2 mmol/L phosphorus (P), from a wastewater treatment plant. Later trials were carried out on a synthetic solution containing a suspended solids loading content of 1 g/L macerated dog food in 1.5% saline (NaCl, laboratory grade, Fisher Scientific) tap water.

The phosphorus effluent was comprised of trickling bed filter effluent sampled from an inter-process channel between trickling filters and humus tanks following tertiary treatment of human cellulose matter. The phosphorus contamination was a result of point and diffuse sources of; human wastes, animal wastes, and human disturbances of land and vegetation (farming practices leading to arable runoff). The synthetic suspended solids solution was generated to mimic raw human cellulose matter in diluted saline water from marine ships. These types of effluent are typical of industry therefore it is meaningful to work with these kinds of effluents.

The pH of effluent volumes were adjusted to desired values using solutions of 8.3 mol/L sodium hydroxide (NaOH, 98%, Fisher Scientific) and 15.8 mol/L nitric acid (HNO_3, 70%, Fisher Scientific). Raw composition of the solutions used is detailed in Table 3.1.

Table 3.1. Physicochemical characteristics of effluent solution used.

Parameter	Tricking filter effluent	Suspended solids effluent
P concentration (mmol/L)	0.2	0.0
Total suspended solids (g/L)	0.0	1.0
Turbidity (NTU)	35.3	209.1
Conductivity (mS/cm^2)	0.8	35.4
pH	7.5	7.2

3.4 Experimental Set-Up

3.4.1 Chemical Coagulation Experiments

Conventional chemical coagulation experiments were carried out by performing a series of jar tests with the addition of 1.5 mol/L ferric chloride solution. A variable speed flocculator (Stuart Scientific, model SW1, UK) was used with 76 × 25 mm flat paddle impellers immersed in cylindrical jars containing 1 L samples of effluent. Two speeds were used during the ferric chloride addition with a rapid mix at 100 rpm for 3 min employed

initially, followed by a slow-stir phase at 25 rpm for 3 min thereafter.[253] Samples were then left to stand quiescently for 30 min to allow solutions to uncoil fully and settle out. The ferric chloride-based coagulant used was prepared from a 40% w/v stock solution of ferric chloride ($FeCl_3.6H_2O$, 97%, Fisher Scientific).

3.4.2 Electrocoagulation Experiments

Prior to each EC experiment, electrodes were immersed in 0.6 mol/L phosphoric acid (H_3PO_4, 85%, Fisher Scientific) for one hour to chemically clean the mild steel plates and to remove any impurities. The electrodes were then rinsed repeatedly with deionised water (Elga, nominal resistivity 18.2 MΩ cm, USA) to remove any excess acid and expose fresh metallic surfaces.

The electrode pack was connected to a single phase 2.1 kW (70 V/30 A) direct current (DC) power supply unit (Wayne Kerr Electronics, model AP7030A, UK) operated in galvanostatic mode. In this mode, current intensity to the electrodes was held constant with the cell potential allowed to vary to maintain the current requirement. The current and cell potential across the electrodes was recorded through the power supply. A peristaltic pump (Cole-Parmer Instrument Company, model Masterflex L/S, UK) was used to pump effluent into the EC cell from an effluent source tank that was held under constant agitation (1,000 rpm) using a magnetic stirrer (Scientific Industries, model MegaMag Genie, USA) and stir bar to maintain effluent homogeneity. Figure 3.4 on the following page shows schematically how the EC system was set up to operate.

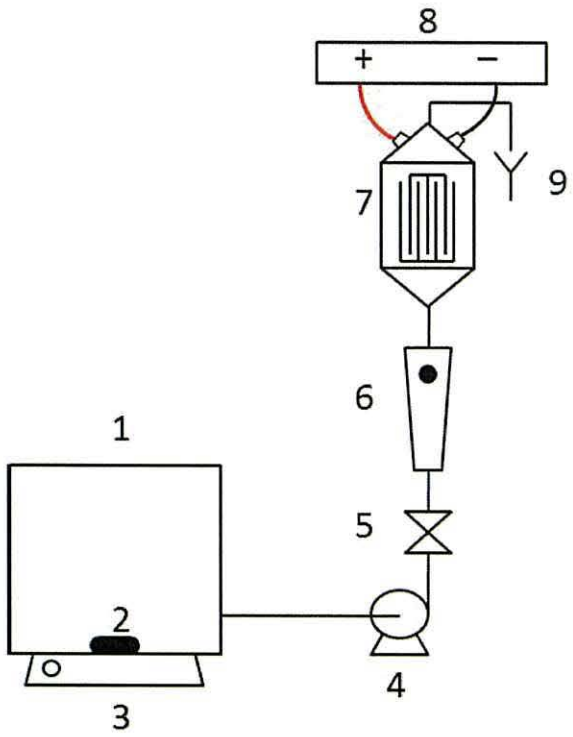

Figure 3.4. Experimental EC system; 1 – effluent source tank; 2 – magnetic stir bar; 3 – magnetic stirrer; 4 – peristaltic pump; 5 – flow control valve; 6 – flow meter; 7 – EC cell; 8 – power supply; 9 – sample collection.

The amounts of iron dissolved during EC experiments were theoretically calculated from a derivation of Faraday's law (Equation 10) and through the establishment of a coagulant dose calibration plot shown in Figure 3.5. This plot expresses the relationship between the amount of iron dissolved and current density at constant flow rate.

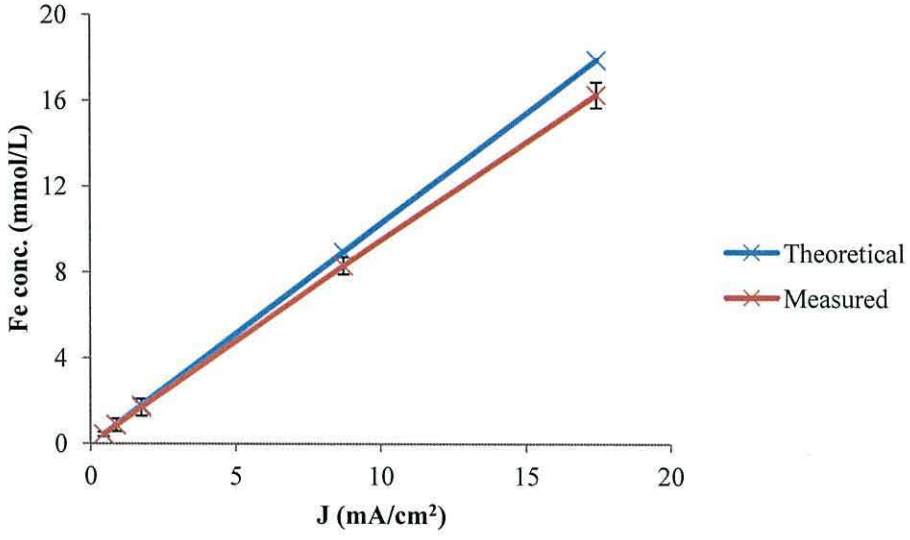

Figure 3.5. Theoretical and actual iron concentration *vs.* current density (error bars shown on *Measured* data points are ± 1 SD).

At the lower current densities of 0.4 to 0.9 mA/cm^2 the deviation between theoretical measurements of electro-dissolved iron and measured concentrations was 1.5% and 2.8%.

At 1.8 mA/cm^2 the difference between theoretical and measured concentrations was 5%, whilst at 8.7 mA/cm^2 and 17.5 mA/cm^2 the deviation increased to 7.2% and 9.1%. The difference is negligible at the lowest current density of 0.4 mA/cm^2 but at the higher settings (0.9 to 17.5 mA/cm^2) the deviation between theoretical and measured was incorporated to attain a true iron concentration at higher current densities. Table 3.2 displays the actual current densities required to deliver true concentrations of iron as calculated from Equation 10 (section 2.5.5).

Table 3.2. Revised current densities to achieve true iron concentrations.

Calculated current density (mA/cm^2)	Theoretical Fe conc. (mmol/L)	Measured Fe conc. (mmol/L)	Deviation between theoretical & measured conc. (%)	Revised current density to achieve true iron conc. (mA/cm^2)
0.44	0.45	0.44	1.50	0.44
0.87	0.90	0.87	2.80	0.89
1.75	1.79	1.70	5.00	1.84
8.73	8.95	8.31	7.20	9.36
17.45	17.91	16.28	9.10	19.04

Subsequently, in order to achieve a measured iron concentration of 17.9 mmol/L, the current density was increased by 9.1% from 17.5 to 19 mA/cm^2 (figures rounded up to 1 decimal place), to take into account the 9.1% deviation between theoretical and measured iron concentrations. This is relevant to sections 5.3.1 and 6.5 in chapters 5 and 6, respectively.

A combined pH/conductivity probe (Hanna Instruments, model HI98129, USA) was used to measure conductivity and pH of the solutions pre and post treatment. All experiments were performed in triplicate at ambient conditions thus temperature was approximately 19 – 25^o C. All experimental variables of EC and chemical coagulation that were studied are presented in Table 3.3.

Table 3.3. Summary of experimental variables studied for EC and chemical coagulation experiments.

Experiment	Parameter	Range tested
Electrocoagulation	Coagulant dose (mmol Fe/L)	0.4 – 17.9
	Conductivity (mS/cm^2)	12.5 – 51.4
	Current density (mA/cm^2)	0.4 – 18.5
	Electrolysis time (sec)	5.0 – 150.0
	Floc retention time (min)	10.0 – 1,440.0
	Inter-electrode distance (mm)	1.5 – 24.0
	pH	3.0 – 11.0
	Pollutant concentration (g/L)	0.1 – 1.0
	Stirrer speed (rpm)	50.0 – 800.0
Chemical coagulation	Coagulant dose (mmol Fe/L)	0.2 – 0.7

3.5 Analysis

A range of techniques were used to measure pollutant removal rates, amount of iron delivered into solution, and characterisation of floc particles produced.

3.5.1 Atomic Absorption Spectrometry

Total iron ($Fe^{2+/3+}$) analysis was carried out using atomic absorption spectrophotometry (AAS) (Agilent Technologies, model 220FS AA, USA). This technique is based upon electron excitement and radiation absorption. A sample, in aqueous form, is aspirated into an air/acetylene gas flame where the element of interest (iron) is dissociated from its chemical bonds and placed in a non-ionised state. The released individual atoms are now capable of absorbing radiation of wavelengths characteristic of the element.[254] Absorbed radiation, provided by an iron hollow-cathode lamp (Agilent Technologies, SpectrAA Fe lamp, USA) filled with argon (Ar), is measured by a photomultiplier mounted on the opposite end of the analyser. The amount of radiation absorbed is proportional to the concentration of the element being determined.

3.5.2 Ultraviolet-visible Spectrometry

Ultraviolet-visible spectroscopy (UV-Vis) (ATI Unicam, model UV 4, UK) was employed to measure concentrations of Fe^{2+} ions only in solution during electrocoagulation trials. Used in conjunction with AAS, this spectrometric method allows for the analysis of both total iron content (AAS) and Fe^{2+} ion content in samples. By subtracting Fe^{2+} concentrations from total iron concentrations, the presence of Fe^{3+} ions is given. This analysis was important in deriving the ratio of Fe^{2+}:Fe^{3+} in EC treated solutions and for indicating the conversion rate of Fe^{2+} to Fe^{3+} post coagulant addition.

The selective capability of UV-Vis to measure Fe^{2+} ions is due to the spectrophotometric 1,10-phenanthroline method of analysis.[255] Ferrous ions reacts with 1,10-phenanthroline to form an orange-red complex $[(C_{12}H_8N_2)3Fe]^{2+}$ the colour of which is dependent on the concentration of Fe^{2+} present. The iron-phenanthroline complex is then extracted out with nitrobenzene and measured at 512 nm against a reagent blank. Figure 3.5 on the following page shows the spectrometric scan from 400 – 600 nm that was ran on a known sample indicating that maximum absorption (λ max) occurred at 512 nm.

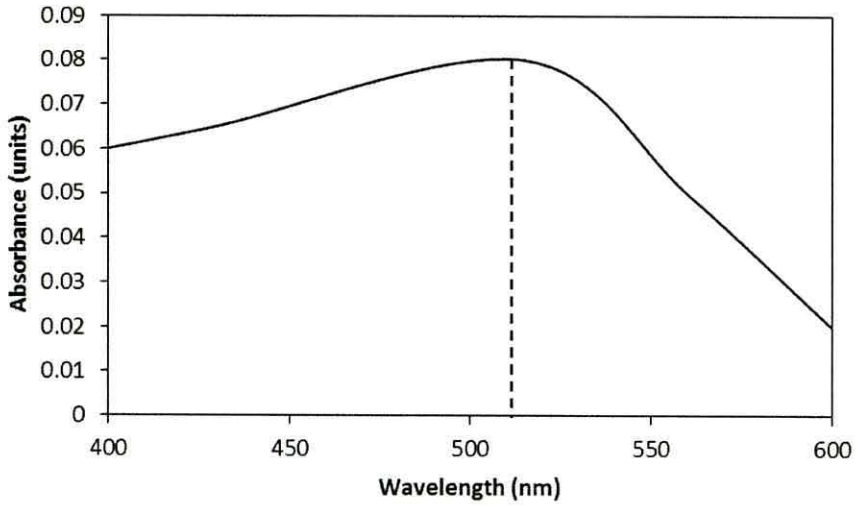

Figure 3.5. UV-Vis spectrometric scan showing maximum absorption peak (λ max) at 512 nm.

3.5.3 Inductively Coupled Plasma-Optical Emission Spectrometry

Phosphorus analysis was carried out to determine the degree of pollutant removal efficacy of floc formed during the EC and chemical coagulation trickling effluent trials. An inductively coupled plasma-optical emission spectrophotometer (ICP-OES) (Jobin-Yvon, model JY138, France) was used to measure phosphorus concentrations in samples collected post-treatment. This technique relies on excited electrons emitting energy at given wavelengths upon their return to ground state. An aliquot of sample is sprayed into an argon flame where it is atomised. Although each element emits energy at multiple wavelengths, the ICP-OES technique depends on selecting a single wavelength for a given element. The intensity of energy emitted is proportional to the concentration present within the sample. By determining which wavelengths are emitted by the sample, along with their intensities, the elemental composition of the sample can be quantified relative to a standard.[256] The efficiency of pollutant removal (e.g. phosphorus), R (%), was calculated using Equation 15:

$$R(\%) = \frac{T_i - T_f}{T_i} \times 100 \qquad \textbf{Equation 15}$$

Where T_i is the raw pollutant concentration (mmol/L) and T_f is the residual pollutant concentration post-treatment (mmol/L).

3.5.4 Turbidity

Before and after EC treatment of the synthetic solids solution, turbidity was recorded using a turbidimeter (Oakton, model T-100, UK). As an optical measurement parameter, turbidity is widely used as a performance marker for water clarity and is often related to total suspended solids concentrations.[257] As such, it was used to monitor solids removal as an indicator of floc efficacy. Results were expressed in nephelometric turbidity units (NTU) with measurement accuracy within ± 2% of the final reading, or 0.05 NTU. A silicon photodiode centred at 90° to the incident light path was used as the photodetector.

3.5.5 Total Suspended Solids

Residual total suspended solids (TSS) concentration in samples treated *via* EC and chemical coagulation were analysed following the standard method of total suspended solids dried at 103 – 105° C.[258]

Homogenised supernatant aliquots of 100 mL volumes from settled samples were vacuum filtered through weighed standard glass-fibre filters (porosity 0.45 μm) and dried for one hour before being left to cool in a desiccator to balance temperature. The dried filters were then re-weighed and the cycle of drying, cooling, desiccating and re-weighing was repeated until constant weights were obtained or until the weight difference was less than 4% of the previous weight. Duplicate samples were carried out in some instances and average weights were in agreement to within 5% of their average. The increase in weight of the dried filters represented the total suspended solids present in the supernatant. Equation 16 outlines the residual TSS calculation carried out.

$$mg\ total\ supended\ solids/L = \frac{(A-B) \times 1000}{\text{sample volume (mL)}} \qquad \textbf{Equation 16}$$

Where A is weight of filter + dried residue (mg), and B is weight of filter only (mg).

3.5.6 Dissolved Oxygen

A portable dissolved oxygen (DO) probe (Hanna Instruments, model HI 9146, USA) was used to measure the amount of gaseous oxygen present in effluent during and after EC treatment. The probe utilised a Clark-type polarographic electrode capable of sensing oxygen concentration in aqueous solutions.

A platinum (Pt) cathode and a silver/silver chloride (Ag/AgCl) reference anode in potassium chloride (KCl) electrolyte separated by a gas-permeable plastic membrane in built into the tip of the dipping probe was immersed into 1 L effluent samples. In order to read a DO concentration, a fixed voltage is applied to the Pt electrode and as oxygen diffuses through the membrane to the cathode, it is reduced whilst oxidation occurs at the Ag/AgCl anode. Accordingly, a current will flow that is proportional to the rate of oxygen diffusing and is in turn related to the concentration of DO. The current is converted to a proportional voltage that is amplified and sent to the reader which converts the voltage reading to a concentration measured in mg/L and displays the read out on the hand held monitor.[259]

3.6 Characterisation

In order to characterise the floc complexes produced during trial work and the impact on the electrodes, a range of techniques were used; cyclic voltammetry, nano-arrayer imaging, scanning electron microscopy, transmission electron microscopy, and zeta potential measurement. These are discussed in turn in the following sub-sections. Characterisation results are given in Chapter 6.

3.6.1 Cyclic Voltammetry

Cyclic voltammetry (CV) was used to characterise the impact of oxygen presence in solution on the surface electrochemistry of the mild steel electrodes used during trials. Trickling filter bed effluent was chosen for the voltammetric studies over the synthetic colloidal solution to minimise solids fouling in the potentiodynamic system. The pH of the effluent was 7.2.

Electrochemical experiments were carried out in a classical three-electrode glass cell. This consisted of a reference electrode, working electrode, and a counter electrode. In these types of experiments, a triangle-wave potential is applied to a system under investigation and the faradaic current response measured. This current is measured over a set of potentials from an initial value to a predetermined end value. After scanning the entire range it is reversed and the potential range is scanned backwards. This is done to allow species that have been oxidised during the forward scan, to be reduced in the reverse scan.

From this, information such as redox potential and electron transfer rate between analyte and electrode is gathered.[260]

For the experiments, the working electrode was positioned horizontally with the active surface (0.13 cm^2) set upwards. The electrolyte was left unstirred during the experiments. Potentials were measured against a saturated calomel electrode (SCE) due to the convenience of this half-cell over a standard hydrogen electrode (SHE) which relies on freshly prepared platinum electrodes, very accurately determined hydrogen chloride (HCl) solution concentration, and the safe provision of a hydrogen (H_2) gas source at 1 atm pressure. These conditions made the SHE difficult to use experimentally. A Pt electrode was used as the counter. The relationship between SCE to SHE is shown in Figure 3.6.

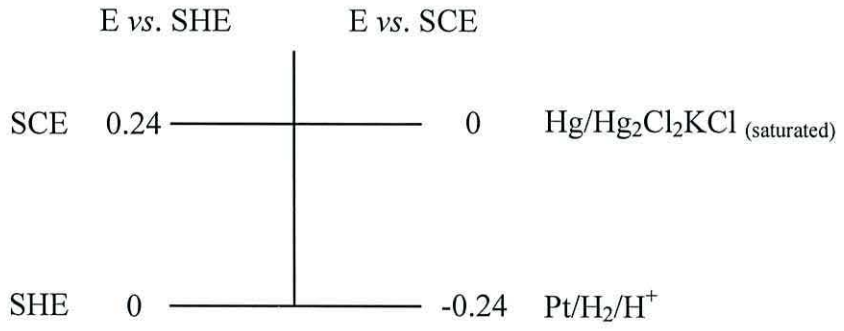

Figure 3.6. Relationship between SHE and SCE.

Cyclic voltammetry experiments were performed at room temperature with a potentiostatic system (EcoChemie B.V., model Autolab PGSTAT30, Netherlands). One successive cycle was performed between -2 V/SCE and 2 V/SCE with a scan rate dE/dt of 100 mV/s. This potential range was chosen so as to induce hydrogen formation in the cathodic part and iron dissolution in the anodic part. High purity nitrogen was used for de-aeration, while ambient air was used for aerating the cell, the gas flow being 150 mL/min in either case.

3.6.2 Nano-arrayer

A nano-arrayer is a surface patterning platform for the dispersal of nanoparticles onto a surface.[261] However, it was the imaging camera used by operators to align nanoparticles onto a substrate that was of interest. Capable of measuring in the micrometre range, the nano-arrayer (Nano eNabler™ System, BioForce Nanosciences Inc., USA) camera was a 8.5 mm colour charge-coupled device (CCD) with 640 × 480 pixel resolution. With this feature it was possible to see individual floc particles within a solution volume.

Samples for imaging were prepared by pipetting one drop of flocculated solution onto a glass slide and covering carefully with a small, thin glass cover-slip. The slide was then placed atop the sample block of the nano-arrayer and the imaging camera lowered until it contacted the cover-slip. The camera was then focussed to provide detailed morphology, shape and size of flocculated particles. Within the software of the analyser it was capable to draw a ruler line (in micrometres) that was used to provide scale to the imaged particles.

3.6.3 Scanning Electron Microscopy

A scanning electron microscope (SEM) (Hitachi, model S-520, Japan) was used to obtain images of used electrode plate surfaces. One litre solutions containing settled floc were decanted to remove the top supernatant volume before being heated at 70° C in an oven for seven days to evaporate the remaining liquid content. Dried floc samples were then prepared for imaging by ultrathin gold coating (Polaron Equipment Ltd, model SEM Sputtering Unit E5000, UK) to prevent a build-up of surface charge on the non-conducting samples. SEM pictures were taken at 10 kV at various magnifications.

Images produced *via* an SEM are the result of a sample undergoing scanning by a focused beam of accelerated electrons. These electrons, emitted by an electron gun held above the sample, carry significant amounts of kinetic energy that are directed downwards through electromagnetic fields and lenses within the vacuum sealed microscope to focus them onto the sample. Once the electron beam hits the sample, the energy carried is dissipated as a variety of signals during interactions with the electrons present within the sample as a consequence of deceleration of the incident electrons in the solid sample. The various signals that are produced such as photons (characteristic X-rays), visible light (cathodoluminescence – CL), secondary electrons and backscattered electrons (BSE) are detected and contain information about the sample's topography. Detectors inside the microscope collect the X-rays, BSE and secondary electrons converting them into a signal that is sent to an imager and relayed onto a display monitor. The electron beam is scanned in a raster scan pattern meaning a sample is progressively scanned in a systematic line-by-line fashion. This produces a highly detailed image of the sample that can be magnified to the micrometre range. [262]

3.6.4 X-Ray Diffraction

X-ray diffraction was performed on a limited number of selected samples to confirm the presence of magnetite in EC derived floc. A Siemens 5000 powder x-ray diffractometer was employed for these investigations. The unit consisted of a constant-potential X-ray generator operating at 45 kV:40 mA with a copper target operated at room temperature. The spectrum scanning rate was set at 2-theta (θ)/min. Flocculated samples suspected of containing magnetite floc particles were prepared in the same way to achieve the dried flocculant as set out in the previous section for SEM. The dried floc was then ground to a fine powder (approximately 10 μm) and placed into the sample holder inside the diffractometer.

X-rays generated in a cathode ray tube *via* heating a filament to produce electrons are accelerated towards the target sample that is rotated by applying a voltage. These electrons bombard the rotating target material dislodging inner shell electrons of the sample material and producing X-ray spectra whose wavelengths are characteristic of the sample material. A detector inside the diffractometer records and processes the X-ray spectra produced and converts the signal to a count rate which is displayed on the machine's software as a graphical output of intensity *vs*. 2-θ. The 2-θ refers to the angle of rotation that the X-ray detector is turned through to collect X-rays diffracted off the sample which is itself rotated at an angle θ. Typically, for powder patterns, data is collected at 2-θ from 5° – 70° and the instrument used to maintain the angle and rotate the sample is a goniometer.[263]

3.6.5 Transmission Electron Microscopy

Transmission electron microscopy (TEM) was carried out to image floc sizes. The technique is very similar to SEM in that a beam of electrons is transmitted through a specimen with images formed from the interactions of those electrons with those present in the sample. The main difference however is the greater amount of detail that can be elicited from samples owing to the utilisation of the small de Broglie wavelength of electrons.[264]

De Broglie wavelength electrons refer to those that express wave-particle duality in quantum mechanics. This enables a TEM analyser to achieve finer detail down to being able to image a single column of atoms in the nanometre range, tens of thousands of times smaller than the smallest resolvable object in a traditional microscope. This technique was

used in conjunction with the nano-arrayer to image floc particles formed under various electrochemical parameters for analysis.

3.6.6 Zeta Potential

Zeta potential, denoted as ζ-potential, is an experimental measure of the effective charge of a particle in a colloidal system as it moves through the solution, providing a direct indicator of solution stability. It is a measure of the potential difference between the dispersion medium and the stationary layer of fluid attached to a dispersed particle.

If particles in a suspension have a large negative or positive ζ-potential they will repel each other due to significant electrostatic repulsive forces dominating and there will be no tendency for them to aggregate. However, if particles have low ζ-potential values this confers that attraction exceeds repulsion and van der Waals forces dominate allowing particles to flocculate. Zeta potential measurements therefore have the capacity of predicting the potential stability of a colloidal system and whether or not it will coagulate.

Colloids with high ζ-potential (negative or positive) are therefore electrically stable while colloids with low ζ-potential will aggregate. Table 3.4 summarises colloidal stability in relation to ζ-potential measurements.

Table 3.4. Colloidal stability chart based upon zeta potential.

Colloidal stability behaviour	ζ-potential (mV)
Rapid coagulation	0 – ±5
Incipient instability	±10 – ±30
Moderate stability	±30 – ±40
Good stability	±40 – ±60
Excellent stability	>±61

The general dividing line between stable and unstable suspensions is taken at either +30 or -30 mV. Particles with ζ-potential greater than +30 mV or more negative than -30 mV are considered stable.[265]

All ζ-potential measurement were carried out on an analyser (Malvern Instruments, Zetasizer 3000 HS, UK) that determines ζ-potential by using a combination of laser Doppler velocimetry and phase analysis light scattering (PALS) to measure particle electrophoretic mobility in an aqueous sample.

A sample receptacle is placed inside the analyser and a laser is shined onto it to provide light to illuminate the particles within the sample. This light source is then split to provide an incident and a reference beam of which the incident laser beam passes through the centre of the sample. The scattered light at an angle of 13° is detected and when an electric field is applied to the sample any particle movement that occurs will cause the intensity of light detected to fluctuate with a frequency proportional to the particle speed. This information is then passed to a signal processer and relayed to a computer which outputs a frequency spectrum that is then used to calculate the electrophoretic mobility and hence zeta potential.

3.7 Experimental Design

The preliminary experimental variables outlined in Table 3.2 were divided into three experimental sets; A – C, as summarised in Table 3.5.

Table 3.5. Summary of electrocoagulation experiments conducted in sets A – C.

Experimental Set	Determinant	Experimental motivation
A	Coagulant concentration effect	Determine critical electrocoagulant mass for flocculation
B	Dissolved oxygen effect	Investigate floc formation in higher oxygenated solutions
C	Coagulant dilution effect	Evaluate floc removal efficiency against dilution

These experimental sets were specifically designed to determine the optimum use and development of the EC reactor and to determine a coagulant dose range. Chapter 5 is devoted to the analysis of key electrochemical parameters involved in EC and quantifying any trend developments in relation to floc formation. The following sub-sections detail the experiments ran.

3.7.1 Experiment Set A

The first set of experiments aimed to establish the minimum EC coagulant concentration where flocculation was observed. Initially, conventional chemical coagulation trials were undertaken on raw trickling effluent to determine a reference iron dose where chemical flocculation occurred. Ferric ion concentrations of 0.2, 0.4, 0.5, 0.7 mmol Fe/L were added to 1 L samples of effluent and adjusted to pH 7 to neutralise the drop in acidity as a consequence of the ferric chloride addition. Samples were then jar-tested and settling times of 0, 10, 20, 30, 40, 50, and 60 min were separately studied by running replicate tests. A settling time of 30 min was found to be the most appropriate duration in the experiments.

Following this, 10 mL supernatant aliquots per treated sample were taken from a fixed depth of 2 cm below liquid surface level for residual phosphorus analysis.

Electrocoagulation experiments were then carried out to determine the required iron dose rate where flocculation would occur electrochemically. This was done to compare the mass of iron needed to induce flocculation between EC and conventional chemical coagulation. An identical iron concentration range of 0.2, 0.4, 0.5, 0.7 mmol Fe/L was tested. Raw effluent was pumped into the EC cell at flow rates of 0.4 – 1.4 L/min whilst current density was held constant at 1 mA/cm^2. One litre samples were collected per coagulant dose investigated and jar-tested followed by a 30 min quiescent phase. Supernatant aliquots of 10 mL were extracted 2 cm below liquid level for residual phosphorus analysis.

3.7.2 Experiment Set B

The second set of experiments was designed to investigate the impact of dissolved oxygen in EC treated effluent on flocculation.

Mixing Regime I

Immediately post-EC treatment two mixing stages were introduced as a method of increasing dissolved oxygen content in treated effluent. Directly from the outlet of the EC cell, coagulated effluent was directed to a 0.5 L volume vessel that was held under constant vigorous agitation (stage 1 mixing) *via* a magnetic stirrer and stir bar set at 100 rpm stirrer speed. Following this, effluent was then transferred to a slow mixing stage (stage 2 mixing) comprised of a 1 L volume vessel gently agitated with a paddle mixer set at 25 rpm stirrer speed. Figure 3.7 on the following page illustrates how the apparatus was set up to include the two mixing stages.

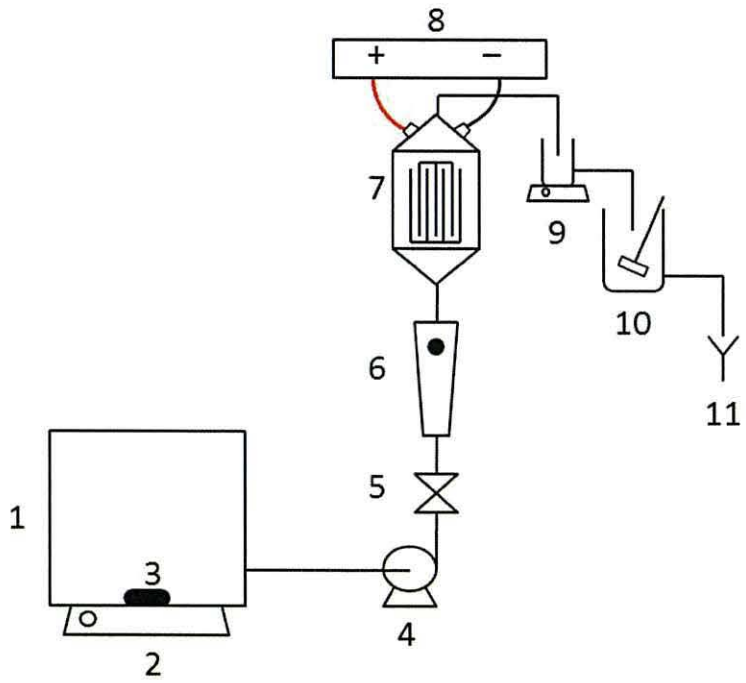

Figure 3.7. EC equipment with mixing stages; 1 – effluent source tank; 2 – magnetic stirrer; 3 – magnetic stir bar; 4 – peristaltic pump; 5 – valve; 6 – flow meter; 7 – EC cell; 8 – power supply; 9 – stage 1 mixing; 10 – stage 2 mixing; 11 – sample collection.

Electrocoagulant derived iron concentrations of 0.2, 0.7, 1.4 and 2.9 mmol Fe/L were tested. Raw effluent was pumped into the EC cell at a constant flow rate of 0.5 L/min and current density was altered from 0.3 – 5.6 mA/cm^2 to achieve the desired coagulant range. Residence times in stage 1 and stage 2 mixing vessels were 1 and 2 min, respectively. One litre samples were collected from the outlet of the stage 2 mixing vessel and subjected to a 30 min quiescent period. Aliquots of 10 mL supernatants volumes were then collected 2 cm below liquid level from the settled samples for residual phosphorus analysis.

Mixing Regime II

A secondary mixing regime was also tested under identical operating parameters but stage 1 mixing vessel was substituted for a smaller 250 mL volume, providing a residence time of 30 sec, and agitated at an increased stirrer speed of 1,000 rpm. This was done to understand if a shorter, faster agitation stage, immediately following EC, would benefit floc formation through altering the levels of dissolved oxygen within the effluent. Once again, 1 L samples were collected after stage 2 mixing and were allowed a 30 min quiescent phase prior to 10 mL supernatant aliquots being extracted 2 cm below liquid surface levels for residual phosphorus analysis.

3.7.3 Experiment Set C

The third set of experiments carried out was based on investigating the generation of a concentrated stream of coagulated effluent and diluting it into a larger volume of raw effluent. This was done with a view of determining if diluting floc, post-generation, could still affect pollutant coagulation and to what extent. As experiment sets A and B were primarily concerned with identifying factors responsible for generating floc, set C was designed to understand the fate of manipulating pre-formed flocculant and its dilution with raw effluent.

Initially, a 0.7 mmol Fe/L coagulant dose (0.5 L/min flow rate; 1.4 mA/cm^2 current density) was delivered into effluent within the EC cell. This dosed effluent from hereon will be referred to as concentrated coagulant effluent (CCE). Following the passage through stage 1 and stage 2 mixing phases, various CCE volumes were collected and introduced into raw effluent volumes to generate 1 L samples of diluted floc. The 1 L samples were allowed a 30 min quiescent phase before 10 mL supernatant aliquots was extracted for residual phosphorus analysis. Table 3.6 details the volumes of CCE and raw effluent used and the dilution ratios investigated.

Table 3.6. Dilution ratios of concentrated treated effluent to raw effluent.

Coagulant dose (mmol Fe/L)	CCE volume (mL)	Raw effluent volume (mL)	Dilution ratio	Final coagulant dose (mmol Fe/L)
0.7	770.0	230.0	1:1.3	0.5
0.7	500.0	500.0	1:2.0	0.4
0.7	250.0	750.0	1:4.0	0.2

3.7.4 Electrochemical Parameter Study

Details of Chapter 5 experiments are presented here in the following sub-sections. These trials were designed to isolate and test individual electrochemical parameters for their effect on floc formation and development. In order to quantify their impact on flocculation, the synthetic solids effluent was used during these trials as greater control over the constituents of the effluent was achievable thereby allowing reproducibility of the effluent. This could not be guaranteed with the trickling bed filter effluent owing to its nature and source.

Residual total suspended solids (TSS) concentrations in treated settled supernatant volumes were used to evaluate electrocoagulation's floc formation response to changing operational parameters.

The preferred method of analysing the effect of parameter changes on floc formation was to return to employing direct dosing without producing CCE and subsequently diluting into raw effluent. This was chosen as it was decided this method would provide a more accurate view of emerging patterns and relationships between the two without the added influence of CCE dilution. A feasibility trial identifying whether flocculation would occur *via* direct dosing revealed that an initial coagulant dose of 1.8 mmol Fe/L was sufficient to induce flocculation and achieve a reduction in the 1 g/L raw TSS concentration of 90%. Consequently, baseline parameters of 0.25 L/min flow rate and 1.8 mA/cm^2 current density (equating to a coagulant dose of 1.8 mmol Fe/L) were observed during the parametric trials. Raw effluent was pumped into the EC cell and whereupon it expelled from the reactor, 1 L samples were collected and jar-tested. Following a 30 min settlement period, supernatant volumes from the settled samples were then analysed for residual TSS. The mass balance changes in TSS between raw and residual concentrations was then used to infer floc efficacy and this was used to allude to any emerging relationships between floc formation and changes in operational parameters. The arrangement of the EC equipment for the parametric studies was therefore reconfigured as shown in Figure 3.4 (section 3.4.2).

Pollutant Loading Studies

The concentration of suspended solids was altered to investigate the effect of pollutant loading on floc formation. For these trials five batches of effluent containing various loadings of 0.1, 0.25, 0.5, 0.75 and 1 g/L was ran through the EC cell. Constant parameters observed were: 0.25 L/min flow rate; 1.8 mA/cm^2 current density; coagulant dose 1.8 mmol Fe/L; electrolysis time 59 sec; inter-electrode distance 3 mm; effluent pH 7.2; effluent conductivity 35 mS/cm^2.

Inter-Electrode Distance Studies

Five different electrode packs were assembled each with various electrode spacing's to test 1.5, 3, 6, 12 and 24 mm inter-electrode distances on floc formation. Each pack was inserted

in turn into the EC chamber and trialled with. Constant parameters observed were: 0.25 L/min flow rate; 1.8 mA/cm^2 current density; coagulant dose 1.8 mmol Fe/L; 1 g/L pollutant loading; effluent pH 7.2; effluent conductivity 35 mS/cm^2.

Coagulant Dose Studies

The amount of coagulant electro-dissolved into solution was experimented with in order to determine its impact on floc formation. Dosages of 0.5, 0.9, 1.8, 9 and 17.9 mmol Fe/L were trialled with at constant flow rate of 0.25 L/min whilst current density was altered from 0.4 to 19 mA/cm^2 to achieve the various coagulant doses using Figure 3.5 in section 3.4.2. Constant parameters observed were: electrolysis time 59 sec; inter-electrode distance 3 mm; 1 g/L pollutant loading; effluent pH 7.2; effluent conductivity 35 mS/cm^2.

Current Density Studies

Current densities of 0.4, 0.9, 1.8, 9.4, and 19 mA/cm^2 were investigated for their effect on flocculation. Constant parameters observed were: 0.25 L/min flow rate; electrolysis time 59 sec; inter-electrode distance 3 mm; 1 g/L pollutant loading; effluent pH 7.2; effluent conductivity 35 mS/cm^2.

Agitation Studies

The stirrer speed of 1 L samples collected post-EC was altered to assess the impact of agitation on floc formation. Speeds of 50, 100, 200, 400 and 800 rpm were tested for an initial 3 min interval on electrocoagulated effluent followed by a constant agitation of 25 rpm for 3 min thereafter. Constant parameters observed were: 0.25 L/min flow rate; 1.8 mA/cm^2 current density; coagulant dose 1.8 mmol Fe/L; electrolysis time 59 sec; inter-electrode distance 3 mm; 1 g/L pollutant loading; effluent pH 7.2; effluent conductivity 35 mS/cm^2.

Electrolysis Time Studies

Time taken for effluent to traverse the cell and be subjected to electrochemical reactions and processes was experimented with to understand the consequences of solution-electrode interface time on floc formation. Electrolysis times of 5, 25, 50, 100, and 200 sec were

investigated through changes in flow rate whilst current density was also altered to target a constant coagulant dose of 1.8 mmol Fe/L. These changes are shown in Table 3.7.

Table 3.7. Flow rate and current density changes to achieve various electrolysis times whilst targeting a 1.8 mmol Fe/L coagulant dose rate.

Electrolysis time (s)	Flow rate (L/min)	Current density (mA/cm^2)
5.00	2.97	20.73
25.00	0.59	4.15
50.00	0.30	2.07
100.00	0.15	1.04
200.00	0.07	0.52

Constant parameters observed were: coagulant dose 1.8 mmol Fe/L; inter-electrode distance 3 mm; 1 g/L pollutant loading; effluent pH 7.2; effluent conductivity 35 mS/cm^2.

Coagulant Retention Time Studies

Retaining a volume of flocculant prior to addition into raw solution was trialled with, with a view of assessing the activity lifetime of floc. Retention times of 0.2, 0.5, 1, 5, 30, 60, 360, 720, and 1,440 min were experimented with by collecting 100 mL volumes of flocculant solution and holding under stirred conditions of 25 rpm for the desired periods of time. These volumes were then introduced into raw volumes of effluent and subjected to the normal flocculation procedure to test their efficacy in pollutant removal. Constant parameters observed were: 0.25 L/min flow rate; 1.8 mA/cm^2 current density; coagulant dose 1.8 mmol Fe/L; electrolysis time 59 sec; inter-electrode distance 3 mm; 1 g/L pollutant loading; effluent pH 7.2; effluent conductivity 35 mS/cm^2.

pH Studies

The pH of effluent entering the EC cell was altered in order to determine the outcome of pH on floc formation. Ranges of pH 3, 4, 5, 6, 7, 8, 9, 10, and 11 were trialled with and sodium chloride addition was altered to maintain constant conductivity in the synthetic effluent. Constant parameters observed were: 0.25 L/min flow rate; 1.8 mA/cm^2 current density; coagulant dose 1.8 mmol Fe/L; electrolysis time 59 sec; inter-electrode distance 3 mm; 1 g/L pollutant loading; effluent conductivity 35 mS/cm^2.

Conductivity Studies

Five batches of effluent were prepared with various amounts of sodium chloride ranging from 5, 10, 15, 20, and 25 g/L to achieve different conductivity levels. The separate volumes were then trialled through the EC cell. Constant parameters observed were: 0.25 L/min flow rate; 1.8 mA/cm^2 current density; coagulant dose 1.8 mmol Fe/L; electrolysis time 59 sec; inter-electrode distance 3 mm; 1 g/L pollutant loading; effluent pH 7.2.

3.8 References

253. Rump, H. H. Laboratory Manual for the Examination of Water, Wastewater and Soil, 3rd edition. Wiley-VCH, 2000.
254. Welz, B., Sperling, M., Resano, M. Atomic Absorption Spectrometr. John Wiley & Sons, 2008.
255. Marczenko, Z., Balcerzak, M. Separation, Preconcentration and Spectrophotometry in Inorganic Analysis. Elsevier, 2000.
256. Taylor, H. E. Inductively Coupled Plasma-mass Spectrometry: Practices and Techniques. Academic Press, 2001.
257. Wu, J. L., Ho, C. R., Huang, C. C. Srivastav, A. L., Tzeng, J. H., Lin, Y. T. Hyperspectral sensing for turbid water quality monitoring in freshwater rivers: empirical relationship between reflectance and turbidity and total solids. Sensors (Basel) 2014; 14 (12): 22670-22680.
258. American Water Works Association (AWWA). Standard Methods for the Examination of Water and Wastewater. American Public Health Association, 2012.
259. Hitchman, M. L. Measurement of Dissolved Oxygen. John Wiley & Sons, 1978.
260. Marken, F., Neudeck, A., Bond, A. M. Cyclic Voltammetry. In Scholz, F. (Ed.) Electroanalytical Methods: Guide to Experiments and Applications, p57-107. Springer, 2010.
261. Hornyak, G. L., Tibbals, H. F., Dutta, J., Moore, J. J. Introduction to Nanoscience and Nanotechnology. CRC Press, 2009.
262. Wells, O. C. Scanning Electron Microscopy. McGraw-Hill, 1974.
263. Pecharsky, V. K., Zavalij, P. Y. Fundamentals of Power Diffraction and Structural Characterization of Materials. Springer, 2009.
264. Williams, D. B., Carter, C. B. Transmission Electron Microscopy: A Textbook for Materials Science. Springer, 2009.
265. Koutsoukos, P. K. Klepetsanis, P. G., Spanos, N. Calculation of Zeta-Potentials from Electrokinetic Data. In Somasundaran, P. (Ed.) Encyclopedia of Surface and Colloid Science Volume 8 (2nd Ed), p1097-1114. CRC Press, 2006.

Chapter 4

Electrocoagulation

4 Electrocoagulation

4.1 Introduction

The results of the coagulation experiments, along with resultant discussions, are given here under the following sub-section headings: (i) experiment set A, (ii) experiment set B, and (iii) experiment set C. Each section has then been further separated into individual trials. Details for individual trials assessing floc behaviour in relation to operational parameters are then given in chapter 5.

4.2 Experiment Set A

Initial experiments were designed to quantify the concentration of iron coagulum needed to induce flocculation from the standard industrial practice of chemical dosing using ferric chloride. This was done to establish a baseline where EC treatment could be assessed and determine any trend in behaviour in coagulant concentration versus flocculation. These experiments also served to understand the performance of EC against the adopted conventional chemical coagulation approach to wastewater treatment.

4.2.1 Chemical Coagulation *vs.* Electrocoagulation

Figure 4.1 on the following page presents the effects of increasing coagulant concentration on the efficiency of phosphate removal (η) obtained from chemical coagulation (denoted as CC) and electrocoagulation (denoted as EC) of the trickling effluent. Error bars have also been included in Figure 4.1 for all data points and all subsequent figures from here on (error bars shown are $\pm$ 1 standard deviation). Please note however, that due to the small errors involved, in certain graph plots the error bars are not as clearly shown, an enlarged plot point in Figure 4.1 is shown to highlight this point.

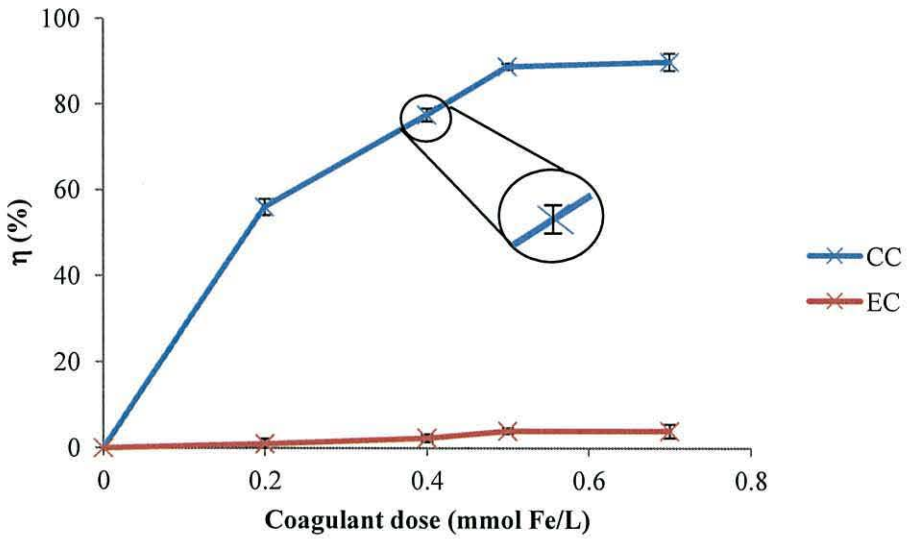

Figure 4.1. Effect of iron concentration on phosphate removal by; (i) chemical coagulation (CC), and (ii) electrocoagulation (EC) (error bars shown are ± 1 SD). Conductivity = 35 mS/cm^2; pH = 7.2; C_0 = 0.16 mmol P/L.

The results show that phosphorus removal efficiency, *via* chemical coagulation, increased from 56% at 0.2 mmol Fe/L to 90% at 0.7 mmol Fe/L. The reduced coagulation performance at low iron concentrations of 0.2 – 0.4 mmol Fe/L suggest that insufficient coagulant was present in solution to effectively reduce the pollutant particles' double layer and enable destabilisation leading to aggregation. At 0.5 mmol Fe/L, coagulation performance was markedly improved with a removal efficiency of 89% recorded. This indicates that particles treated at this coagulant concentration and beyond (0.7 mmol Fe/L), approached their isoelectric point resulting in mass destabilisation and improved precipitation of pollutant phosphorus particles.[266]

However, the removal efficiency derived from EC treatment were significantly lower in comparison with removal rates of only 0 – 4% recorded. Figure 4.2 on the following page shows the samples treated *via* chemical coagulation and EC at the various dose rates selected.

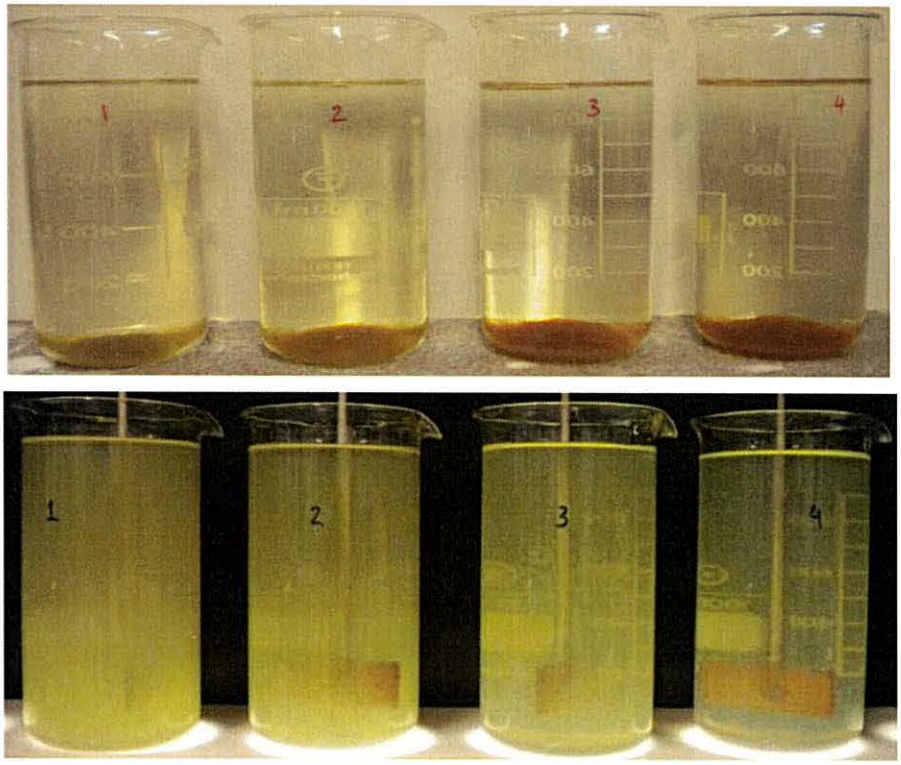

Figure 4.2. ***Top.*** **Chemical coagulated samples post-30 min settlement.** ***Bottom.*** **Electrocoagulated samples post-30 min settlement. Coagulant concentrations, left – right: 0.2, 0.4, 0.5, 0.7 mmol Fe/L.**

Figure 4.2 reveals that coagulation and precipitation of flocculated particles occurred at all chemical iron doses. However, no flocculation occurred during the EC coagulant dosing trials. Consequently, with no flocculation of phosphorus particles occurring, this resulted in the poor removal efficiency results shown in Figure 4.1. The lack of flocculation observed may be explained by the oxidative state of the electrochemically released iron ions into solution compared to ions delivered chemically. Table 4.1 details the proposed oxidation states of liberated iron ions as a function of their source material.

Table 4.1. Oxidation state of iron ions during chemical coagulation and electrocoagulation.

Treatment	Iron cation source	Iron oxidation state during dosing
Chemical coagulation	Ferric chloride	Fe^{3+}
Electrocoagulation	Mild steel electrode	Fe^{2+}

During chemical coagulation, iron is delivered into solution in the ferric form (Fe^{3+}) from its chloride salt. However, during EC, iron cations are electro-dissolved into solution in the ferrous state (Fe^{2+}). The difference in oxidation states is due to the favoured production of Fe^{2+} over Fe^{3+} during EC operation. Table 4.2 on the following page summarises the standard electrode potentials for the formation of Fe^{2+} and Fe^{3+} taken from the electrochemical series.

Table 4.2. Standard reduction potentials of Fe^{2+} and Fe^{3+}.

Equilibrium	Standard electrode potential (V)
$Fe^{2+}_{(aq)} + 2e^- \rightarrow Fe_{(s)}$	– 0.44
$Fe^{3+}_{(aq)} + 3e^- \rightarrow Fe_{(s)}$	– 0.04

From Table 4.2 the standard electrode potential (E^o) values imply that the production of Fe^{2+} is thermodynamically favoured over Fe^{3+} production as the E^o for the half reaction of $Fe^{2+}_{(aq)}$ to $Fe_{(s)}$ is more negative than that of $Fe^{3+}_{(aq)}$ to $Fe_{(s)}$.

As a result in the difference of iron oxidation state's between chemical coagulation and EC, there was an associated difference in the mechanism of pollutant removal. Sweep-floc coagulation is associated with Fe^{3+} based coagulant solutions as it forms insoluble $Fe(OH)_3$ flocs that can physically enmesh pollutant particles and precipitate them out. Ferrous based solutions are associated with charge neutralisation coagulation mechanism.[145,267] Previous studies have shown that flocs produced under charge neutralisation are weaker as there are fewer physical bonds between the flocs.[268] Thus, floc strength is reduced and size diminishes, particularly with the application of shear force, as that imposed from the paddle mixers during the jar-testing stage, post EC. In contrast, flocs formed under sweep-floc conditions are bonded stronger, form larger sized complexes and are resistant to shear forces.[269] This difference in Fe^{2+}/Fe^{3+} coagulation performance is attributable to the higher solubility of hydroxides and lower positive charges associated with Fe^{2+} compared to Fe^{3+} thus making it a poorer coagulant and explaining the superior performance of chemical coagulation over EC.

4.2.2 Section Conclusions

At the coagulant dosing range tested and with the current set up in use, only chemical coagulation provided flocculation and removal of pollutant species. Electrocoagulation treatment failed in producing any observable floc and consequently had inferior pollutant removal rates. It has been argued that differences in released iron oxidation states of Fe^{2+} and Fe^{3+} between the two coagulation methods has accounted for the contrast in performance.

4.3 Experiment Set B

As the form of iron delivered into solution during set A trials was different between the two coagulation systems, a direct comparison between EC and chemical coagulation was

not applicable. In chemical coagulation the released iron was in the form Fe^{3+} whereas for EC, the delivered iron was in the form Fe^{2+}.

In order to accurately determine a minimum EC coagulant concentration where flocculation would occur, a new set of experiments (set B) were established to determine the conditions required for the electrochemical generation of Fe^{3+} ions in solution. This was done to replicate the same iron cationic oxidation state involved during chemical coagulation and attempt to promote similar flocculation. To achieve this, mixing stages were introduced immediately post-EC treatment to promote oxidation through increasing dissolved oxygen (DO) content in dosed effluent. Figure 3.7 represents the setup of apparatus devised to achieve this. During this experiment set, two mixing regimes were investigated to determine optimal conditions for increasing DO levels in treated effluent and thus quantify the effect of oxygen concentration on floc development and growth. Both are discussed in turn.

4.3.1 Mixing Regime I

An expanded coagulant dosing range of 0.2 – 2.9 mmol Fe/L was tested and mixing regime I imposed that comprised of:

- Stage 1 mixing vessel; 0.5 L volume (residence time 1 min)/500 rpm agitation,
- Stage 2 mixing vessel; 1 L volume (residence time 2 min)/25 rpm agitation.

One litre samples were collected from the outlet of the stage 2 mixing vessel and subjected to settlement times of 30 min. Following this, residual phosphorus concentrations in sample supernatants were measured and removal efficiencies determined. The results recorded are shown in Figure 4.3 (denoted as Mix I) on the following page, along with the previous removal efficiencies of the chemical coagulation (CC) trials and EC trials conducted in section 4.2.1.

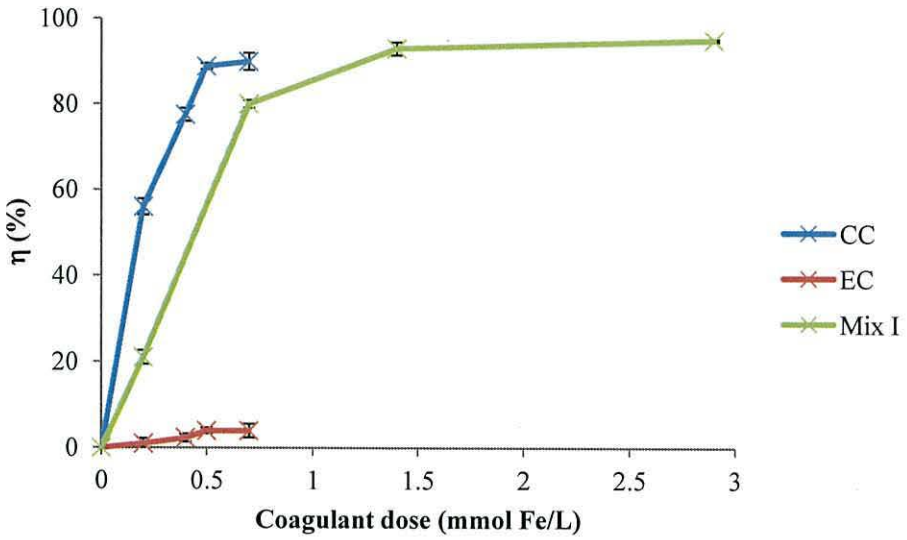

Figure 4.3. Effect of aeration on phosphate removal in electrocoagulated samples (Mix I) compared to electrocoagulation alone (EC), and chemical coagulation (CC) (error bars shown are ± 1 SD). Conductivity = 35 mS/cm^2; pH = 7.2; C_0 = 0.16 mmol P/L.

The results show that removal efficiencies during the EC mixing regime I samples were markedly improved upon with a maximum removal efficiency of 95% recorded at an aerated coagulant dose of 2.9 mmol Fe/L. Even at the lowest coagulant concentration tested of 0.2 mmol Fe/L, a removal efficiency of 21% was recorded compared to 0% during the EC only trials. In order to compare between all the trials ran Table 4.3 summarises the phosphorus removal efficiencies recorded at 0.7 mmol Fe/L coagulant dose.

Table 4.3. Phosphorus removal at 0.7 mmol Fe/L coagulant dose, per trial

Treatment	Pollutant removal rate (%)
Chemical coagulation	90.0
EC Mixing Regime I	80.0
Electrocoagulation	4.0

It can be seen from Table 4.3 that with the introduction of the mixing stages, this allowed treated effluent expelling from the EC cell to become aerated, a factor which led to an improvement in phosphorus removal efficiency at the 0.7 mmol Fe/L coagulant dose. Figure 4.4 on the following page reveals the EC/aerated samples after 30 min settlement.

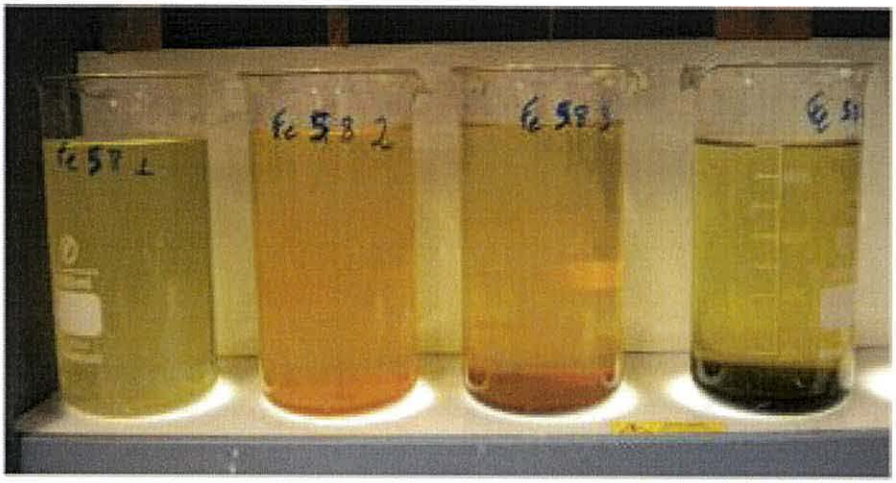

Figure 4.4. Electrocoagulated samples subjected to fast and slow mixing phases, 30 min post-settlement with various iron doses. Coagulant concentrations, left – right: 0.2, 0.7, 1.4, 2.9 mmol Fe/L.

In Figure 4.4 it can be seen that the introduction of the mixing stages substantially aided in floc formation and development. A clear progression of small particle formations at 0.2 mmol Fe/L, through to large sweep-floc $Fe(OH)_3$ flocculants, characterised by orange/green precipitate and high phosphorus removal efficiencies of the same magnitude order as those measured during the chemical coagulation tests, were recorded. The aeration stages therefore promoted the oxygenation of the EC treated effluent expelling from the cell, increasing DO content, which led to the oxidation of electrolytically dissolved Fe^{2+} to Fe^{3+}. In order to substantiate this claim, Fe^{2+} and Fe^{3+} analysis along with DO concentration analysis was carried out on samples taken immediately expelled from the EC cell, during stage 1 mixing, and during stage 2 mixing. The results are reported in Figure 4.5 on the following page.

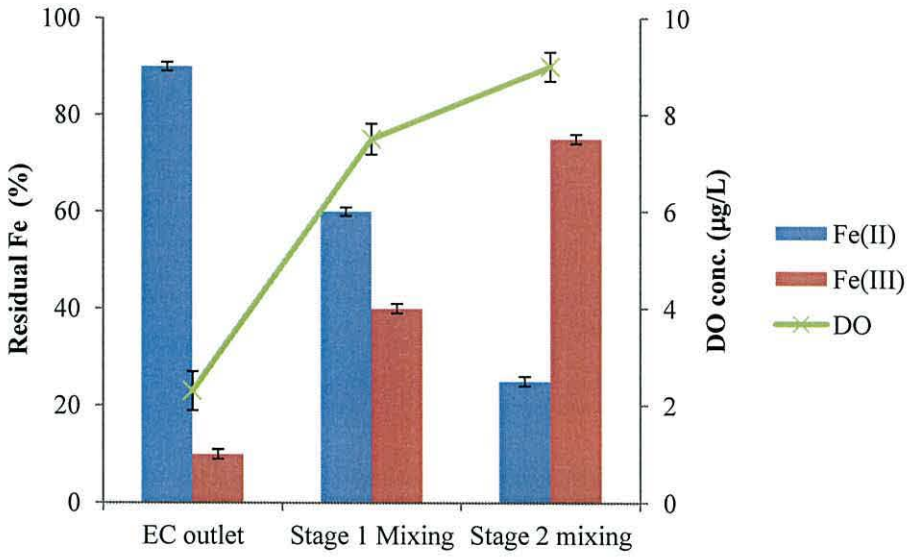

Figure 4.5. Percentages of Fe^{2+}/Fe^{3+} remaining in solution and dissolved oxygen (DO) concentrations at various EC treatment stages (error bars shown are ± 1 SD).

From Figure 4.5 it can be seen that as the mixing regime was imposed on treated effluent post-EC, the percentage of ferrous and ferric concentrations varied. Immediately post-EC, 90% of iron in solution was in the ferrous form, after stage 1 this reduced to 60% and finally down to 25% during stage 2 mixing. Conversely, the amount of ferric remaining in solution increased at the expense of ferrous due to its oxidation by increased DO content, attributable to the incorporation of the mixing stages. This decrease in Fe^{2+} linked to increases in DO is consistent with studies of Fe^{2+} oxidation published in the literature.[178,270,271] In effluent immediately collected post-EC cell, the DO concentration was measured at 2.3 µg/L, whereas in stage 1 and stage 2 mixing it had increased to 7.5 µg/L and 9 µg/L.

This increase in ferric concentration, as a direct result of the various mixing stages imposed, along with the increment of coagulant dose of 0.7 – 0.9 mmol Fe/L, is consistent with the observation of sweep-floc coagulation occurring, as characterised by the production of larger-sized floc particles and the orange/green precipitate formed at the bottom of the sample beakers.

To conclude, it was found that satisfactory flocculation (sweep-floc mechanism) was found to occur at a minimum oxygenated electrocoagulant dose of 0.7 mmol Fe/L. For chemical coagulation however, the minimum dose found was 0.2 mmol Fe/L.

4.3.2 Mixing Regime II

As improvements in phosphorus removal efficiencies were recorded with the introduction of the aeration stages, mixing regime II was investigated with a view of assessing the impact of a shorter stage 1 mixing residence time and faster agitation on DO availability and floc formation. Consequently, mixing regime II comprised of:

- Stage 1 mixing vessel; 0.25 L volume (residence time 30 sec)/1,000 rpm agitation,
- Stage 2 mixing vessel; 1 L volume (residence time 2 min)/25 rpm agitation (unchanged from mixing regime I).

It was postulated that a shorter residence time during stage 1 mixing, agitated at a faster stirrer speed, would fulfil two purposes: (i) faster agitation would ensure quicker aeration of treated effluent increasing the DO content in solution and inducing complete oxidation of Fe^{2+} to Fe^{3+}, and (ii) shorter residence time would transfer newly converted Fe^{3+} ions faster to the stage 2 mixing phase, designed to promote floc formation processes and the production of $Fe(OH)_3$. Figure 4.6 on the following page shows samples dosed with 0.2 – 2.9 mmol Fe/L and subjected to mixing regime II, along with samples that were subjected to mixing regime I, for comparison.

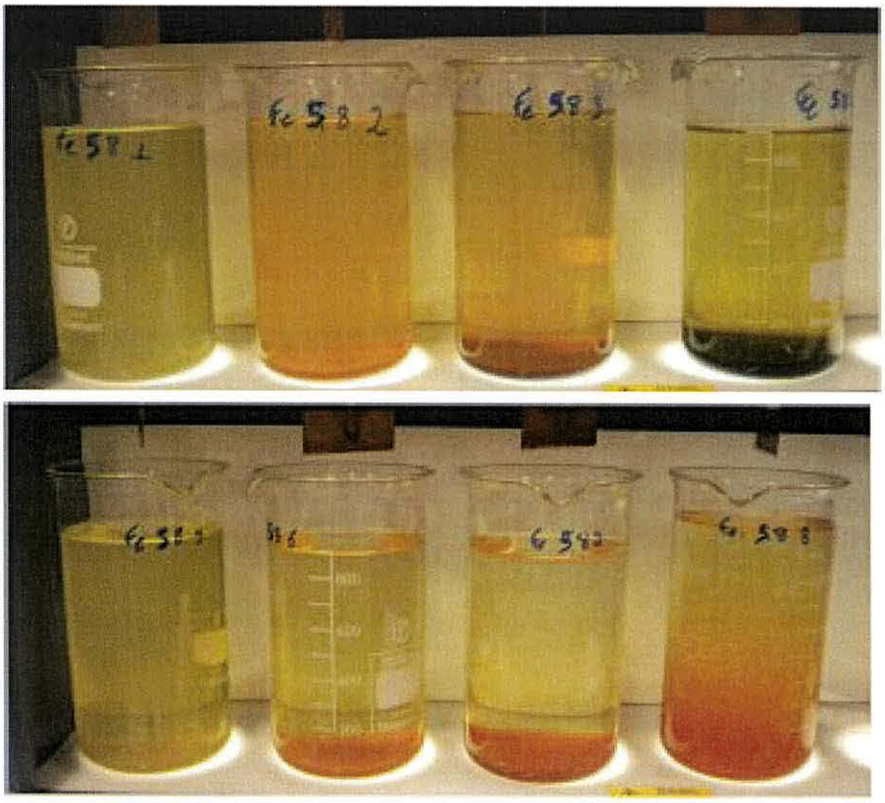

Figure 4.6. ***Top.*** **Samples subjected to mixing regime I.** ***Bottom.*** **Samples subjected to mixing regime II (post-15 min settlement). Coagulant concentrations, left – right: 0.2, 0.7, 1.4, 2.9 mmol Fe/L.**

The samples in which mixing regime I was imposed, a steady progression from $Fe(OH)_2$ to $Fe(OH)_3$ production is observed. However, in samples that were subjected to a shorter, greater turbulent stage 1 mixing step (mixing regime II), with the exception of the 0.2 mmol Fe/L dosed sample, all other samples produced the desired $Fe(OH)_3$ floc. This further supports the postulation that the oxidation state of the generated iron hydroxide floc is strongly influenced by the DO content availability within the treated effluent.[146,272]

In support of the faster mixing regime II benefitting floc formation through increased DO content, Figure 4.7 on the following page compares the phosphorus removal efficiencies during the chemical coagulation, EC only, and EC mixing regime I and II trials (denoted as Mix II in Figure 4.7).

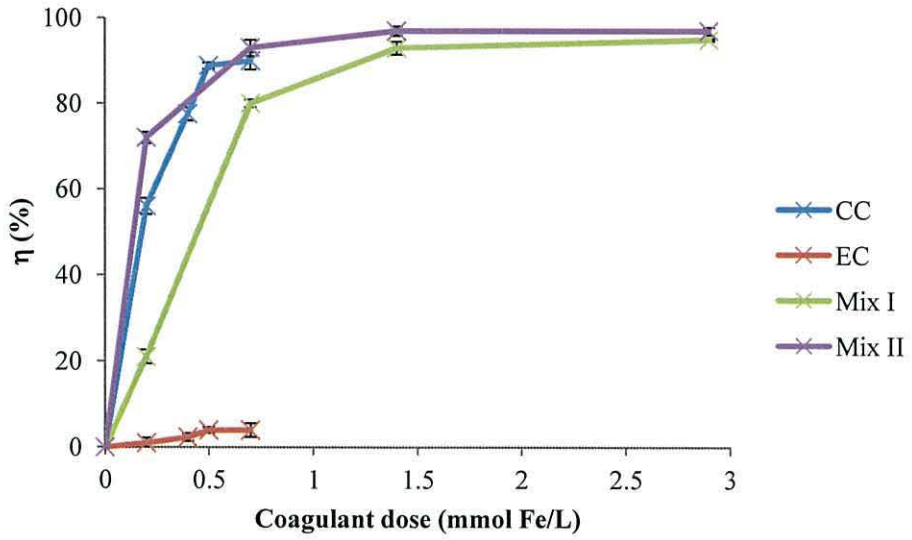

Figure 4.7. Effect of mixing regimes (Mix I/Mix II) post-EC on phosphate removal compared to electrocoagulation only (EC) and chemical coagulation (CC) (error bars shown are ± 1 SD). Conductivity = 35 mS/cm^2; pH = 7.2; C_0 = 0.16 mmol P/L.

For all samples tested, further increases in removal rates were recorded in samples subjected to mixing regime II compared to the previous trials. The highest phosphorus removal efficiency of 97% was recorded at a coagulant dose of 1.4 mmol Fe/L. At 0.2 mmol Fe/L, the lowest removal efficiency of 72% was recorded. Table 4.4 directly compares the phosphorus removal efficiencies for all trials ran dosed at 0.7 mmol Fe/L.

Table 4.4. Phosphorus removal efficiencies at 0.7 mmol Fe/L coagulant dose, per trial.

Treatment	Pollutant removal efficiency (%)
EC Mixing Regime II	93.0
Chemical coagulation	90.0
EC Mixing Regime I	80.0
Electrocoagulation	4.0

In comparing the removal rates for the various trials ran at a coagulant dose rate of 0.7 mmol Fe/L, it can be seen that employing mixing regime II, immediately after EC treatment produced the highest phosphorus removal efficiency of 93% recorded thus far.

4.3.3 Section Conclusions

It has been shown that with the introduction of a fast/short mixing stage preceding a slow/long mixing stage, pollutant removal increased and outperformed chemical coagulation at the 0.7 mmol Fe/L dose. This is due to the promotion of Fe^{3+} conversion as a result of vigorously aerating and oxidising oxygen starved effluent expelling from the EC cell. This aided in promoting the oxidation of electro-dissolved Fe^{2+} to Fe^{3+} and the

formation of sweep floc $Fe(OH)_3$ precipitates. Results thus far have revealed strong trends in two key EC operational areas:

- Favourable sweep floc development is dependent upon the formation of Fe^{3+} ions from the oxidation of electrolytically dosed Fe^{2+} ions.
- Increasing the agitation of EC treated effluent, *via* higher mixing rates, promotes formation of desired Fe^{3+} through increasing the yield of available DO in treated effluent solutions.

4.4 Experiment Set C

With the discovery of satisfactory floc formation and a 93% phosphorus removal efficiency recorded at an EC coagulant dose of 0.7 mmol Fe/L, attention was turned to investigating the dilution of coagulum produced. This was carried out with a view of assessing whether treated effluent, dosed at an initial coagulant concentration of 0.7 mmol Fe/L, could be diluted with raw effluent down to lower concentrations of 0.2 – 0.5 mmol Fe/L, whilst still effecting pollutant flocculation and removal. It was postulated that by doing this, it could be demonstrated that pollutant removal, on par with chemical coagulation, could be carried out at EC dose rates below 0.7 mmol Fe/L, albeit not *via* direct dosing as in experiment set A. This approach of producing a concentrated stream of treated effluent and diluting into a larger volume of raw effluent to induce flocculation in the overall final body of pollutant water will be referred to hereon in as coagulant dilution. Experiment set C trials were therefore designed to expose any trend development in diluting coagulated effluent on floc formation by assessing phosphorus removal efficiencies and residual iron concentrations in treated samples.

4.4.1 Coagulant Dilution

Figure 4.8 on the following page compares phosphorus removal efficiency results from experiment set A (section 4.2.1), in which direct dosing of 0.2 – 0.5 mmol Fe/L coagulant was carried out *via* EC and conventional chemical coagulation, to the EC coagulant dilution experiments (denoted at Dil. I in Figure 4.8) in which an initial treated effluent volume of 0.7 mmol Fe/L dose was diluted with varying raw effluent volumes to achieve final coagulant concentrations of 0.2 – 0.5 mmol Fe/L.

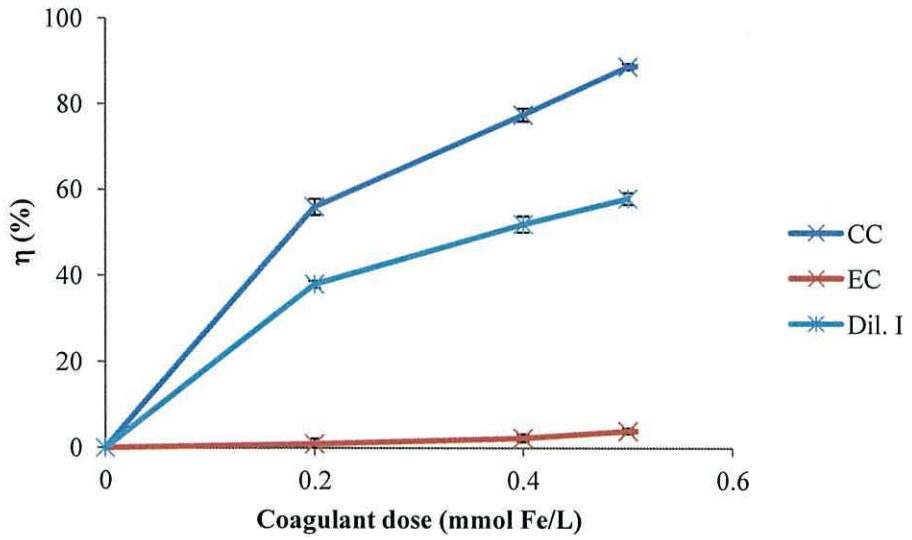

Figure 4.8. Chemical coagulation (CC) and EC direct dosing *vs.* EC coagulant dilution (Dil. I) (error bars shown are ± 1 SD). Conductivity = 35 mS/cm^2; pH = 7.2; C_0 = 0.16 mmol P/L.

From Figure 4.8 it can be seen that the coagulant dilution method improved phosphorus removal efficiencies from 4% to 58% (at 0.5 mmol Fe/L dose), when compared to EC direct dosing. This increase in phosphorus removal can be attributed to the difference in stage development of floc derived from the coagulant dilution method than that from direct dosing.

During coagulant dilution, a volume of effluent is dosed at 0.7 mmol Fe/L within the EC cell and then transferred onto two mixing phases. These phases, one short residence time/fast mixing and the other long residence time/slow mixing, are designed to maximise the formation and development of $Fe(OH)_3$ sweep-floc particles through the oxidation of Fe^{2+} ions to Fe^{3+}. This has been demonstrated in section 4.3.2. Consequently, this volume of dosed effluent is densely populated with sweep-floc complexes containing active absorption sites. Once introduced into a larger volume of raw effluent, these flocs are ready to instantly absorb and bridge with pollutant particles forming physical bonds between them creating larger insoluble aggregates that co-precipitate out.

Despite the dilution of the initial small volume of concentrated coagulant effluent (CCE) into a larger untreated volume, the overall effect is of introducing pre-formed active absorption sites (sweep-flocs) into raw wastewater that are capable of very fast and effective pollutant removal. If the example of diluting 250 mL of CCE at 0.7 mmol Fe/L into 750 mL of raw effluent is examined, whilst a coagulant concentration dilution factor

of four times has occurred (final dose 0.2 mmol Fe/L), the phosphorus removal efficiency is 38% compared to 1% for dosing directly with 0.2 mmol Fe/L.

This difference in pollutant removal between dosing directly and diluting a concentrated volume of pre-dosed solution can be explained using Brownian coagulation theory.[273,274]

Brownian Coagulation Theory

Brownian motion refers to the continuous random movement of particles suspended in a fluid. Brownian coagulation or perikinetic flocculation occurs when, as a result of their random motion, particles collide and stick together. The theory of Brownian coagulation is based upon the Smoluchowski equation which counts the number of particles as a result of collisions and which is determined by particle size, density, and the transport mechanisms involved in the system.[275]

Using this theory is has been shown that particles of different size within a poly-disperse suspension coagulate faster than that between particles of the same size due to the tendency for small size particles to attach to larger ones.[276] If applied to the results shown in Figure 4.8, this finding is supported. During the coagulant dilution method a small volume of dosed effluent (optimised to form $Fe(OH)_3$ floc) was introduced into raw effluent. The size of the introduced flocs in comparison to the discrete pollutant ions was ample, approximately 15 – 20 μm (section 6.4 provides a fuller description and analysis of floc sizes). Thus, Brownian coagulation occurred very quickly in which the microscopic pollutant particles attached themselves to the macroscopic flocs resulting in co-precipitation of ferric hydroxide-pollutant complexes and an improvement in phosphorus removal. In contrast, the direct dosing method involved the release of Fe^{2+} ions. As the effective ionic radius of a ferrous ion is 75 pm and the radius of a phosphorus ion is 58 pm,[277] the size difference is negligible and therefore Brownian coagulation would not have occurred as readily, supported by the poor removal efficiency of 1% shown in Figure 4.8.

This proposition has merit in that similar work conducted has also shown that solutions containing discrete pollutant particles, which are almost indefinitely stable, flocculate rapidly when seeded with pre-grown flocs as in the coagulant dilution method.[278]

Furthermore, and perhaps more poignant, is the fact that due to the dispersion of ferrous ions directly into raw effluent at low concentration (0.2 mmol Fe/L), the requirement for effective coagulation through sweep-floc would have been severely diminished owing to the poor collisional interactions of Fe^{2+} with OH^- ions to form the desired $Fe(OH)_3$ sweep-flocs.

However, despite improvements in pollutant removal recorded, the removal efficiencies for the coagulant dilution method remained relatively low (38 – 58%) when compared to chemical coagulation (56 – 90%). The highest phosphorus removal efficiency of 58% was recorded at the lowest coagulant dilution, 1:1.3 (treated effluent to raw effluent), which produced the highest final coagulant dose concentration of 0.5 mmol Fe/L. As final coagulant dose rates decreased down to 0.4 mmol Fe/L and 0.2 mmol Fe/L (through larger dilutions of 1:2 and 1:4 of treated effluent to raw effluent), phosphorus removal efficiency further decreased. The results indicate that diluting coagulant concentration reduces pollutant removal. In order to understand this trend, the following section explores electrical double layer compression theory in an attempt to explicate the relationship between the two.

Electrical Double Layer Compression

The Stern double layer model, which is a combination of the Helmholtz and Guoy-Chapman models,[279,280,281,282,283] is the conventional way of visualizing the ionic environment in which a charged pollutant particle resides, and can explain how electrical repulsive forces maintain its solubility in an aqueous media. Figure 4.9 on the following page illustrates the Stern and Diffuse Layer's that make up the electrical double layer (EDL).

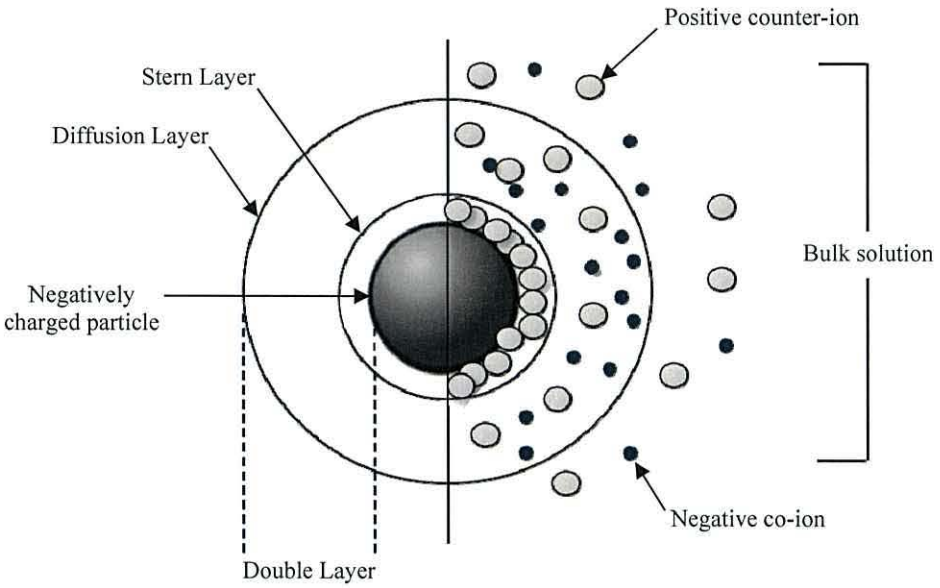

Figure 4.9. Diffuse double layer model: left side depicts order of layers and right side depicts concentrations of ions.

A negatively charged pollutant particle in solution is surrounded by a layer of positive ions that firmly attach to it. This layer of counter-ions is referred to as the Stern layer.[284] Additional positive ions remain attracted to the negative pollutant particle but are now repelled by the establishment of this layer as well as by the presence of other positive ions attempting to approach the particle. Similarly, there is a lack of negative ions immediately within the vicinity of the Stern Layer as they are repelled by the strong negative charge on the pollutant particle. A dynamic equilibrium results forming a diffuse layer which contains a high concentration of positive ions near the Stern layer that gradually declines with distance, and a low concentration of negative ions that gradually increases with distance from the pollutant particle.[285] These concentrations eventually equalise until an equilibrium of positive and negative ions is reached with the normal counter and co-ion concentrations in the bulk solution. This double layer which surrounds each pollutant particle explains why pollutants remain soluble in solution.[286]

When two particles approach each other and their electrical double layers begin to overlap, the resultant similar charges between the two cause electrostatic repulsion to dominate and force the particles apart.[287] The level of energy required to overcome this repulsion exponentially increases as the particles are driven closer together. In order for agglomeration to occur, the two particles must have sufficient kinetic energy (through mass and speed) to exceed this energy barrier. Once the energy barrier has been overcome,

the net interaction energy is all attractive and van der Waal's forces can dominate inducing agglomeration.[288]

For flocculation to occur, the energy barrier should be lowered to such an extent, or preferably eliminated, so that the net interaction is always attractive. This can be accomplished by neutralising the charge on pollutant particles and involves the addition of coagulant.[289]

Coagulant dosing in contaminated effluents introduces $Fe(OH)_3$ which can adsorb onto the surface of pollutant particles. This results in a zero net charge of the pollutant particle and compression of its double layer eliminating its repulsive energy barrier. The more coagulant that is added the lower the energy barrier becomes. Figure 4.10 on the following page represents a net interaction curve diagram formed by subtracting the attraction curve from the repulsion curve.

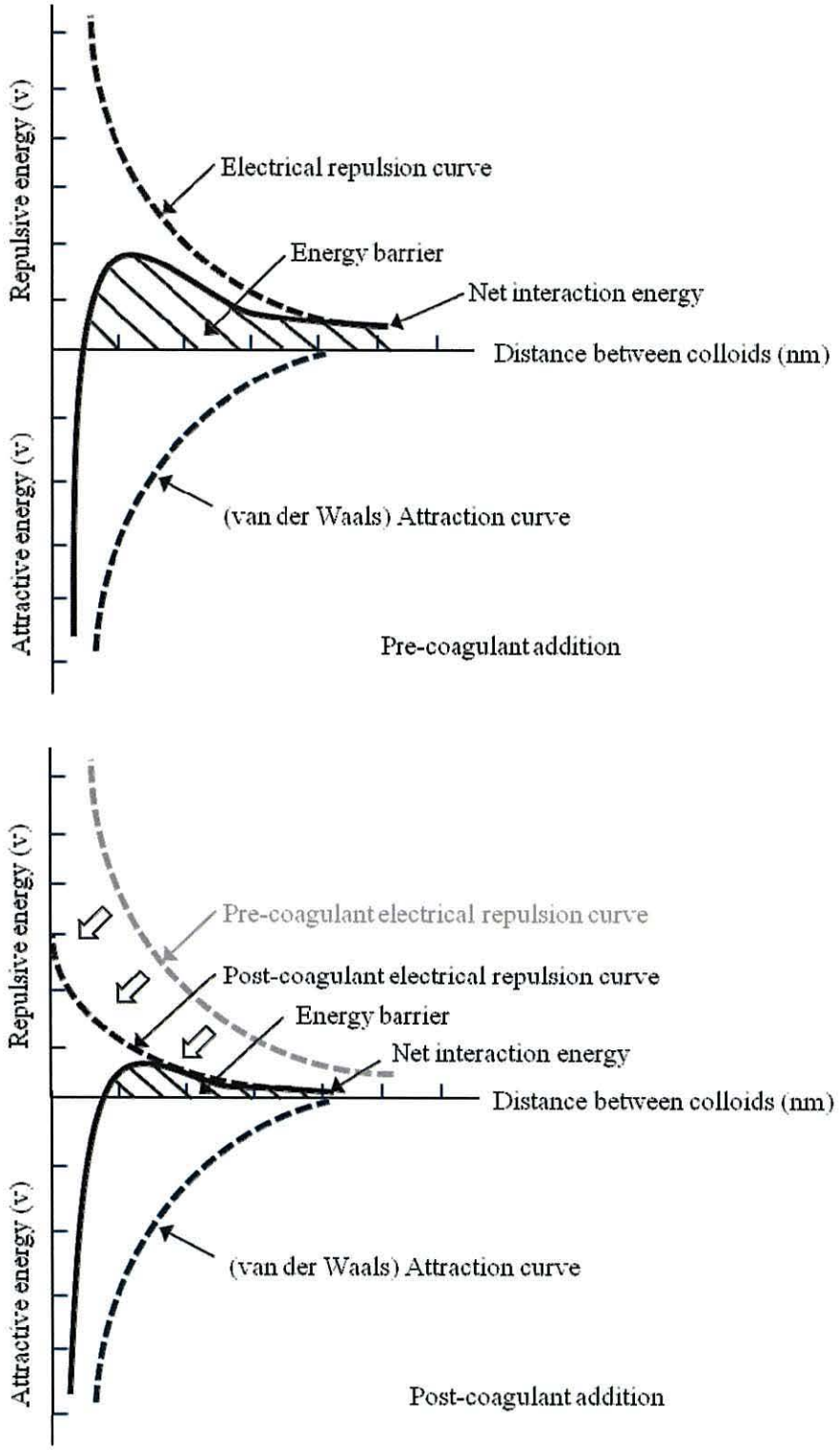

Figure 4.10. Net interaction curve diagrams: (*top*) pre-coagulant addition, (*bottom*) post-coagulant addition. Addition of coagulant lowers repulsion curve.[288]

Figure 4.10 shows the net effect of coagulant addition on the repulsion energy curve and the resultant difference in the energy barrier area pre and post-coagulant addition. The smaller the overall energy barrier area produced the greater charge neutralisation of pollutant particles has occurred. Subsequently, flocculation can occur as the compression

of double layers surrounding pollutant particles has occurred and the repulsive energy is diminished allowing for particle agglomeration.

Therefore, with the addition of sufficient coagulant, adsorption onto pollutant particles occurs leading to charge neutralisation and double layer compression which reduces the repulsion energy curve diminishing its influence. The degree to which charge neutralisation and subsequent double layer compression can occur is related to the amount of coagulant in solution. During the coagulant dilution trials, the concentration of coagulum was reduced from 0.7 to 0.5 – 0.2 mmol Fe/L. As a consequence this reduced the number of flocs in solution available for adsorption which impacted on the degree of charge neutralisation that could occur and subsequent double layer compression. This resulted in differences in lowering of the repulsion curve.

In order to demonstrate the relationship between coagulant concentration and double layer compression, Figure 4.11 on the following page represents ion density variation in the diffuse layer of pollutant particles in low concentration and high concentration coagulant solutions.

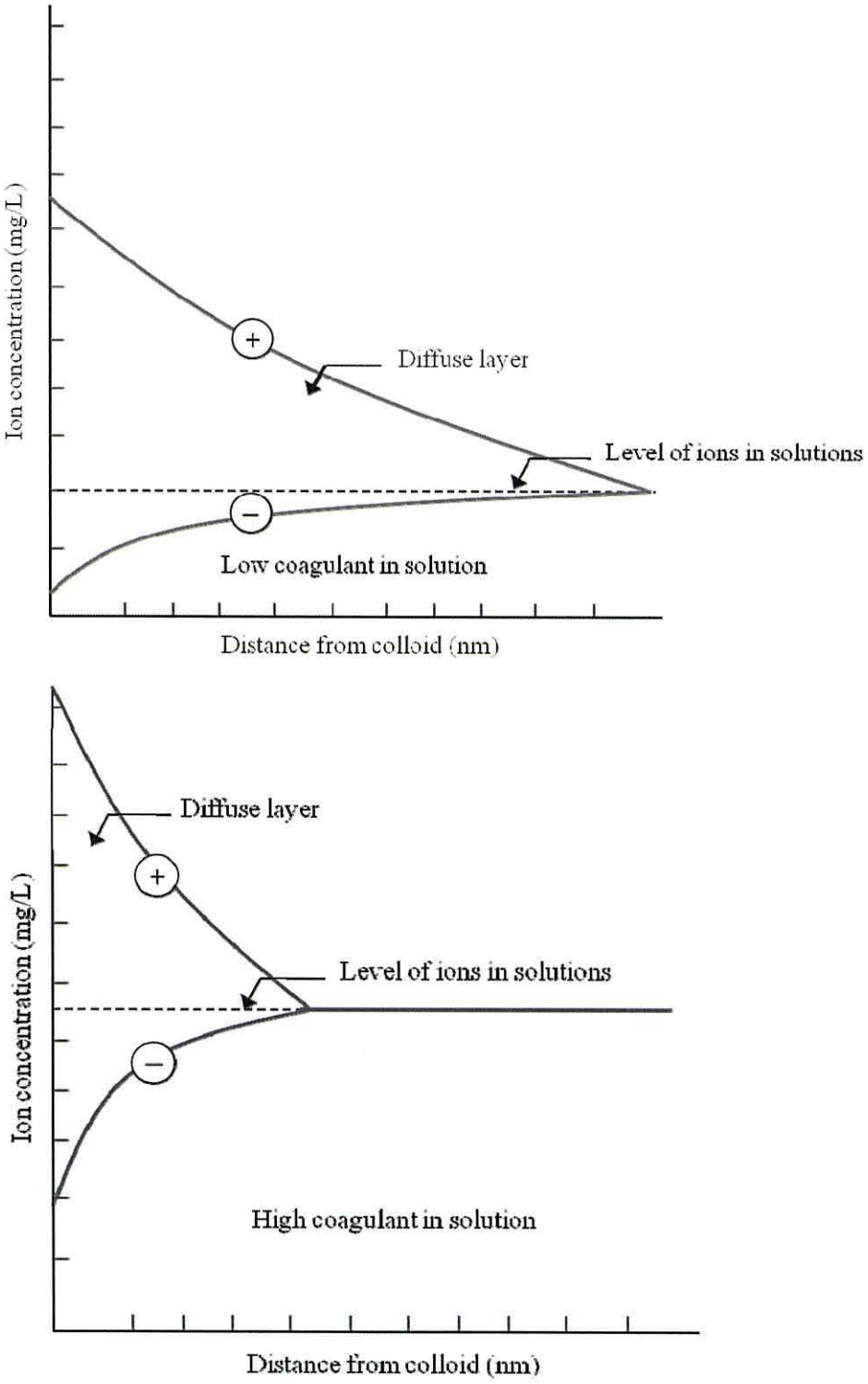

Figure 4.11. Variation of ion density in the diffuse layer as a function of coagulant concentration: (*top*) low coagulant in solution, (*bottom*) high coagulant in solution.[288]

The thickness of the double layer is dependent upon the charge of the pollutant particle attracting counter and co-ions to it. A high coagulant dose neutralises the charge on pollutant particles through adsorption of $Fe(OH)_3$ resulting in the breakdown of the Stern and diffuse layers and overall compression of the electrical double layer. This leads to

flocculation and is evident by the 93% phosphorus removal efficiency recorded in Table 4.4 (section 4.3.2).

Decreasing the coagulant concentration however, such as diluting a dose of 0.7 mmol Fe/L to 0.5 – 0.2 mmol Fe/L, reduces adsorption levels onto pollutant particles due to a reduction in $Fe(OH)_3$ concentrations and thus a reduction in charge neutralisation.

Consequently, the Stern and diffuse layers remain and the double layer is thick surrounding pollutant particles maintaining them discrete in solution. The results in Figure 4.8 reflect this showing that as dilution increased; pollutant removal decreased owing to a reduction in coagulant concentration reducing the degree of charge neutralisation and double layer compression. Ultimately, with compression reduced at the lower coagulant concentrations, the electrical repulsion energy was not reduced sufficiently and so flocculation was inhibited. This led to a drop of 34% in phosphorus removal efficiency as coagulant concentrations was diluted down to 0.5 – 0.2 mmol Fe/L.

In comparing the average coagulant diluted phosphorous removal efficiencies to the chemical coagulation results in Figure 4.8, expectantly it can be noted that the former are on average 34% lower than the latter. Whilst a significant improvement in pollutant removal is recorded *via* the floc dilution method over EC direct dosing, there is still a significant difference in removal efficiencies between EC and chemical coagulation.

A final set of experiments was therefore established in which higher coagulant doses of 1.1 and 1.4 mmol Fe/L were diluted down to 0.5 – 0.2 mmol Fe/L. This was done to assess the influence of higher initial coagulant doses and subsequent dilution on flocculation through analysing phosphorus removal efficiencies.

4.4.2 Greater Initial Dosing

Figure 4.12 on the following page compares phosphorus removal efficiencies from the previous section (4.4.1) with trials ran in which the initial coagulant dose was increased; initially to 1.1 mmol Fe/L (denoted at Dil. II in Figure 4.12) and subsequently diluted down to 0.5 – 0.2 mmol Fe/L, and then to 1.4 mmol Fe/L (denoted as Dil. III in Figure 4.12) and diluted down similarly.

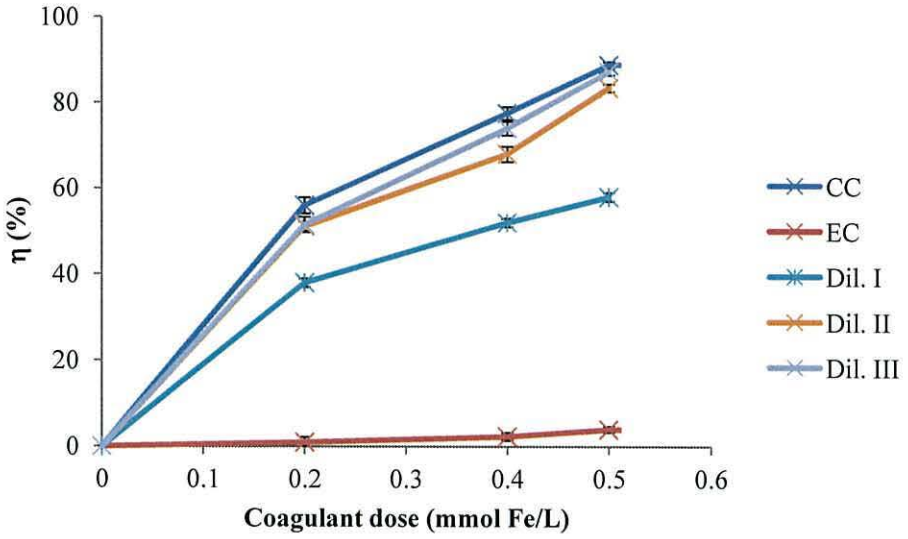

Figure 4.12. Influence of varying initial coagulant dose (prior to dilution) *vs.* chemical and electrocoagulation direct dosing (error bars shown are ± 1 SD). Conductivity = 35 mS/cm^2; pH = 7.2; C_0 = 0.16 mmol P/L.

Based on results shown in Figure 4.12 it can be concluded that pollutant removal efficiencies increased by an average of 27% and 30% as the initial coagulant concentration increased to 1.1 and 1.4 mmol Fe/L, prior to dilution. Table 4.5 summarises the phosphorus removal efficiencies at the lowest coagulant concentration of 0.2 mmol Fe/L for each trial recorded in Figure 4.12.

Table 4.5. Phosphorus removal efficiencies per trial.

Treatment	Initial coagulant dose (mmol Fe/L)	Final coagulant dose (mmol Fe/L)	P removal efficiency (%)
Chemical coagulation	0.2	0.2	56.0
EC coagulant dilution III	1.4	0.2	52.0
EC coagulant dilution II	1.1	0.2	51.0
EC coagulant dilution I	0.7	0.2	38.0
Electrocoagulation	0.2	0.2	1.0

It can be seen that as the initial coagulant concentration increased from 0.7 – 1.4 mmol Fe/L, prior to dilution down to a final dose rate of 0.2 mmol Fe/L, phosphorus removal increased from 38 – 52%. This removal efficiency of 52% is comparable to the 56% removal efficiency recorded during conventional chemical coagulation. It has therefore been demonstrated that achieving analogous pollutant removal rates between EC and chemical coagulation is possible by manipulating the electrochemical dosing system to maximise the development of generated floc. A correlation has also been demonstrated between the initial coagulant concentration prior to dilution, and the efficacy of resultant floc produced in removing pollutants. It is postulated that the improvement in results is a consequence in the shift of balance between floc particle growth rate and nucleation rate.

The following section aims to delineate the relationship between growth rate versus nucleation rate and its influence on flocculation.

Floc Particle Growth Rate vs. Nucleation Rate

For flocs to form, a series of conditions must be satisfied. Firstly, there must be a supply of building material gained, by adsorption of $Fe(OH)_3$ coagulant onto pollutant particles. Secondly, sufficient adsorption and charge neutralisation must occur for the thermodynamic state to be conducive to particle aggregation. The supply rate of coagulant for destabilising and producing nucleation sites is dependent on its abundance in solution and is a function of concentration.[290]

A high coagulant concentration will increase the rate of nucleation within solution but at the cost of floc growth rate.[291] This is a result of increasing the super-saturation of the solution shifting the balance towards favouring nucleation over growth. Equation 17 describes the precipitation rate of $Fe(OH)_3$ that is dependent upon the degree of super-saturation.

$$SS = \frac{[Fe^{3+}][OH^-]^3}{K_s} \qquad \textbf{Equation 17}$$

Where K_s is the solubility constant of ferric hydroxide. Therefore, with the addition of a high coagulant dose this increases the super-saturation of the solution which increases the nucleation rate considerably relative to the floc growth rate.[292] The result is a suspension with flocs that are smaller in size but greater in number that, because of this characteristic, can remove a larger proportion of pollutant due to the overall larger surface area available for adsorption.

Figure 4.13 on the following page diagrammatically represents the relationship between coagulant dose, nucleation rate and floc formation.

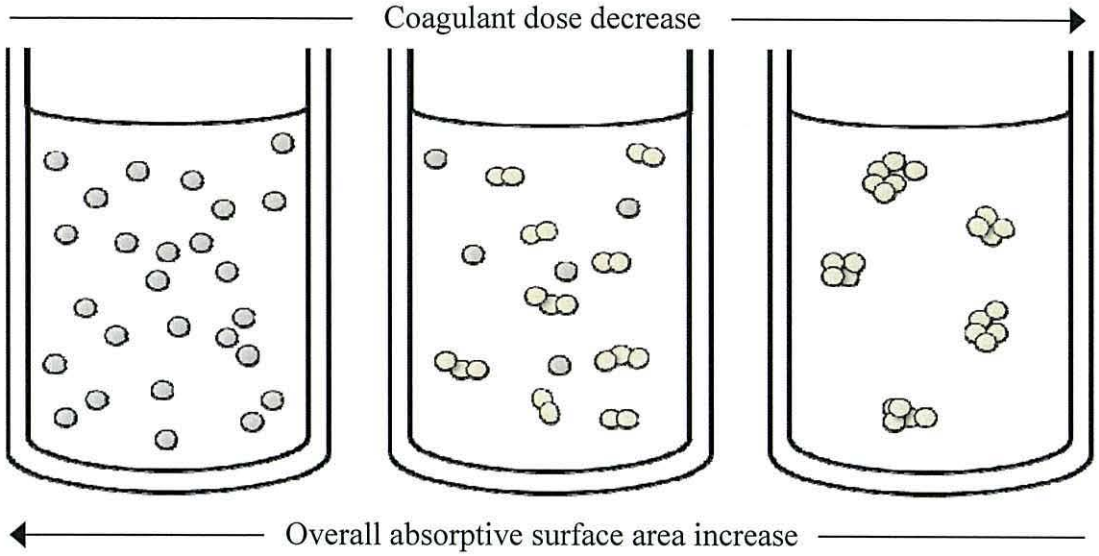

Figure 4.13. Floc formation: floc nucleation mechanism (left) versus floc growth mechanism (right).

Therefore, as initial coagulant concentration increased from 0.7 – 1.4 mmol Fe/L prior to dilution, the resultant treated samples contained flocs successively smaller in size but larger in number. Upon dilution, the concentrations were all reduced to a constant 0.2 mmol Fe/L but the size of the flocs remained unchanged. Consequently, the solution treated at 1.4 mmol Fe/L and diluted down to 0.2 mmol Fe/L had smaller sized flocs present than the solution treated at 0.7 mmol Fe/L and diluted to 0.2 mmol Fe/L. This resulted in a greater overall surface area for adsorption in the initially higher dosed sample which led to a greater degree of charge neutralisation occurring and effectuated an increase in pollutant removal.

In order to verify the proposed explanation, residual total iron analysis was carried out on settled supernatant volumes of the treated samples. Figure 4.14 on the following page summarises the results recorded.

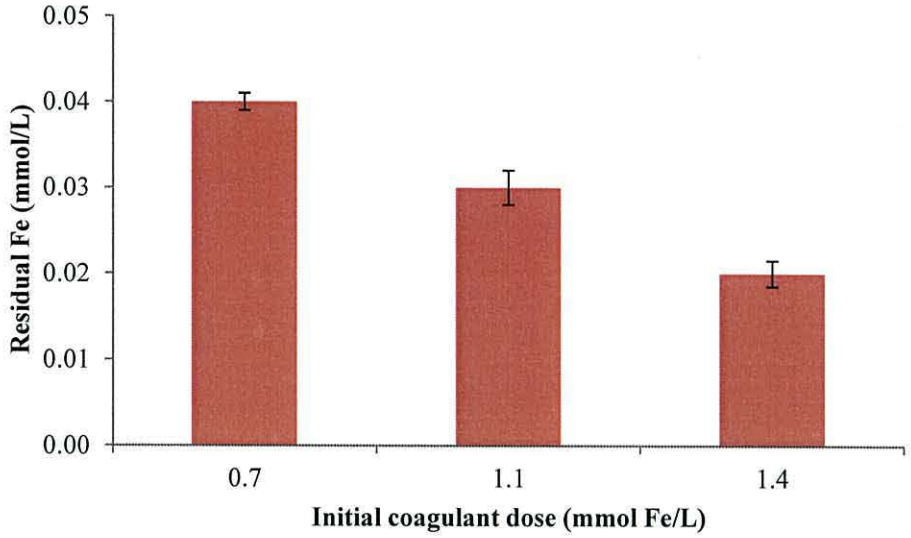

Figure 4.14. Residual total iron in samples diluted to final coagulant concentration of 0.2 mmol Fe/L *vs.* initial coagulant concentration (error bars shown are ± 1 SD).

It can be seen that as the initial dose of coagulant increased from 0.7 – 1.4 mmol Fe/L, the residual iron concentration decreased. This behaviour is concurrent with the theory proposed in that at the higher initial coagulant doses, super-saturation of $Fe(OH)_3$ increased. This drove the rate of $Fe(OH)_3$ nucleation to exceed the rate of floc growth which consequently left less iron in solution as more was effectively being absorbed and/or retained by the precipitate. Increases in the super-saturation of $Fe(OH)_3$ nuclei therefore favours their aggregation and an improvement in flocculation.[293]

4.4.3 Section Conclusions

It has been demonstrated that raw effluent containing discrete particles flocculate rapidly when seeded with pre-grown flocs as a function of Brownian coagulation method. This is proven by recorded increases in P removal at lower coagulant concentrations if dilution of a concentrated volume of coagulated effluent is carried out. Furthermore, it has also been shown that the promotion of floc nucleation rate over growth rate leads to improved pollutant removal efficiencies.

4.5 References

266. Kiliç, M. A. A Parametric Comparative Study of Electrocoagulation and Coagulation of Aqueous Suspensions of Kaolinite and Quarts Powders. PhD thesis, School of Natural and Applied Sciences, Middle East Technical University, 2009.

267. Murugananthan, M., Bhaskar, G., Raju, G., Prabhakar, S. Removal of sulphide, sulphate, and sulphite ions by electrocoagulation. Journal of Hazardous Materials 2004; 109: 37-44.
268. Li, T., Zhu, Z., Wang, D., Yao, C., Tang, H. Characterization of floc size, strength and structure under various coagulation mechanisms. Powder Technology 2006; 168: 104-110.
269. Leentvaar, J., Rebhun, M. Strength of ferric hydroxide flocs. Water Research 1983; 17 (8): 895-902.
270. Singer, P. C., Stumm, W. The solubility of ferrous iron in carbonate bearing waters. Journal of the American Water Works Association 1970; 62: 198-202.
271. Stumm, W., Morgan, J. J. Aquatic Chemistry. Wiley-Interscience, 1981.
272. Babu, R. R., Bhadrinarayana, N. S., Meera, K. M., Begum, S., Anantharaman, N. Treatment of tannery wastewater by electrocoagulation. Journal of the University of Chemical Technology and Metallurgy 2007; 42 (2): 201-206.
273. Veshchunov, M. S. On the Theory of Brownian Coagulation. Journal of Engineering Thermophysics 2010; 19 (2): 62-74.
274. Azarov, I. B., Veshchunov, M. S. Development of the New Approach to the Brownian Coagulation Theory: Transition Regime. Journal of Engineering Thermophysics 2010; 19 (3): 128-137.
275. Smoluchowski, M. Drei Vorträge über Diffusion, Brownsche Molekularbewegung und Koagulation von Kolloidteilchen. Physikalische Zeitschrift 1916; 17: 557-571.
276. Matteson, M. J., Dobson, R. L., Glenn, R. W., Kukunoor, N. S., Waits, W. H., Clayfield, E. J. Electrocoagulation and separation of aqueous suspensions of ultrafine particles. Colloids and Surfaces A: Physicochemical and Engineering Aspects 1995; 104 (1): 101-109.
277. Shannon, R. D. Revised effective ionic radii and systematic studies of interatomic distances in halides and chalcogenides. Acta Crystallographica 1976; A32: 751-767.
278. Agrawal, D. C., Raj, R., Cohen, C. Nucleation of flocs in dilute colloidal suspensions. Journal of the American Ceramic Society 1989; 72 (11): 2148-2153.
279. von Helmholtz, H. Ueber einige Gesetze der Vertheilung elektrischer Ströme in körperlichen Leitern mit Anwendung auf die thierisch-elektrischen Versuche. Annalen der Physik und Chemie, Leipzig 1853; 89: 211-233.
280. Gouy, G. M. Sur la Constitution de la Charge Électrique à la Surface d'un Électrolyte. Comptes Rendus de L'Académie des Sciences 1910; 149: 654.
281. Chapman, D. L. A contribution to the theory of electrocapillarity. Philosophical Magazine 1913; 25: 475.
282. Stern, O. Zur Theorie der Elektrolytischen Doppelschicht. Zeitschrift Fur Elektrochemie 1924; 30: 508.
283. Grahame, D. C. The Electrical Double Layer and the Theory of Electrocapillarity. Chemical Reviews 1947; 41: 441-501.
284. Lyklema, J. Fundamentals of Interface and Colloid Science 1995; 2: 3-208.
285. Bogotsky, V. S. Fundamentals of Electrochemistry. Wiley-Interscience, 2006.
286. Derjaguin, B., Landau, L. Theory of the stability of strongly charged lyophobic sols and of the adhesion of strongly charged particles in solutions of electrolytes. Acta Physico-Chemica URSS 1941; 14: 633
287. Russel, W. B., Saville, D. A., Schowalter, W. R. Colloidal Dispersions. Cambridge University Press, 1989.
288. Ravina, L. Coagulation & Flocculation. Zeta-Meter Inc, 1993.
289. Sincero, A. P., Sincero, G. A. Physical-chemical Treatment of Water and Wastewater. IWA Publishing, 2002.

290. Bache, D. H., Gregory, R. Flocs in Water Treatment. IWA Publishing, 2007.
291. González, T., Domínguez, J. R., Beltran de Heredia, J., Garcia, H. M., Sanchez-Lavado, F. Aluminium sulphate as coagulant for highly polluted cork processing wastewater: Evaluation of settleanility parameters and design of clarifier-thickener unit. Journal of Hazardous Materials 2007; 148: 6-14.
292. Domínguez, J. R., Beltran de Heredia, J., González, T., Sanchez-Lavado, F. Evaluation of ferric chloride as a coagulant for cork processing wastewaters. Influence of the operating conditions on the removal of organic matter and settleability parameters. Industrial and Engineering Chemistry Research 2005; 44: 6539-6548.
293. Amuda, O. S., Amoo, I. A. Coagulation/flocculation process and sludge conditioning in beverage industrial wastewater treatment. Journal of Hazardous Material 2007; 141 (3): 778-783.

Chapter 5

Electrochemical Parameter Study

5 Electrochemical Parameter Study

5.1 Introduction

This chapter explores the relationships between electrochemical parameters and resultant floc produced *via* direct dosing method. The results displayed here are designed to show trends and patterns in operational parameters and floc production. Parameters are divided into three sections: (i) preliminary test work parameters, (ii) process parameters, and (iii) chemical parameters.

5.2 Preliminary Test Work Parameters

In order to decide on the range of experimental parameter values, a number of preliminary trials were carried out which are summarised in the next three sub-sections.

5.2.1 Effect of Pollutant Loading on Flocculation

Figure 5.1 on the following page presents total suspended solids (TSS) and turbidity removal efficiencies for pollutant concentrations (C_0) over the range 0.1 – 1 g/L. As a reproducibility check, one set of conditions (C_0 = 0.5 g/L) was repeated five times (n = 5), with the averaged response reported. All other conditions were carried out in triplicate and error bars have also been included in all figures (error bars shown are ±1 standard deviation (SD)).

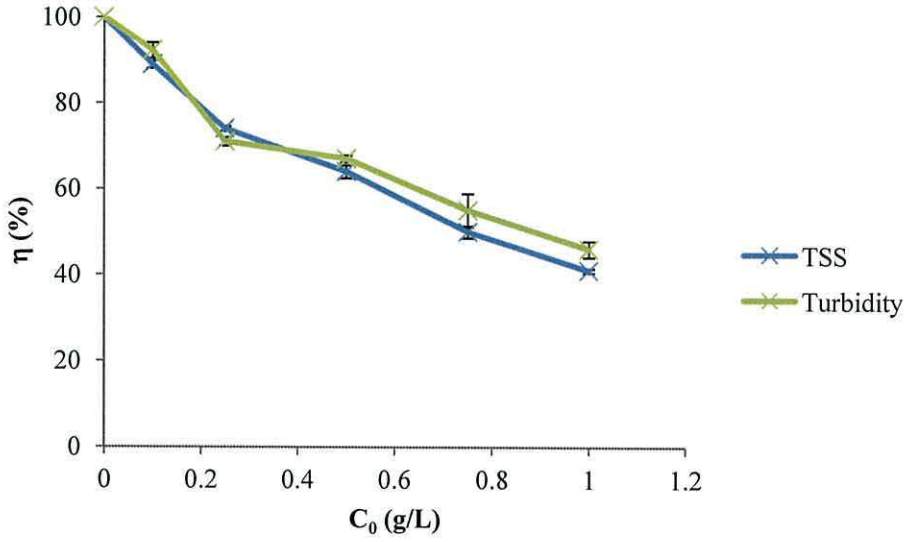

Figure 5.1. Pollutant removal efficiencies as a function of pollutant loading (error bars shown are ±1 SD). Current density = 1.8 mA/cm^2; flow rate 0.25 L/min; electrolysis time = 59 sec; coagulant dose = 1.8 mmol Fe/L; conductivity = 35 mS/cm^2; pH = 7.2; inter-electrode distance = 3 mm.

When pollutant C_0 was increased whilst coagulant dose remained constant, TSS removal efficiency decreased from 89% at 0.1 g/L to 41% at 1 g/L and turbidity from 92% to 46%. The effect of increasing initial pollutant concentration therefore requires a response increase in coagulant dose. This is attributable to the fact that the charged hydroxo-cationic complexes formed during EC are limited in their adsorption of suspended colloids and therefore effectively have a cut-off limit for being able to physically enmesh them. A point is therefore reached whereby the flocs formed have their available adsorption sites fully occupied and cannot adsorb anymore suspended solids. In order to overcome this, more coagulant is needed to be delivered into solution to provide more active adsorption sites and enmesh a greater quantity of colloidal matter.

5.2.2 Effect of Inter-electrode Distance on Flocculation

Removal of TSS and turbidity at inter-electrode spacing's of 1.5, 3, 6, 12 and 24 mm was studied in order to derive the impact of electrode spacing on flocculation. Variation of pollutant removal efficiencies as a function of inter-electrode distance is presented in Figure 5.2 on the following page.

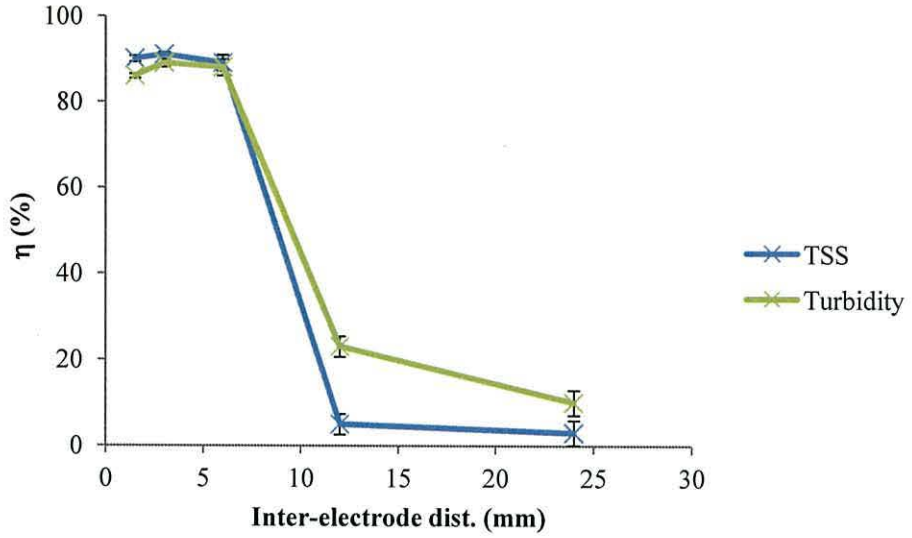

Figure 5.2. Removal efficiencies as a function of inter-electrode distance (error bars shown are ± 1 SD). Current density = 1.8 mA/cm^2; flow rate 0.25 L/min; coagulant dose = 1.8 mmol Fe/L; conductivity = 35 mS/cm^2; pH = 7.2; C_0 = 1 g/L.

Figure 5.2 shows negligible change in pollutant removal efficiencies from 1.5 to 6 mm followed by a dramatic reduction in removal efficiencies at 12 and 24 mm gap spacing's. Upon disassembling the electrode packs it was found that the 12 and 24 mm gap packs were blocked with raw effluent. A quick experiment to understand the natural settling behaviour (settlement velocity) of the raw effluent was conducted by the timed, downward movement of the solid-liquid interface in a graduated vessel.

A 1 L measuring cylinder was filled with homogenised raw effluent and the time taken for the interface between the solid-liquid boundary to traverse a 5 cm distance, delineated by marked lines drawn on the cylinder, revealed that the raw effluent had a settlement velocity of 1.2 mm/s. Calculating the flow through velocity of the effluent through the various electrode packs gaps was then done and the velocities per gap are displayed in Table 5.1.

Table 5.1. Flow through velocities per inter-electrode distance.

Inter-electrode distance (mm)	Flow through velocity (mm/s)
1.5	8.4
3.0	4.2
6.0	2.1
12.0	1.1
24.0	0.5

As illustrated in Table 5.1, the flow through velocities through the 12 and 24 mm gap electrode packs was 1.1 and 0.5 mm/s, below the 1.2 mm/s settlement velocity of the raw effluent. Consequently, the raw suspended solids were not being pushed up, through, and

out of the EC reactor. Thus, sedimentation of effluent occurred in between the electrode gaps of 12 and 24 mm, leading to the poor and inaccurate pollutant removal efficiencies recorded at those spacing's.

A second set of experiments was therefore carried out in which the flow through velocity of the raw effluent through all electrode packs was maintained at 2.1 mm/s, almost double the settlement velocity of the raw effluent (at 1.2 mm/s), thus avoiding any sedimentation occurring within the electrode gaps. In order to do this, the flow rate and current density was altered to accommodate the changes in electrode pack spacing's whilst still maintaining a constant coagulant dose of 1.8 mmol Fe/L. Table 5.2 delineates the parameters instigated during the second set of inter-electrode distance experiments to maintain constant flow through velocity. Results from the second set of experiments are shown in Figure 5.3.

Table 5.2. Parameters implemented to achieve constant coagulant dose of 1.8 mmol Fe/L and flow through velocity of 2.1 mm/s at various inter-electrode distances.

Inter-electrode distance (mm)	Flow rate (L/min)	Current density (mA/cm^2)
1.50	0.06	0.40
3.00	0.12	0.80
6.00	0.25	1.80
12.00	0.50	3.30
24.00	1.00	6.70

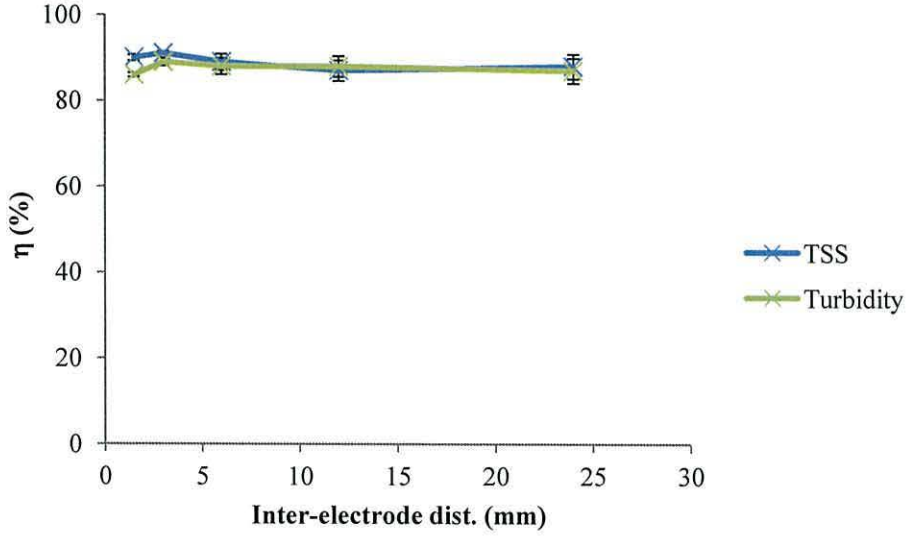

Figure 5.3. Effect of inter-electrode distance on pollutant removals at constant flow through velocity (error bars shown are ± 1 SD). Coagulant dose = 1.8 mmol Fe/L; conductivity = 35 mS/cm^2; pH = 7.2; C_0 = 1 g/L.

From Figure 5.3 there is no change in removal efficiencies despite changes in inter-electrode distance if a constant coagulant dose is maintained (through altering flow rate and current density accordingly). Therefore it can be argued that this set of experiments further proves that coagulant dose is the dominant factor in flocculation.

However, a final set of experiments was carried out in order to understand electrode gap spacing's on flocculation but this time, the operation of the system was switched from a galvanostatic operation to a potentiostatic operation. This was done to remove the constant current factor and assess the system's response directly to changes in electrode distance. Figure 5.4 displays the pollutant removal efficiencies recorded per inter-electrode distance investigated.

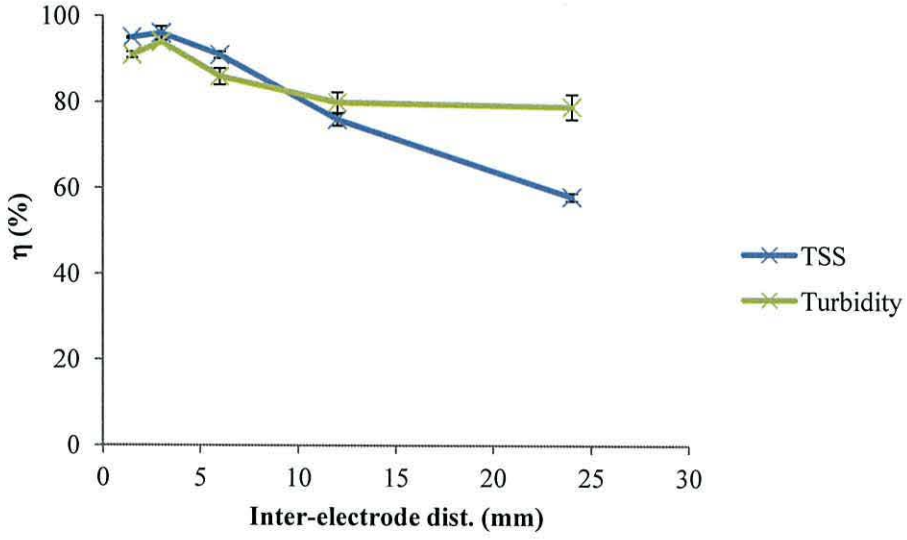

Figure 5.4. Removal efficiencies as a function of inter-electrode distance (error bars shown are ± 1 SD). Flow rate 0.25 L/min; conductivity = 35 mS/cm^2; pH = 7.2; C_0 = 1 g/L.

The analysis revealed that TSS removal efficiency increased from 58% to 96% as electrode distance decreased from 24 to 3 mm. A similar decrease in turbidity (79% down to 94%) was also recorded with maximum removal efficiency for all pollutants observed at inter-electrode distance of 3 mm. However, further reduction in inter-electrode spacing down to 1.5 mm did not increase the process efficiency. This suggests that electrode spacing plays an important part on floc generation and as electrode distance decreases flocculation increases characterised by improved pollutant removal efficiencies. This relationship is relevant down to 3 mm but spacing's smaller than this show a curtailing of removal efficiencies indicating floc formation is not continually improved as distance grows

smaller. The overall trend of diminishing flocculation as inter-electrode distance increases can be explained by variations in Ohmic loss (IR drop).

Ohmic Loss

During the process of EC, a potential is applied across anodes and cathodes inducing electron transfer and the electro-oxidation of the anode material into solution. As treatment continues, metal hydroxide accumulation develops on anodic surfaces and scale can form on cathodic surfaces leading to electrode passivation.[294,295] This phenomena is exaggerated at increased inter-electrode distances as the electrophoretic movement of cations and hydroxides away from their electrode sources slows, and a thick concentration boundary layer within the electrode gaps develops that increases with electrode distance. Consequently, the applied potential during treatment increases over time at constant current input which equates to an increase in Ohmic loss (IR resistance) that in turn inhibits the rate of anodic oxidation. As the rate of anodic oxidation slows, numbers of cations dissolved into solution decreases. As these cations are responsible for the formation of flocculant, floc formation is detrimentally impacted upon. This leads to poor aggregation of suspended solids and pollutant adsorption as illustrated by the reduced TSS removal efficiencies as electrode spacing's increased from 3 to 24 mm. At close electrode spacing's, resistance to current flow in the solution medium is lower and this facilitates the electrochemical removal of TSS. Variation in IR drop is governed by Equation 11 in section 2.4.1.

Equation 11 infers that at constant anodic surface area and solution conductivity, IR increases with the increment of inter-electrode distance. The increase in IR drop is not recommended for EC as this leads to greater energy consumption and higher operating costs.

However, as shown in Figure 5.4, decreasing from 3 to 1.5 mm saw no increase in TSS or turbidity removal suggesting flocculation does not continually improve as electrode distance draws nearer. This is in spite of Equation 16 suggesting that a shorter gap would favour IR drop minimisation. This could be a result of the surface charge of the double layer surrounding the suspended solids suppressing the removal efficiency.[183,296] It was decided to keep the distance between electrodes at 3 mm which was the optimal distance in the EC reactor determined experimentally.

5.2.3 Effect of Coagulant Dose on Flocculation

The effect of coagulant concentration on flocculation *via* direct dosing inferred from the study parameter removal efficiencies, is presented in Figure 5.5. Coagulant dose was varied from 0.5, 0.9, 1.8, 9 and 17.9 mmol Fe/L.

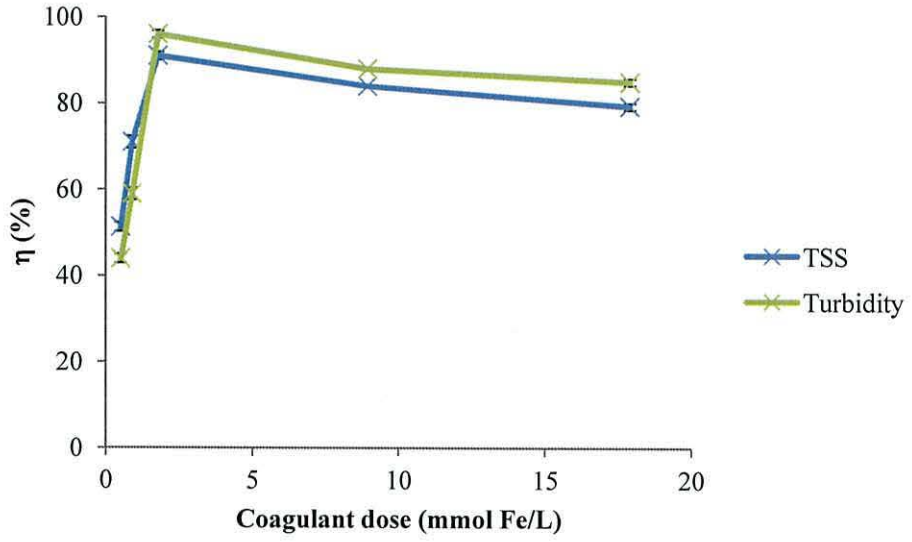

Figure 5.5. Pollutant removal efficiencies as a function of coagulant dose (error bars shown are ± 1 SD). Flow rate = 0.25 L/min; electrolysis time = 59 sec; conductivity = 35 mS/cm^2; pH = 7.2; C_0 = 1 g/L; inter-electrode distance = 3 mm.

As coagulant dose increased from 0.5 to 1.8 mmol/L, TSS removal increased from 51% to 91% and turbidity from 44% to 96%. Therefore, as coagulant amount increased, removal efficiencies increased and a dependency relationship is revealed. However, as coagulant dose increased to 9 and 17.9 mmol/L, the relationship changed. Reduced removal efficiencies of 84% and 79% were recorded for TSS and 88% and 85% for turbidity. This latter trend may be explained by floc density changes and the fractal nature of floc aggregates as discussed below.

Floc Density

For EC treatment it is desirable to produce high-density flocs as, for a given mass, the fluid drag during settleability within a water column is reduced leading to fast sedimentation rates. This floc trait can be achieved under diffusion-limited aggregation (DLA) conditions in which no repulsion is encountered between colliding particles and that each collision leads to attachment and aggregate growth.[297] Under these conditions, particle-cluster floc growth mechanism is proposed whereby a pollutant particle is able to penetrate some way

into an adolescent floc structure before becoming enmeshed and forming part of the flocculant matrix. This mechanism of floc growth is conceptualised in Figure 5.6.

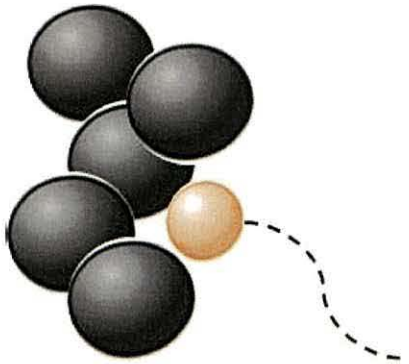

Figure 5.6. Particle-cluster floc growth mechanism; typically at low coagulant dosages.

Formation of flocs *via* particle-cluster mechanism produces high density, compact flocs with high fractal dimensions. In order to generate this flocculant, aggregates must be initially small in size and this is associated with low coagulant doses.[144] The reason being that at low coagulant concentrations, Brownian collision coefficient is low owing to less Fe^{3+} and hydroxyl groups in solution thus the interaction of ions to form $Fe(OH)_3$ coagulant and its subsequent flocculation with pollutant particles is less. The consequence is that much smaller adolescent floc aggregates are formed, however these structures can produce high fractal dimension, high density flocs that settle out quickly due to particle-cluster growth mechanism.

As coagulant concentration increases however, greater concentrations of ions are released into solution and thus Brownian collision coefficient is significantly increased leading to many Fe^{3+} and OH^- interactions and the formation of large adolescent floc. Subsequently, floc formation is brought about by cluster-cluster aggregation in which self-similar aggregate flocs of comparable size combine to form larger mature floc aggregates. These are much more open structures that are highly permeable and are characterised by low fractal dimensions and low density. Consequently, their sedimentation rates are slow. The concept of cluster-cluster growth is illustrated in Figure 5.7 on the following page.

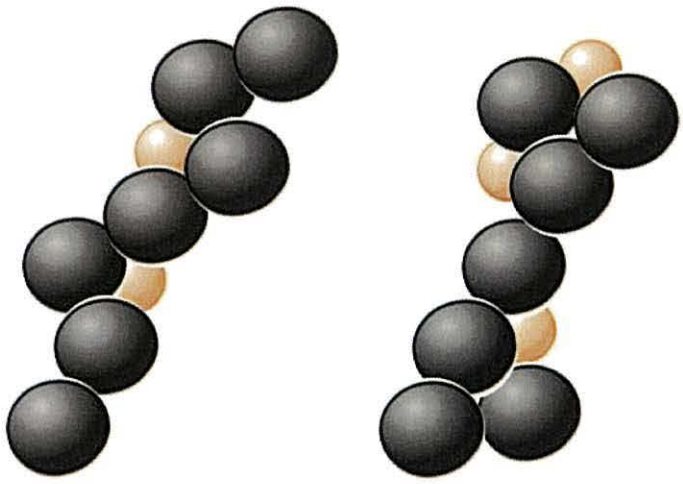

Figure 5.7. Cluster-cluster floc growth mechanism; associated with high coagulant dosages.

The overall effect is that as coagulant concentration increases, floc growth mechanism shifts from one of particle-cluster mechanism, in which compact flocs of high density with d_F about 2.6 is dominant, to one of cluster-cluster growth mechanism characterised by formation of larger, open-structured low density flocs with d_F about 1.8.[298]

This model can be overlaid onto the results in Figure 5.5 whereby it can be attributed that particle-cluster mechanism prevails for coagulant doses of 0.4 – 1.9 mmol Fe/L, as TSS removal efficiency increased from 51% to 91%, but thereafter cluster-cluster floc growth mechanism prevails as removal efficiency decreased from 91% to 84% at 9 mmol Fe/L, and 79% at 17.9 mmol Fe/L. This model is represented in Figure 5.8.

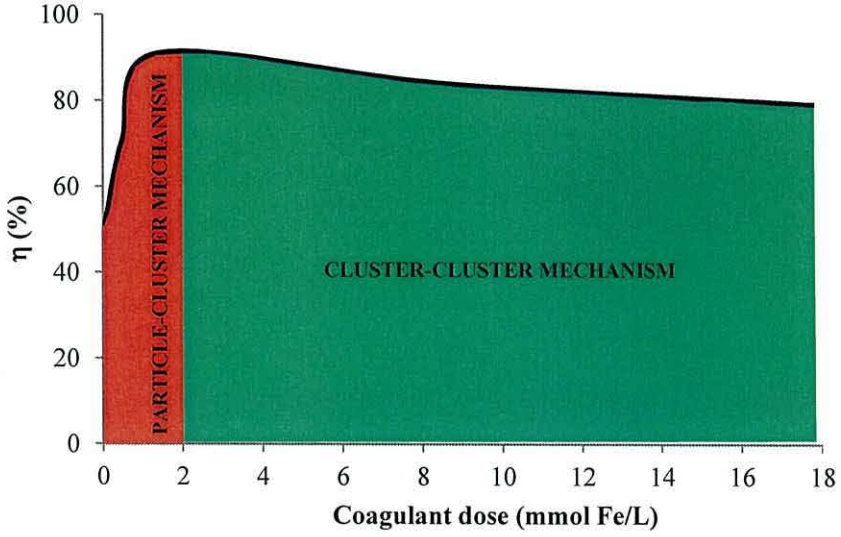

Figure 5.8. Expected floc growth mechanisms at varying coagulation dose.

The impact therefore of higher coagulant concentrations on flocculation is that floc aggregates produced are larger, open structured and less dense leading to poor sedimentation rates and recalcitrant levels of pollutants are left in solution producing reduced removal efficiencies. Whilst floc sizes may be increased at higher coagulant doses, their fractal nature means their effective densities are markedly decreased.[299]

The behaviour recorded during these trials is in contrast however to the finding's recorded in section 4.4.2. During these trials, it was discovered that nucleation rate was favoured over growth rate as coagulant concentration increased. This led to the production of smaller flocs that were greater in number which led to more adsorption and improved pollutant removal efficiencies. The difference however can be explained by the two approaches to EC that was adopted. In section 4.4.2, concentrated coagulant effluent (CCE) was produced that was then blended with raw effluent and subsequently diluted. For the trials reported in this section EC was carried out in continuous mode and under direct dosing conditions and therefore the mechanisms involved are different.

For the coagulant dilution method, EC treatment was configured to promote nucleation rate over growth rate, subsequently this led to smaller floc production at higher coagulant concentration but with the overall effect of improved pollutant removal efficiency. For the current trials, direct dosing of coagulant into effluent was imposed. The prevailing floc mechanisms involved were therefore influenced by particle-cluster or cluster-cluster floc growth mechanism as a result of direct dosing.

5.2.4 Section Conclusions

Experimental variables, specifically pollutant loading, inter-electrode distance and coagulant concentration were evaluated for their effect on flocculation. It can be concluded that the following statements were found for the aforementioned parameters:

- At constant coagulant input, increases in initial concentration of pollutants in a sample wastewater led to reduction in their removal efficiencies. This is a direct result of limited active adsorption sites available within flocs formed at a constant coagulum dose that once occupied, cannot receive any more pollutant particles as concentration increases. In order to overcome this more coagulant has to be delivered into solution and this may be derived stoichiometrically.

- Ohmic loss due to metal hydroxide formation over time on anodic surfaces and passivation of cathodic surfaces is exaggerated as inter-electrode distance increases due to slower electrophoresis rate of ions away from their source electrodes that builds a thick concentration boundary layer within electrode gaps. This drop in IR and subsequent potential increase inhibits the rate of anodic oxidation and desired electrochemical reactions diminishing the concentration of iron cations released into solution. This in turn affects flocculation leading to decreased removal efficiencies.
- Increases in coagulant dose rate during direct dosing treatment method leads to formation of larger sized, open-structured flocs that, due to their low fractal nature have depreciable floc densities and increased drag. This results in slower sedimentation rates and poorer pollutant removal efficiencies.

Following the preliminary test work, pollutant loading was maintained at 1 g/L, inter-electrode distance was optimally maintained at 3 mm, and coagulant dose was experimentally determined to be most efficient at 1.8 mmol Fe/L.

5.3 Process Parameters

The sections present herein detail the impact of four operational parameters on flocculation, that of; current density, stirrer rate, electrolysis time and coagulant retention time.

5.3.1 Effect of Current Density on Flocculation

Some authors have published findings stating that current density can influence pollutant removal efficiencies during EC treatment,[300] therefore this parameter was investigated for its effect on flocculation. Figure 5.9 on the following page shows the impact of current density along with power consumption.

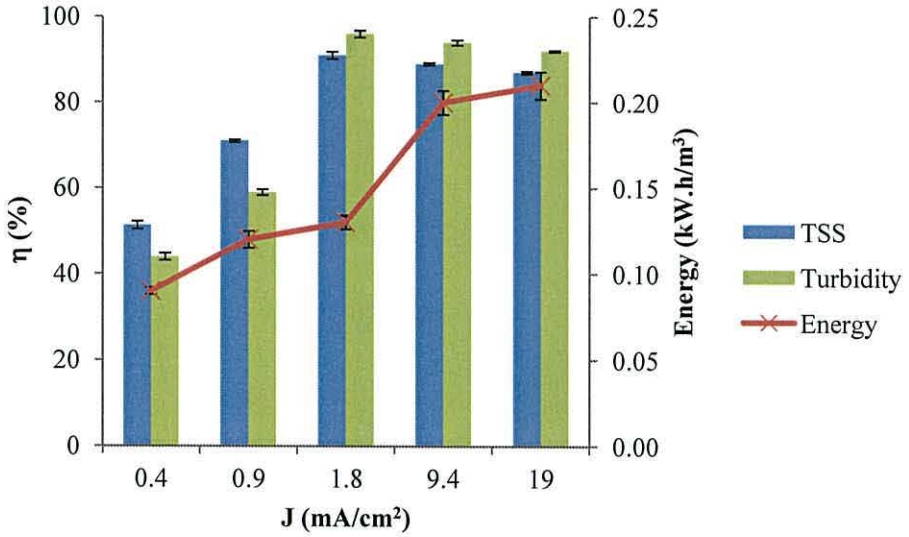

Figure 5.9. Pollutant removal efficiencies and power consumption as a function of current density (error bars shown are ± 1 SD). Flow rate = 0.25 L/min; electrolysis time = 59 sec; conductivity = 35 mS/cm^2; pH = 7.2; C0 = 1 g/L; inter-electrode distance 3 mm.

Figure 5.9 depicts removal efficiencies increasing with increasing current density from 0.4 to 1.8 mA/cm^2. Beyond this however, and removal efficiency improvements are negligible. Figure 5.7 therefore reveals that low current density has a reduced impact on flocculation, whereas at higher current density flocculation is greatly improved characterised by higher removal efficiencies.

During EC, two processes inducing flocculation can be identified; (i) charge neutralisation, and (ii) sweep-floc coagulation. At low current density (identified in Figure 5.9 as 0.4 – 0.9 mA/cm^2), released Fe^{2+} cations contributed to charge neutralisation of pollutant particles as the isoelectric point of said particles was reached. During this mechanism, sorption processes dominated and loose aggregates formed. As current density increased (up to 1.8 mA/cm^2), more cations were electro-dissolved and the generation of $Fe(OH)_3$ occurred which adsorbed and enveloped pollutant particles precipitating them out *via* a mechanism called sweep-floc coagulation.[213]

In support of this, it has been reported in other works that at high current densities, the formation of $Fe(OH)_3$ prevails and has a better coagulating character than $Fe(OH)_2$ associated with low current and charge neutralisation.[254,301] This is evident in Figure 5.9 as at 0.4 mA/cm^2, maximum pollutant removal efficiencies of 51% (TSS) and 44% (turbidity) were recorded. However, at 19 mA/cm^2 higher removal efficiencies of 87% (TSS) and 92% (turbidity) were recorded.

There is an argument therefore to promote the use of high current density to achieve results. In practical terms such a conclusion does not sanction the use of high current density. Figure 5.9 also details power requirement per current density and reveals that as current density increased so did power consumption. Consequently, an increase in current density from 0.4 to 19 mA/cm^2 was accompanied by a power increment from 0.09 to 0.21 $kW.h/m^3$. A balance between optimum removal efficiency and power consumption is therefore needed and this dictates the cost of EC. For this study, the optimal current density found was 1.8 mA/cm^2 at which power consumption was 0.13 $kW.h/m^3$.

5.3.2 Effect of Agitation on Flocculation

As coagulation is generally considered a two stage process of particle transport and particle attachment, agglomerating particles must first collide with each other and secondly adhere upon collision.[302] Consequently, rapid dispersion of coagulum is initially required to introduce adolescent micro-flocs to pollutant particles and generate sufficient kinetic energy to allow them to interact and form physical bonds thereby increasing the size of aggregating molecules. This is accomplished through fast agitation for a short time period. Flocculation is then dependant on slow agitation that allows flocs to further collide, bridge together, mature and ultimately settle out as their size increases. This is usually aided by slow mixing. This forms the basis of a jar-test and in order to assess the impact of stirrer speed on flocculation the initial fast agitation phase was varied between 50 – 800 rpm for 3 min intervals to determine its effect on floc formation. Figure 5.10 on the following page shows the effect of altering stirrer speed on TSS and turbidity removal.

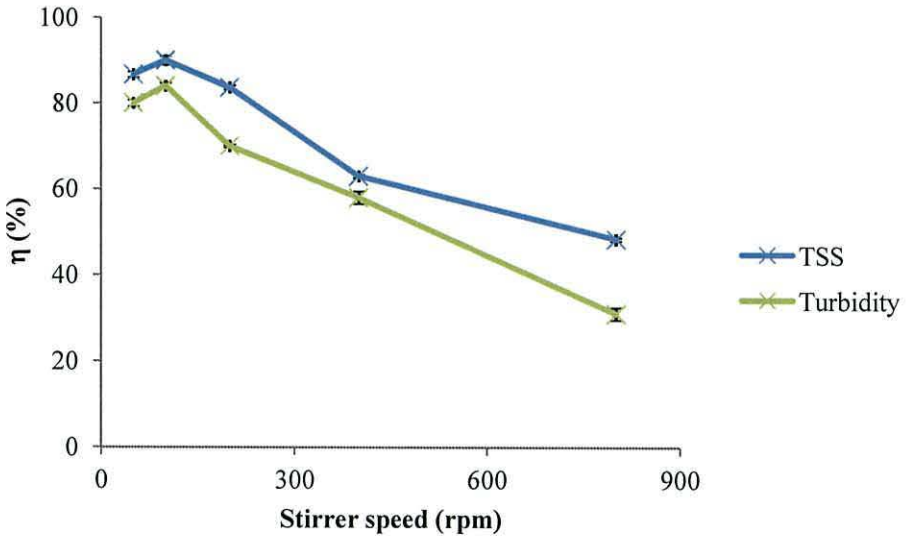

Figure 5.10. Pollutant removal efficiencies as a function of stirrer speed (error bars shown are ± 1 SD). Current density = 1.8 mA/cm^2; flow rate 0.25 L/min; electrolysis time = 59 sec; coagulant dose = 1.8 mmol Fe/L; conductivity = 35 mS/cm^2; pH = 7.2; C_0 = 1 g/L; inter-electrode distance = 3 mm.

The overall trend shown in Figure 5.8 is that of decreasing pollutant removal efficiencies at higher stirrer speeds indicating that flocculation was disrupted as stirrer speed increased. Initially, at the lowest setting of 50 rpm removal efficiencies recorded were 87% for TSS and 80% for turbidity, increasing to 90% (TSS) and 84% (turbidity) at 100 rpm stirrer speed. This initial increase can be explained through adequate stirrer speeds being employed that allowed $Fe(OH)_3$ particles to interact with pollutant particles forming adolescent floc without being subjected to too high a shear rate that detrimentally affected floc size and stability. Beyond 100 rpm stirrer speed the results indicate that the shear rate at faster agitation conditions was too great and floc degradation was experienced delineated by the reduction in removal efficiencies.

The following section discusses the factors that dominate inter-particle collision rates under shear and affect floc growth and formation, also known as orthokinetic flocculation.

Orthokinetic Flocculation

Under perikinetic flocculation (see section Brownian Coagulation Theory) particle-particle collisions are diffusion controlled and dependent on Brownian motion defined by the Smoluchowski treatment theory. This is in contrast to orthokinetic flocculation in which collisions are induced by fluid motion as a direct result of an external mixing source, such as an impeller action, that promotes particle-particle contact. The strength of flocs is of

great importance in (orthokinetic) flocculation due to the shear action imposed by the presence of the mixing source.

Under shear conditions, flocs grow until they reach a certain limiting size, which depends on the applied shear rate.[303] As such, during initial floc formation, aggregation dominates over floc breakage, however as floc size increases, the importance of breakage overrides this relationship and thus, steady-state floc size is governed by the prevailing shear/stress conditions. The rate of particle collisions are fundamental to the rate of floc growth (R_{floc}) which can be defined as the rate of difference between aggregation and floc breakage (R_{br}).[245] Aggregation can be written as the rate of particle collision, R_{col} and a collision efficiency factor α which refers to the fraction of collisions that result in attachment. Thus, the overall rate of floc growth may be expressed as shown in Equation 18:

$$R_{floc} = \alpha R_{col} - R_{br} \qquad \textbf{Equation 18}$$

Under shear conditions αR_{col} decreases as the floc size increases due to the number of particles in the system diminishing thus reducing interparticle collisions.[304] The fundamentals of orthokinetic flocculation can now be applied to the results illustrated in Figure 5.10.

The initial increase, for example recorded in the TSS removal efficiency, from 50 rpm (87%) to 100 rpm (90%) is consistent with adequate shear conditions fragmenting larger flocs into smaller ones that are capable of re-aggregating with each other. The density of these re-aggregated flocs is higher than before and due to their restructuring following fragmentation from their original larger sizes, they are now more compact. As a result, at 100 rpm, agitation was optimal in providing shear conditions that broke floc formations into smaller fragments that could re-aggregate forming new denser, compact flocs allowing for greater and faster removal and sedimentation of pollutants from solution. This is due to compact flocs having more inter-particle contacts owing to the fact that any given particle inside a floc structure will have more close neighbours to bond with. Since the strength of a floc depends on the number and strength of bonds between particles, more compact structures means stronger flocs.[305]

Beyond 100 rpm stirrer speed however and removal efficiencies decreased from 90% to 48% for TSS and 84% to 31% for turbidity. Consequently, as agitation increased, shear

forces imposed on the flocculating system saw floc breakage occur to an irreversible state whereby sheared flocs could not re-aggregate.[306,307,308] For irreversible breakage the collision efficiency is reduced and $\alpha = 0$. Subsequently, flocs at the higher stirrer speeds which were subjected to greater shear, were degraded and adsorbed pollutants were desorbed leading to the lower removal efficiencies recorded.[309]

Figure 5.11 shows the relationship of stirrer speed to shear rate (y) and indicates at which point, with regard to shear rate, floc breakup was experimentally determined.

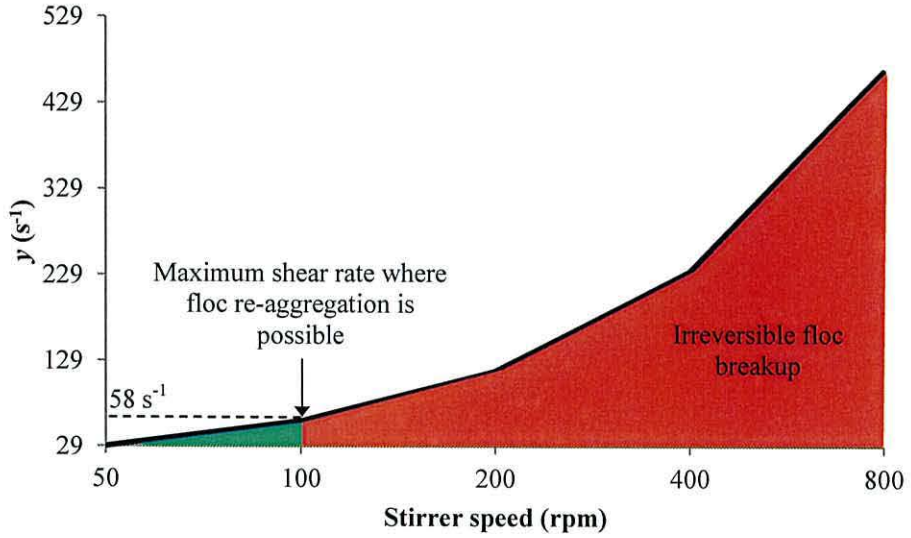

Figure 5.11. Shear rate in respect of stirrer speed delineating where, experimentally determined, shear rate causes floc breakage.

Shear rate (y) is expressed as a ratio between the stirrer frequency rotation n and the ratio between the diameter of the mixing paddle and mixing vessel k as shown in Equation 19:[310]

$$y = \frac{4 \times \pi \times n}{1 - k^2} \qquad \textbf{Equation 19}$$

Where k is the ratio between stirrer diameter and stirrer vessel ($k = d/D$) and in this instance, the diameter of the paddle mixer was 8 cm and the diameter of the mixing vessel was 10 cm, therefore the value of k was 0.8. Stirrer frequency rotation n was converted from the various revolutions per minute (50, 100, 200, 400, 800 rpm) to the SI units s^{-1} by dividing the rpm values by 60, as 60 rpm equals 1 s^{-1}. Consequently, the calculated value

of shear rate per stirrer speed investigated is summarised in Table 5.3 and forms the graph shown in Figure 5.11.

Table 5.3. Shear rate values calculated from rpm's

Stirrer speed (rpm)	Shear rate (s^{-1})
50	29
100	58
200	116
400	233
800	465

As can be seen from Figure 5.11, the maximum shear rate at which floc re-aggregation was possible was 58 s^{-1}. Shear rates in excess of this led to irreversible floc break-up and poorer pollutant removal levels.

5.3.3 Effect of Electrolysis Time on Flocculation

The effect of electrolysis time was studied at constant coagulant input of 1.8 mmol Fe/L from 5 – 200 sec, through lowering current density and flow rate proportionally per electrolysis time investigated. Figure 5.12 illustrates the removal efficiency of TSS and turbidity, as a function of electrolysis time.

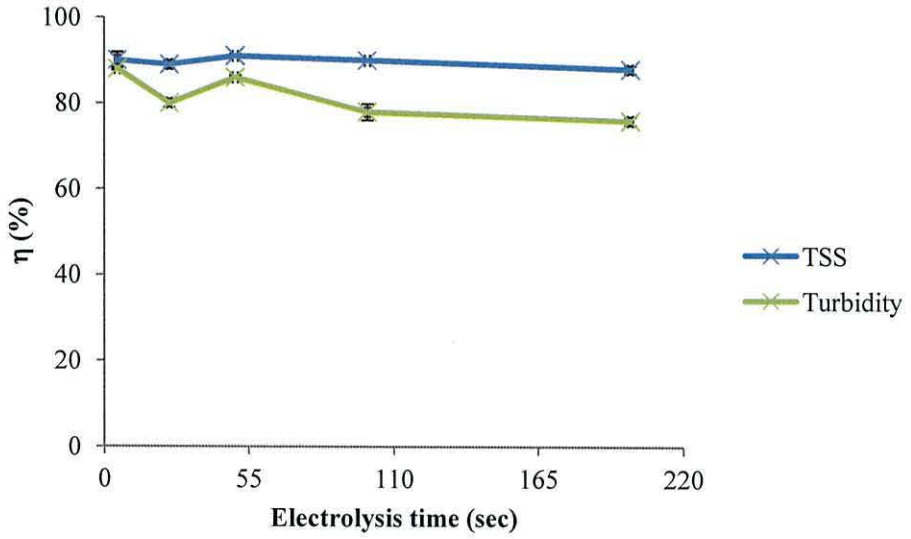

Figure 5.12. Removal efficiencies as a function of electrolysis time (error bars shown are ± 1 SD). Coagulant dose = 1.8 mmol Fe/L; conductivity = 35 mS/cm^2; pH = 7.2; C_0 = 1 g/L; inter-electrode distance = 3 mm.

The results highlight that electrolysis time has no effect on pollutant removal at constant coagulant dosage. This finding establishes and supports that the dominant operating parameter in affecting flocculation and inducing pollutant removal is coagulant

concentration and that within the time frame of the experiments, floc had time to form and stabilise, and therefore electrolysis time does not affect performance.

5.3.4 Effect of Coagulant Solution Retention Time on Flocculation

In order to understand floc lifetime and its activity over time, trials were designed to investigate this aspect. Flocculant solutions at constant coagulant concentration were generated and collected into 100 mL volumes and stored under stirred conditions (25 rpm) for set periods of time in open conditions at room temperature. After holding for set periods, the flocculant samples were introduced into raw effluent volumes and the standard flocculation procedure carried out. Trials were done with a view of assessing floc deactivation over time with regard to pollutant removal. Figure 5.13 on the following page shows TSS and turbidity removal efficiencies over time ranging from 0.2 – 1,440 min.

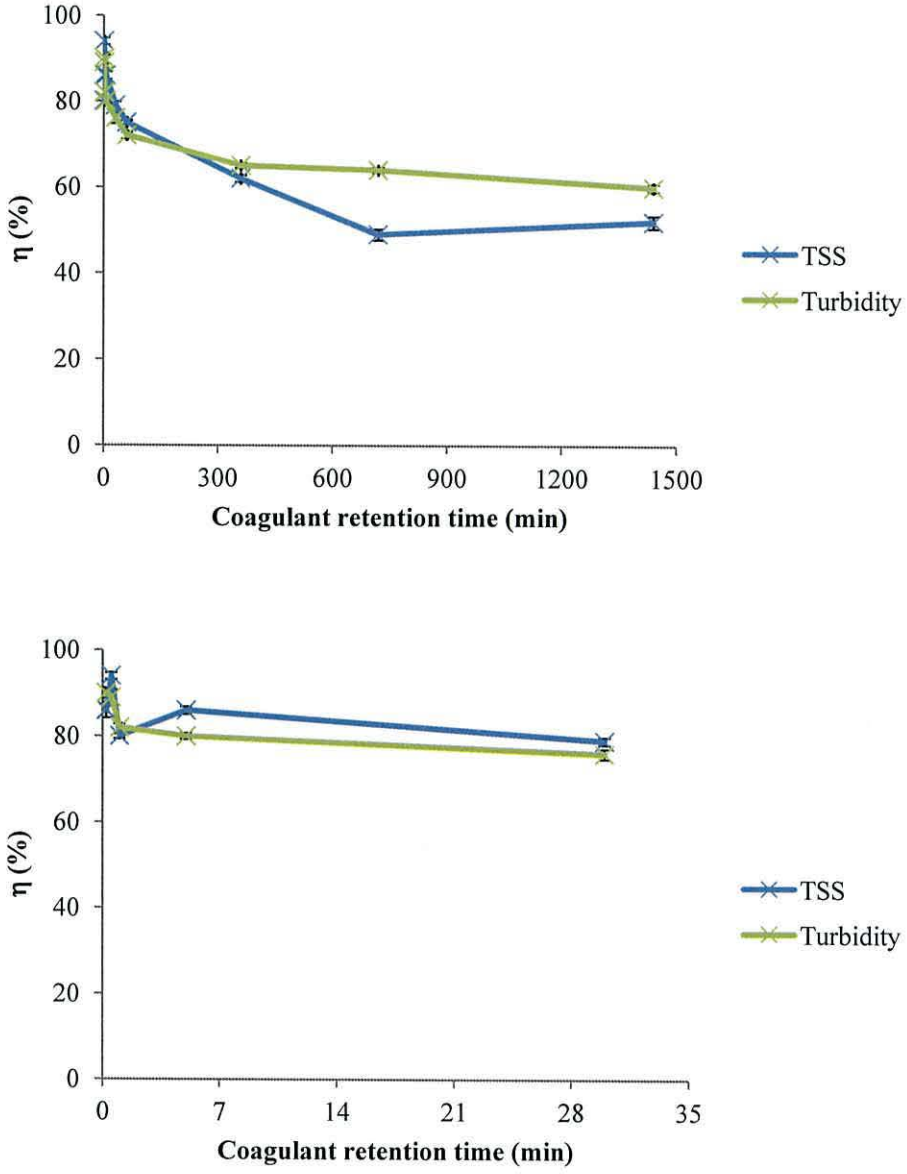

Figure 5.13. ***Top.*** **Pollutant removal efficiencies as a function of all coagulant solution retention times investigated.** ***Bottom.*** **Removal efficiencies for retention times 0.2 – 30 min (error bars shown are ± 1 SD). Current density = 1.8 mA/cm^2; flow rate 0.25 L/min; electrolysis time = 59 sec; coagulant dose = 1.8 mmol Fe/L; conductivity = 35 mS/cm^2; pH = 7.2; C_0 = 1 g/L; inter-electrode distance = 3 mm.**

The overall trend shown is one of decreasing pollutant removal efficiencies as floc retention time increases. During the first 5 min this loss is negligible; however from 30 min to 1,440 min, removal efficiencies decrease from 79% to 52% for TSS and 76% to 60% for turbidity. This suggests that floc has a limited lifetime beyond 5 min before it becomes deactivated and a loss in performance occurs. The reason for this could be related to the formation of magnetite (Fe_3O_4) over time.[311,312] The following section details the progression of floc during the time trials and relates decreasing pollutant removal efficiencies to changes in the oxidation of iron ions in solution.

Surface Charge Variation

Throughout the trials, supernatant samples were filtered (for residual TSS concentration analysis) and the membranes used retained and photographed for their visual record of colour change over time. This is shown in Figure 5.14.

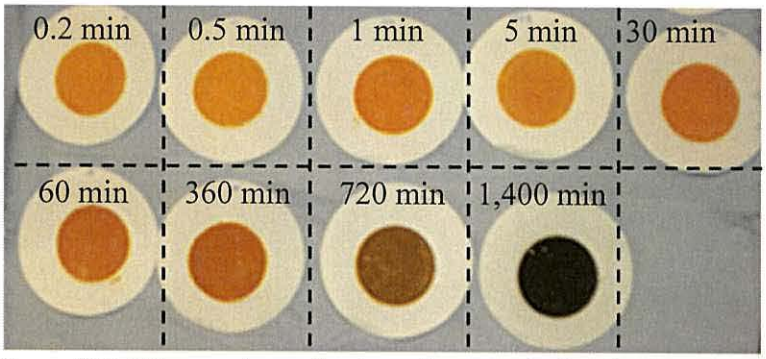

Figure 5.14. Filter membrane discolouration per retention time investigated.

It can be seen that a gradual change in colour from light to dark orange is noted between 0.2 – 360 min, followed by gradation to dark brown and finally black indicating the presence of Fe_3O_4 (magnetite).[313] It is believed that the magnetite formation starts with oxidation of $Fe(OH)^+$ (the dissolved form of $Fe(OH)_2$) in water shown in Equation 20:[314]

$$Fe(OH)_{2(s)} \rightarrow [Fe(OH)]^+_{(aq)} + OH^- \qquad \textbf{Equation 20}$$

Subsequently, the oxidation of $[Fe(OH)]^+$ through the ingression of oxygen into solution over time takes place as follows (Equation 21):

$$2[Fe(OH)]^+_{(aq)} + \tfrac{1}{2}O_2 + H_2O \rightarrow [Fe_2(OH)_3]_{(aq)} + OH^- \qquad \textbf{Equation 21}$$

The intermediate form $[Fe_2(OH)_3]^{+3}$ can combine with another $[Fe(OH)]^+$ to form $Fe_3O(OH)_4^{2+}$, illustrated in Equation 22, which has the equivalent Fe^{2+}/Fe^{3+} ratio as magnetite.

$$[Fe_2(OH)_3]^{+3}_{(aq)} + [Fe(OH)]^+_{(aq)} + 2OH^- \rightarrow Fe_3O(OH)_4^{2+}{}_{(aq)} + H_2O \qquad \textbf{Equation 22}$$

At high oxidation rate or low pH value, it will further oxidize to goethite (FeO(OH)). However, if the concentration of dissolved oxygen in water is low, as was the case in the sample left for 1,400 min, slow oxidation takes place and dehydroxylation occurs before

oxidation so that the intermediate ($[Fe_2(OH)_3]^{+3}$) coverts to magnetite according to Equation 23:

$$Fe_3O(OH)_4^{2+}{}_{(aq)} + 2OH^- \rightarrow Fe_3O_{4(s)} + 3H_2O \qquad \textbf{Equation 23}$$

Consequently, as time progressed and oxygen slowly diffused into solution, this allowed EC generated floc to convert to Fe_3O_4 which had a negative impact on coagulation and pollutant removal efficiencies, illustrated in Figure 5.13. This point is supported by Figure 5.15 that reveals particle shift against a magnet that was held up to the side of the 1,400 min sample beaker. It shows particle shift occurring towards the magnetic force indicating the presence of Fe_2O_3 particles.

Figure 5.15. Particle shift towards a magnetic force that was held against the beaker wall.

The precipitate in sample 1,400 min was then filtered, dried and analysed and the formation of magnetite was confirmed by XRD as shown in Figure 5.16 on the following page.

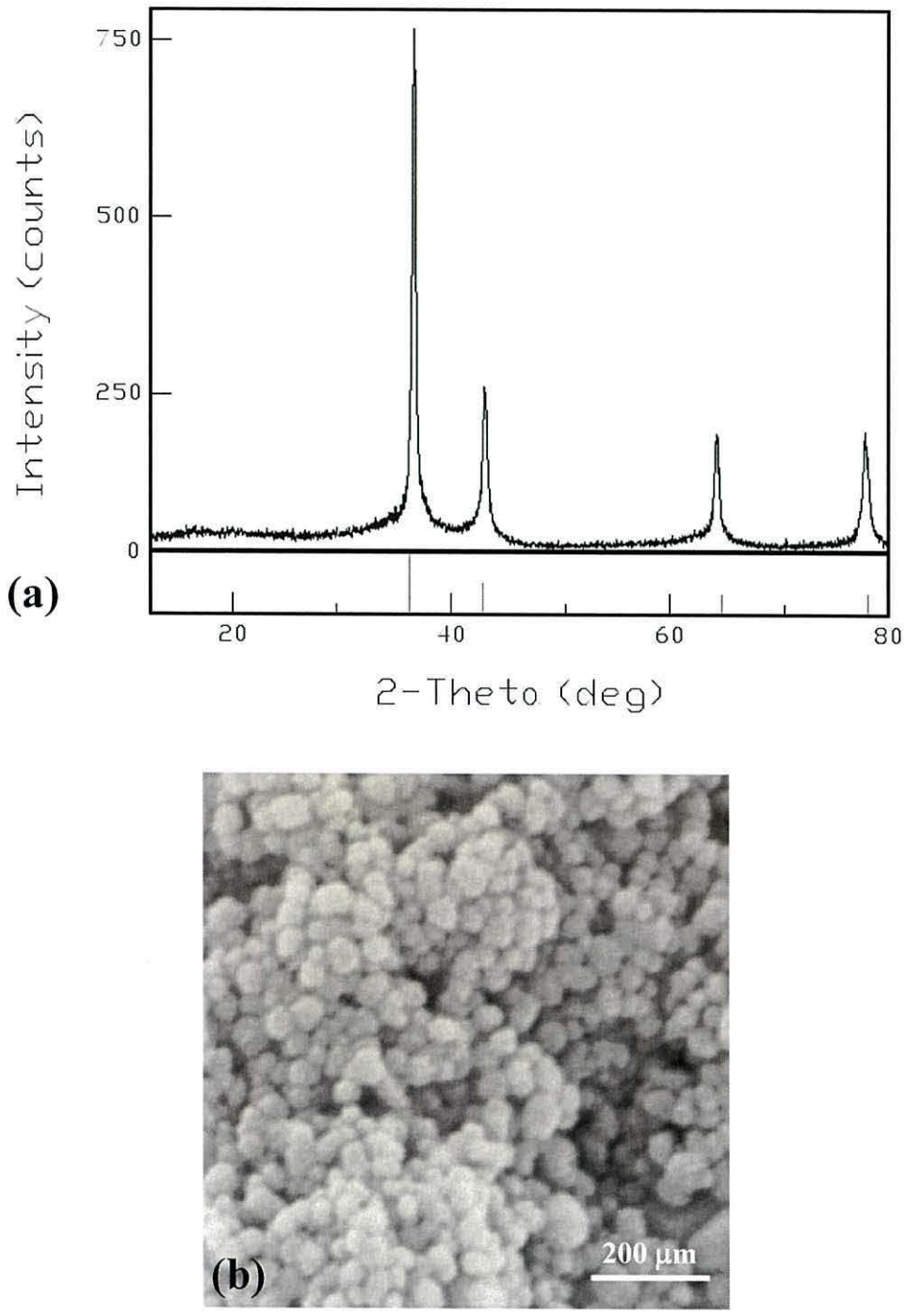

Figure 5.16. (a) X-ray diffraction of magnetite formed at 1,400 min coagulant retention time, (b) SEM image of magnetite formed at 1,400 min coagulant retention time.

As shown in Figure 5.16(a), the precipitate gives rise to peaks corresponding to magnetite. The morphology and size of the solids are also shown in Figure 5.16(b) by SEM analysis. The solids were spherical in shape and approximately 50 – 100 µm in diameter.

5.3.5 Section Conclusions

Process parameters of current density, stirrer speed, electrolysis time and coagulant retention time were investigated for their effects on floc formation. The following conclusions can be drawn from the studies undertaken:

- Changes to current density revealed its impact on pollutant removal and energy consumption. It was found that at current densities below 1.8 mA/cm^2, charge neutralisation dominated the pollutant removal mechanism characterised by low removal efficiencies. At current densities at or in excess of 1.8 mA/cm^2, and the dominate pollutant removal mechanism was found to be sweep-flocculation characterised by high removal efficiencies. Therefore a current density boundary separating the two different removal mechanisms was found. In addition, below the boundary of 1.8 mA/cm^2 energy consumption was low whereas beyond the boundary energy consumption increased. Consequently, a balance between removal efficiency and power consumption was found at current density 1.8 mA/cm^2 which related to a 0.13 $kW.h/m^3$ power consumption.
- In the case of agitation (stirrer speed) impacting on flocculation, flocculating suspensions are governed by prevailing shear conditions and will reach a steady state. When the shear rate increases above a critical level, experimentally determined at 58 s^{-1}, flocs will break until a new steady state is reached. In some cases, because of the irreversible nature of floc breakage, flocs are unable to re-grow if broken at a higher shear rate. Irreversible floc breakage was found to occur at stirrer speeds in excess of 100 rpm. Measuring the shear energy required to break individual flocs or those in a suspension is therefore of high operational importance.
- Electrolysis time was found to impact negligibly in that various electrolysis times from 5 to 200 sec had no significant effect on flocculation at constant coagulant dosage. It can be concluded therefore that the overall dominant process parameter that affects floc formation and coagulation of pollutant particles is coagulant concentration.
- Floc has been found to have a deactivation period after 30 min, whereby the ingress of oxygen in retained flocculant solutions kept in suspension through slow (25 rpm) stirring allows the conversion of floc to magnetite.

5.4 Chemical Parameters

The effects of two chemical parameters; pH and conductivity, were investigated for their impact on floc formation.

5.4.1 Effect of pH on Flocculation

The removal of TSS and turbidity of wastewater at various pH was investigated at constant coagulant concentration to determine its effect on flocculation. Figure 5.17 shows this effect.

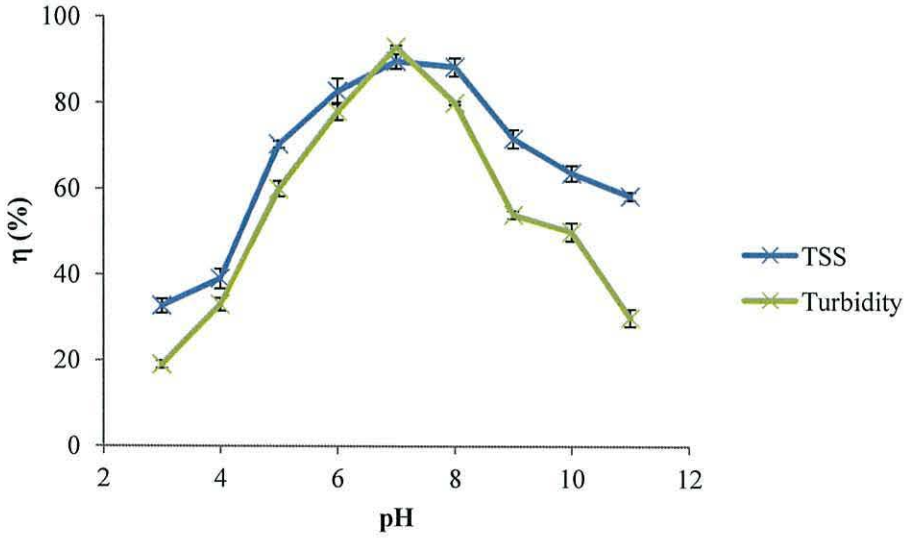

Figure 5.17. Pollutant removal efficiencies as a function of pH (error bars shown are ± 1 SD). Current density = 1.8 mA/cm^2; flow rate = 0.25 L/min; electrolysis time = 59 sec; coagulant dose = 1.8 mmol Fe/L; conductivity = 35 mS/cm^2; C_0 = 1 g/L; inter-electrode distance = 3 mm.

In the pH range studied, pH 7 recorded the highest pollutant removal efficiencies of 90% for TSS and 93% for turbidity. Increasing pH to 11 saw a marked deterioration in removal rates down to 58% for TSS and 30% for turbidity. In the pH range 3 – 7, as pH increased, pollutant removal efficiencies also increased. The results indicate that pH had a substantial impact on flocculation and can be attributed to the iron speciation that occurred with changes in solution pH.

Iron speciation vs. pH

As observed in Figure 5.17, descending from pH 7 to 3, removal efficiency decreased. This behaviour can be explained by the amount of total iron concentration remaining in solution

as Fe^{2+}. Figure 5.18 summarises the percentage of Fe^{2+} in solution after 3 min mixing at 100 rpm under atmospheric conditions with changing pH.

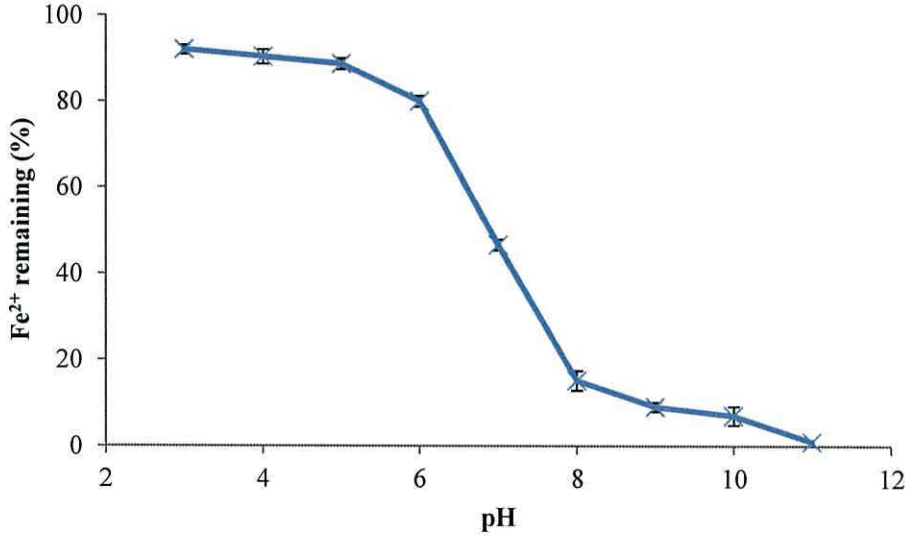

Figure 5.18. Percentage of Fe^{2+} remaining in solution after 3 min mixing as a function of pH under open atmospheric condition (error bars shown are ± 1 SD).

At low pH (3 – 6) Fe^{2+} percentages were measured at 92% decreasing to 80%. This drop was due to faster oxidation of Fe^{2+} to Fe^{3+} as a result of pH increase. This is consistent with results in the higher pH range of 8 to 11 that showed a dramatic reduction in Fe^{2+} remaining as a percentage of total iron. Percentages of 15% (pH 8), 9% (pH 9), 7% (pH 10) and 1% (pH 11) were recorded. These findings reveal that an increase in pH from 6 to 7 is equivalent to an increase in Fe^{2+} oxidation based on Equations 24 and 25:[178]

$$4Fe^{2+}_{(aq)} + O_{2(g)} + 2H_2O_{(l)} + 8OH^-_{(aq)} \rightarrow 4Fe(OH)_3(s) \qquad \textbf{Equation 24}$$

$$\frac{d[Fe^{2+}]}{dt} = -k[Fe^{2+}]\,P_{O2}\,[OH^-]^2 \qquad \textbf{Equation 25}$$

Where k is the rate constant, P_{O2} is the partial pressure of oxygen, and brackets $[i]$ represent molar concentration. It can de deduced therefore that increases in OH^- ion concentration, that occur during the EC process, result in greater Fe^{2+} oxidation and the precipitation of desired $Fe(OH)_3$. Therefore the following holds true for the results that were recorded.

At low pH, the conversion of Fe^{2+} to Fe^{3+} is incomplete as oxidation of Fe^{2+} is slow due to hydroxides at the cathode not being used up. Consequently, it can be assumed that limited pollutant removal recorded in the low pH range in Figure 5.17 is a result of charge

neutralisation mechanism where floc strength is derived from weak van der Waals bonding forces. At neutral pH, oxidation is fast and the formation of $Fe(OH)_3$ is dominant leading to the desired sweep-floc removal mechanism and enmeshment and precipitation prevails leading to high pollutant removal efficiencies shown in Figure 5.17. As pH continues to increase into the alkali region, near complete oxidation of Fe^{2+} to Fe^{3+} is recorded in Figure 5.18, but the increase in OH^- ion concentration leads to the formation of $Fe(OH)_4^-$ through Equation 26:

$$Fe^{3+} + 4H_2O \rightarrow Fe(OH)_4^- + 4H^+ \qquad \textbf{Equation 26}$$

The nature of $Fe(OH)_4^-$ allows it to re-solubilise back into solution and therefore lose its precipitant capability hence the poor removal efficiencies recorded at pH 8 to 11 in Figure 5.17. Based on the experiments carried out in this section and work done by other authors,[315] a pH-Fe speciation diagram can be overlaid onto Figure 5.18 and this is shown in Figure 5.19.

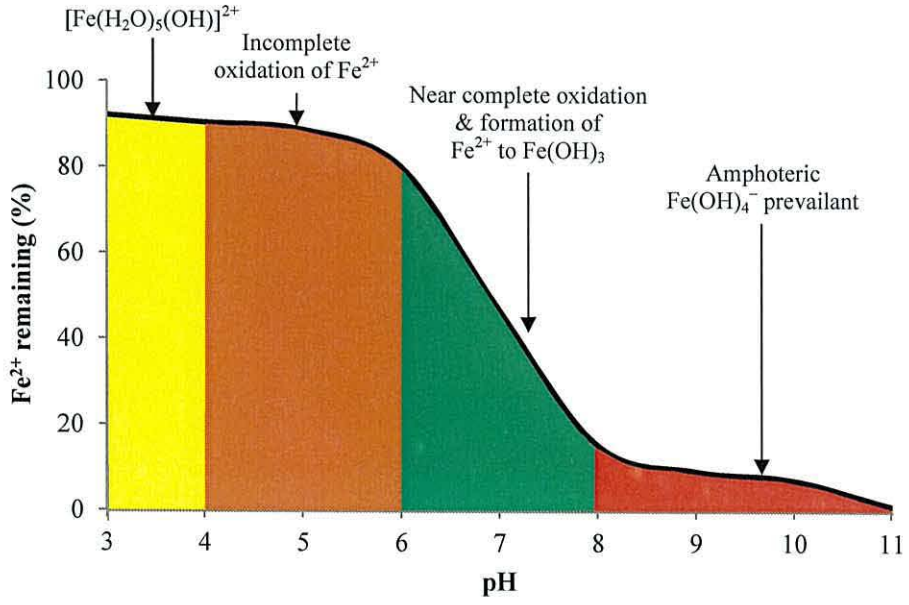

Figure 5.19. pH-iron speciation diagram.

5.4.2 Effect of Conductivity on Flocculation

The sodium chloride concentration of the synthetic solution was varied in order to evaluate the impact of solution conductivity on flocculation. The addition of sodium chloride is also known to diminish the effect of passivation on electrodes.[238]

Table 5.4 shows the relationship between sodium chloride concentration, measured conductivity, and working potential at a constant current density of 1.8 mA/cm^2.

Table 5.4. NaCl addition *vs.* conductivity, at constant current density 1.8 mA/cm^2.

NaCl concentration (g/L)	Conductivity (mS/cm)	Measured potential (V)
5.0	12.5	2.7
10.0	24.6	2.5
15.0	35.2	2.1
20.0	45.0	1.9
25.0	51.4	0.9

As expected, the conductivity of suspensions increased linearly with increasing sodium chloride addition. An increase in conductivity decreases the Ohmic drop between electrodes and therefore the potential required to maintain a constant current is reduced resulting in related energy consumption savings. Figure 5.20 displays TSS and turbidity removal efficiencies against varying conductivity with associated power consumptions.

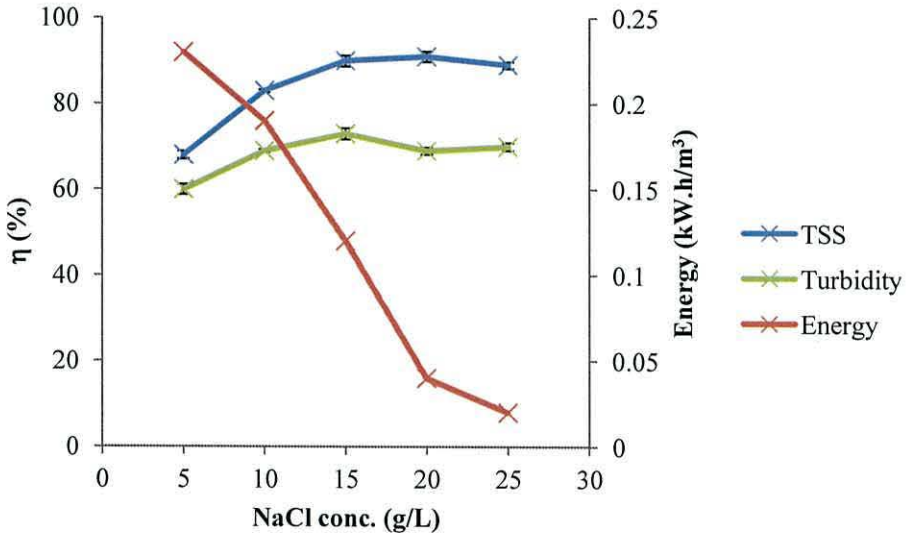

Figure 5.20. Pollutant removal efficiencies and power consumption as a function of conductivity (error bars shown are ± 1 SD). Current density = 1.8 mA/cm^2; flow rate = 0.25 L/min; electrolysis time = 59 sec; coagulant dose = 1.8 mmol Fe/L; pH = 7.2; C_0 = 1 g/L; inter-electrode distance = 3 mm.

During each experiment, the measured pH remained constant. At sodium chloride concentrations of 5 and 10 g/L, TSS removal efficiency was moderate at 68% and 83% and turbidity removal was at 60% and 69%. As sodium chloride content increased to 15 – 25 g/L, removal efficiencies rose to a maximum of 91% for TSS and 73% for turbidity. It can be concluded therefore that as sodium chloride concentration increased, so did the system's performance. Therefore the effect of sodium chloride addition is the intensification of the ionic strength of the suspension.

The ionic strength of a solution is a measure of the concentration of ions in that solution.[300] Greater ionic strength will cause cell potential to drop as the increase in ion concentration from the addition of sodium chloride compresses the double layer surrounding the suspended colloids leading to improved charge neutralisation and coalescence.[316,317]

Above 15 g/L of sodium chloride (related conductivity 35 mS/cm), there was negligible change in system performance and pollutant removal efficiencies were essentially identical thereafter; 90%, 91%, and 89% for TSS and 73%, 69% and 70% for turbidity. In order to remove the influence of conductivity on further experiments, for all remaining electrochemical studies, sodium chloride concentration was maintained at 15 g/L in tap water (1.5% w/v).

With regard to power consumption, Figure 5.20 shows a trend of decreasing consumption as conductivity increased. This is related to cell voltage decreases with increasing wastewater conductivity at constant current density, as illustrated in Table 5.4. It may be considered therefore that higher conductivity is more desirable for better system efficacy.

5.4.3 Section Conclusions

Chemical variables of pH and conductivity were investigated with a view of discerning any trends in changes of either with flocculation. The following statements can be concluded from the experiments undertaken in this section:

- Optimal pH for flocculation in a colloidal system was found to be at neutral pH owing to the predominance of $Fe(OH)_3$ formation. In acidic conditions it has been found that oxidation of Fe^{2+} to Fe^{3+} is incomplete and is reflected in poor pollutant removal efficiencies. As pH shifts towards neutrality the percentage of total iron remaining as Fe^{2+} decreases due to an escalation in rapidity of oxidation to Fe^{3+}. Alkali pH's however also reveal a decline in pollutant removal efficiencies postulated to be due to the conversion of $Fe(OH)_3$ to amphoteric $Fe(OH)_4^-$ re-solubilising back into solution and desorbing previously absorbed contaminants.
- Conductivity was found to improve flocculation as sodium chloride concentration increased up to an optimal 15 g/L. Beyond this; improvements in pollutant removal efficiencies were negligible. It has also been found that addition of sodium chloride presents more ions in solution diminishing system resistance and cell potential as a

result of decreasing the Ohmic drop between electrodes. This also had added benefits of suppressing the Double Layer surrounding colloidal particles and ensuring good flocculation. It was also found that higher conductivity led to reduced energy consumption making for a more desirable system performance.

5.5 References

294. Belmont, C., Ferrigno, R., Leclerc, O., Girault, H. H. Coplanar interdigitated band electrodes for electrosynthesis. Part 4: Application to sea water electrolysis. Electrochimica Acta 1998; 44 (4): 597-603.
295. Virkutyte, J., Rokhina, E., Jegatheesan, V. Optimisation of Electro-Fenton denitrification of a model wastewater using a response surface methodology. Bioresource Technology 2010; 101 (5): 1440-1446
296. Saleem, M., Bukhari, A. A., Akram, M. N. Electrocoagulation for the treatment of wastewater for reuse in irrigation and plantation. Journal of Basic and Applied Sciences 2011: 7 (1); 11-20
297. Meakin, P. Fractal aggregates. Advanced Colloid Interface Science 1988; 8: 249-331
298. Gregory, J. The role of floc density in solid-liquid separation. Filtration and Separation 1998; 35 (4): 366-371
299. Lagvankar, A. L., Gemmell, R. S. A size-density relationship for flocs. Journal of the American Water Works Association 1968; 60: 1040-46.
300. Yılmaz, A. E., Boncukcuoğlu, R., Kocakerim, M. M., Keskinler, B. The investigation of parameters affecting boron removal by electrocoagulation. Journal of Hazardous Materials 2005; B125: 160-165.
301. Zaroual, Z., Azzi, M., Saib, N., Chainet, E. Contribution to the study of electrocoagulation mechanism in basic textile effluent. Journal of Hazardous Materials 2006; 131: 73-78.
302. Amirtharajah, A., O'Melia, C. R. Coagulation processes: destabilisation, mixing and flocculation. In Pontius, F. W. (Ed.) Water Quality and Treatment. A Handbook of Community Water Supplies. McGraw-Hill, 1990.
303. Brakalov, L. B. A connection between the orthokinetic coagulation capture efficiency of aggregates and their maximum size. Chemical Engineering Science 1987; 42: 2373-2383.
304. Aubert, C., Cannell, D. S. Restructuring of colloidal silica aggregates. Physical Review Letters 1986; 56: 738-741.
305. Francois, R. J. Strength of aluminium hydroxide flocs. Water Research 1987; 21: 1023-1030.
306. Spicer, P. T., Pratsinis, S. E., Raper, J., Amal, R., Bushell, G., Meesters, G. Effect of shear schedule on particle size, density, and structure during flocculation in stirred tanks. Powder Technology 1998; 97 (1): 26-34.
307. Gregory, J., Dupont, V. Properties of flocs produced by water treatment coagulants. Water Science and Technology 2001; 44: 231-236.
308. Bayar, S., Yildiz, Y. Ş., Yilmaz, A. E., İrdemez, Ş. The effect of stirring speed and current density on removal efficiency of poultry slaughterhouse wastewater by electrocoagulation. Desalination 2011; 280: 103-107.
309. Fischer, W. R., Schwertmann, U. The formation of hematite from amorphous iron (III) hydroxide. Clays & Clay Minerals 1975; 23: 33-37.

310. Bobic, B., Babic, M. Mitrovic, S., Bobic, I., Jovanovic, M. T. Experimental investigation and calculation of shear rate, shear stress and power for mixing of semi-solid mixtures of ZA27 alloy and ZA27/Al_2O_3 composites with large Al_2O_3 patricles. Association of Metallurgical Engineers of Serbia 2011; 17 (1): 1-12.
311. Parga, J. R., González, G., Moreno, H., Valenzuela, J .L. Thermodynamic studies of the strontium adsorption on iron species generated by electrocoagulation. Desalination and Water Treatment 2012; 37: 244-252.
312. Tsouris, C., DePaoli, D. W., Shor, J. T., Hu, M. Z.-C., Ying, T.-Y. Electrocoagulation for magnetic seeding of colloidal particles. Colloids and Surfaces A: Physicochemical and Engineering Aspects 2001; 177: 223-233.
313. Dufour, J., Marron, J. O., Negro, C., Latorre, R., Formoso, A., Lopez-Mateos, F. Mechanism and kinetic control of the oxyprecipitation of sulphuric liquors from steel pickling. Chemical Engineering Journal 1997; 68: 173-187.
314. Golder, A. K., Samanta, A. N., Ray, S. Removal of trivalent chromium by electrocoagulation. Separation and Purification Technology 2007; 53: 33-41.
315. Burgot, J. L. Ionic Equilibria in Analytical Chemistry. Springer, 2012.
316. Kobya, M., Can, O. T., Bayramoglu, M. Treatment of textile wastewaters by electrocoagulation using iron and aluminium electrodes. Journal of Hazardous Materials 2003; B100: 163-178.
317. Lin, S. H., Peng, C. F. Treatment of textile wastewater by electrochemical method. Water Research 1994; 28: 277-282.

Chapter 6

Characterisation

6 Characterisation

6.1 Introduction

In this chapter floc produced under varying operational parameters are shown along with impacts of electrocoagulation on surface morphology and electrochemical changes at the electrode surfaces used during trial work.

6.2 Electrokinetic Studies

Zeta potential measurements were taken to characterise and quantify the charge of floc particles with a view of better understanding the performance of EC and determine removal mechanism.

6.2.1 Zeta Potential *vs.* Coagulant Concentration

The results in Figure 6.1 show changes in zeta potential (ζ) against varying coagulant concentration. As discussed previously (see section Electrical Double Layer Compression) pollutants are maintained in suspension by electrostatic repulsion between particles. The ζ-potential provides an effective measurement of the charge on a particle. Addition of coagulant could suppress the electric Double Layer surrounding suspended particles, thus reducing repulsion and encouraging aggregation of the pollutant.

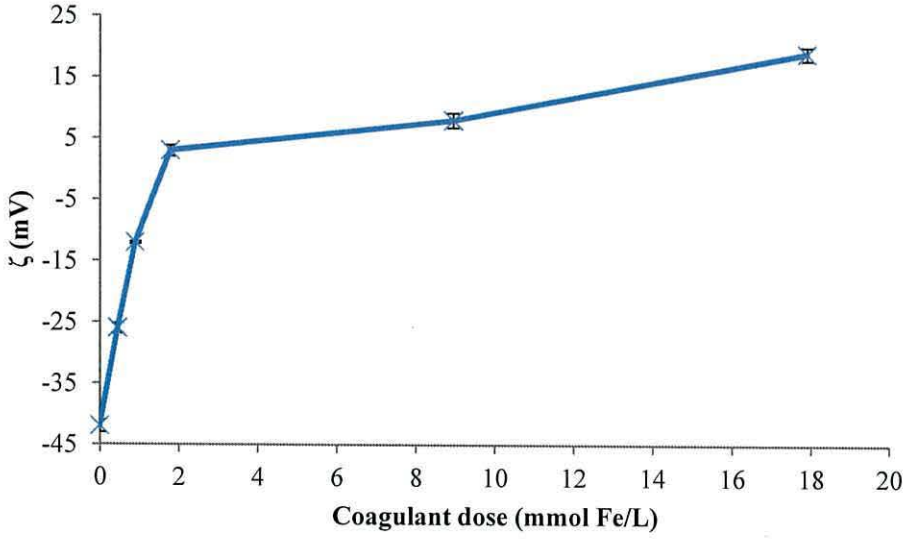

Figure 6.1. Zeta potential as a function of coagulant concentration (error bars shown are ± 1 SD).

It can be seen that the raw synthetic effluent (with no coagulant addition) was stable at –42 mV. This is in accordance with other authors that have demonstrated that naturally occurring colloidal systems acquire a ζ-potential of between –5 and –40 mV.[318,319,320,321] As coagulant addition was increased ζ-potential increased to –12 mV, however the concentrations (0.5 and 0.9 mmol Fe/L) can be regarded as being insufficient to effectively reduce particles' Double Layer and enable mass destabilisation and aggregation as only 71% TSS and 59% turbidity removal efficiencies were recorded at this point (see Figure 5.3). Only at a coagulant concentration of 1.8 mmol Fe/L do particles approach their isoelectric point (point at which a colloidal system is least stable) and flocculation was markedly improved by TSS and turbidity removal efficiencies of 91% and 96% being recorded. Beyond addition of 1.8 mmol Fe/L and ζ-potential increased to a maximum of 19 mV at a coagulant concentration 17.9 mmol Fe/L. This is a result of excessive $Fe(OH)_3$ molecules in solution neutralising the negative charge of suspended particles in solution and conferring a positive replacement charge on particle surfaces, thus re-dispersing the particles. This is supported by results in Figure 5.3 that show a decrease in pollutant removal efficiencies at higher coagulant concentrations.

6.2.2 Zeta Potential *vs.* pH

Figure 6.2 shows ζ-potential versus pH during the trials that were carried out in section 5.4.1, along with the position of the isoelectric point (at 0 mV).

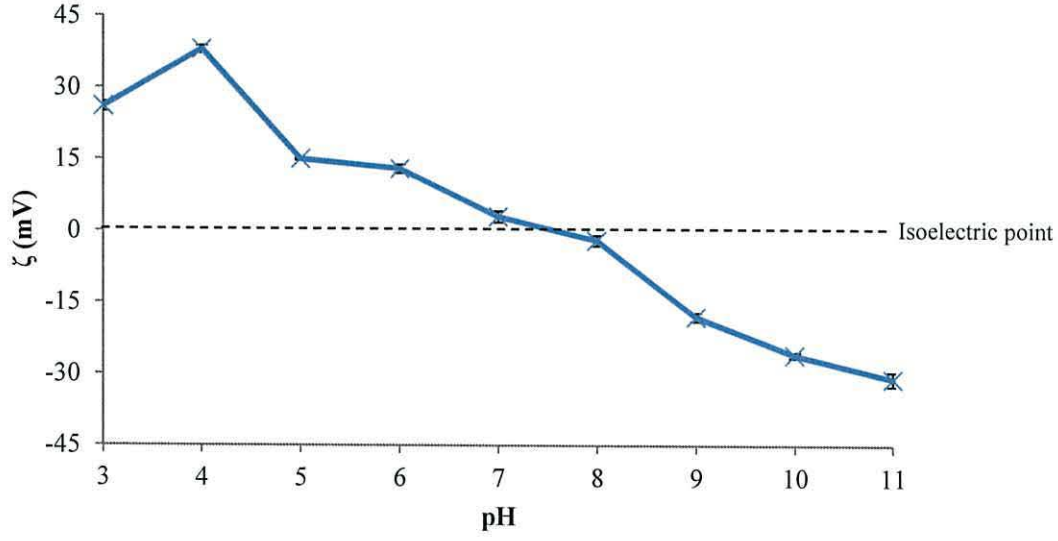

Figure 6.2. Zeta potential as a function of pH (error bars shown are ± 1 SD).

From the plot it can be deduced that pH's below 8 led to positive values of the ζ-potential and higher values of pH caused negative ζ-potential. This behaviour could be explained in terms of the charge of the suspended colloidal particles, which were positive due to the adsorption of cations such as Fe^{2+}, $Fe(OH)^{2+}$, and negative due to the adsorption of negatively charged ions in the form $Fe(OH)_4^-$ as a result of their prevalence in solution dependant on pH conditions. Consequently, zones can be incorporated into the plot that can show areas of stability and instability of the colloidal system at various pH. In Figure 6.2 the isoelectric point (0 mV) is approximately at pH 7, and ζ-potential values between 0 ± 15 mV can be considered unstable and where flocculation is expected to occur, whilst ζ-potential values lying outside this range can be considered as stable where flocculation is compromised. Zones displaying stable and unstable areas in Figure 6.2 are identified in Figure 6.3.

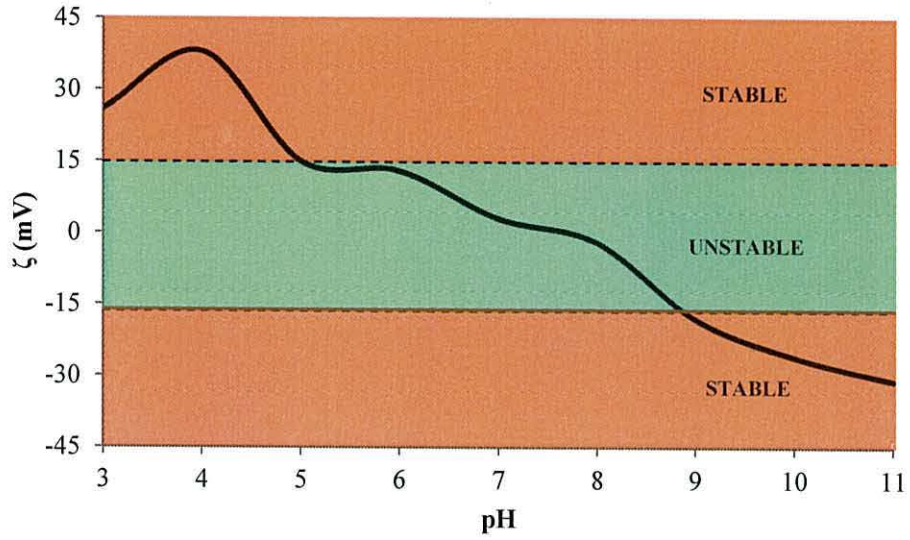

Figure 6.3. Zeta potential as a function of pH with zonal markings indicating areas of suspension stability (no flocculation expected) and areas of suspension instability (flocculation expected).

Furthermore, extrapolated from the results in Figure 6.2, some inferences can be made regarding removal mechanism. Flocculation is a result of the precipitation of iron hydroxides and their aggregation and formation of polymeric hydro-complexes with pollutant particles. Consequently, these complexes and hydroxide particles are positively charged if the pH is below their isoelectric point as addition of acid causes a build-up of positive charge and hence they are adsorbed on the surface of the colloids producing charge suppression and coagulation. If the pH of the solution is beyond the isoelectric point of the hydroxide precipitate then the hydroxide particles will be negatively charged (generation of $Fe(OH)_4^-$) and no charge suppression of the colloid particles is possible. In

this situation colloid coagulation can only occur if the amount of hydroxide precipitate is sufficient enough for bridge formation and sweep-floc enmeshment mechanism to prevail. As a result, a final zoning of the plot in Figure 6.3 can be the addition of predicted removal mechanisms of charge neutralisation (at low pH 3 – 7) and sweep-floc (at high pH 7 – 11) to effectuate pollutant removal from solution, as shown in Figure 6.4.

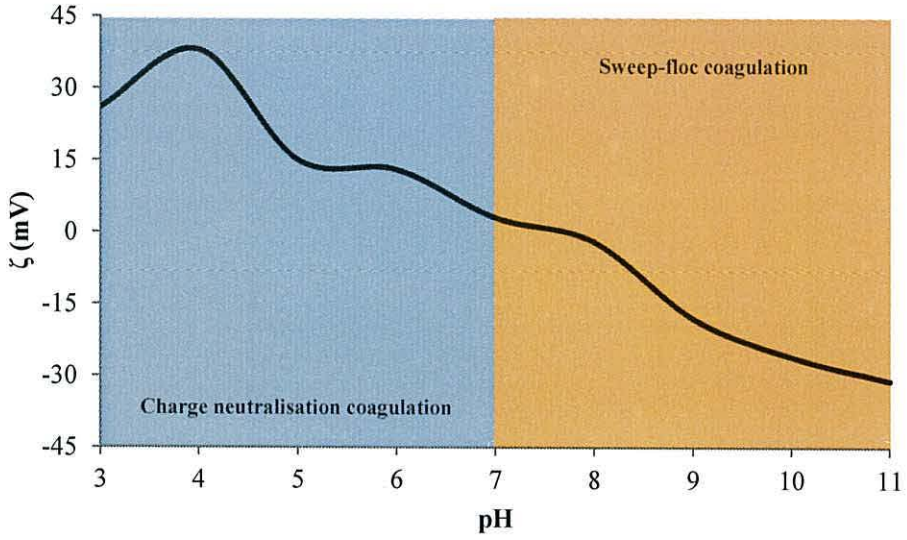

Figure 6.4. Zeta potential as a function of pH with zonal markings indicating where charge neutralisation and sweep-floc coagulation is expected to occur.

6.3 Voltammetry Studies

The voltammetric response of a mild steel electrode in trickling filter bed effluent was measured and is depicted in Figure 6.5 on the following page. This effluent was chosen as the synthetic suspended solution used in Chapter 5 suffered from solids present in the solution.

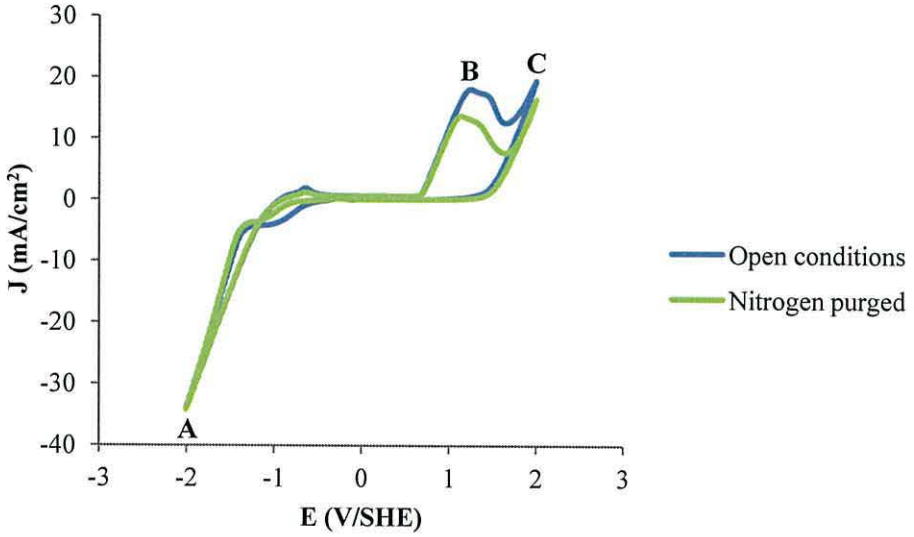

Figure 6.5. Cyclic voltammogram obtained from mild steel disc electrode in trickling filter bed effluent under open conditions and nitrogen purging, at 100 mV/sec scan rate and pH 7.5. Scan initiated at 0 V, E_1 = -2, E_2 = 2 V.

The voltammetric response in Figure 6.5 shows that the dissolution of iron in the effluent is limited in the potential region of –0.5 to 0.7 V, as depicted by the current plateau, but at potential above this region, the current density increased as potential increased. This shows that the extent of iron dissolution is a function of the potential applied. Cathodic peak A at –2 V is related to hydrogen evolution described by Equation 27:

$$2H_2O_{(l)} + 2e^- \rightarrow 2OH^-_{(aq)} + H_{2(g)} \qquad \textbf{Equation 27}$$

Anodic peak B at 1.25 V within the active dissolution region is due to the formation of $Fe(OH)_2$,[322] and is related to Equation 28:

$$Fe^{2+}_{(aq)} + 2H_2O_{(l)} \rightarrow Fe(OH)_{2(s)} + H_{2(g)} \qquad \textbf{Equation 28}$$

Peak C is representative of $Fe(OH)_3$ formation as dissolved Fe^{2+} is further oxidised to ferric hydroxide (Equation 29):

$$2Fe^{2+}_{(aq)} + 5H_2O_{(l)} + \tfrac{1}{2}O_{2(g)} \rightarrow 2Fe(OH)_{3(s)} + 4H^+_{(aq)} \qquad \textbf{Equation 29}$$

This is exaggerated in the open conditions voltammogram, whereby the presence of oxygen hastens the conversion of Fe^{2+} to Fe^{3+} and its subsequent precipitation to $Fe(OH)_3$ is enhanced, compared to the voltammogram conducted in nitrogen purged conditions.

6.4 Floc Imaging

Transmission electron microscope images of floc produced under three different coagulant dosages are shown in Figure 6.6.

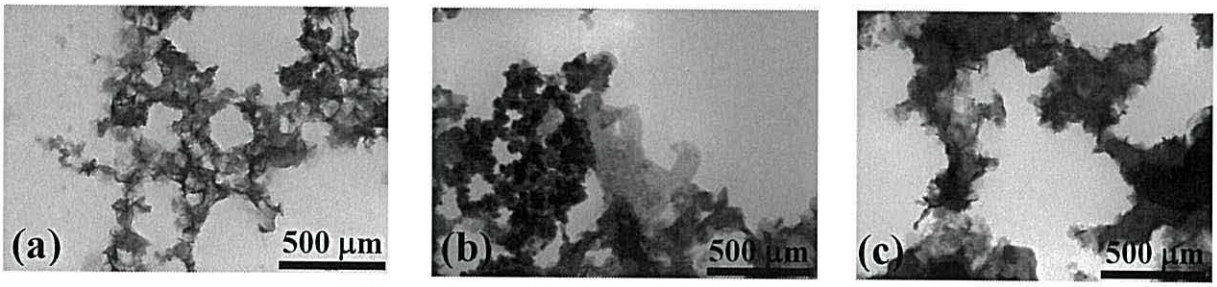

Figure 6.6. TEM images of floc formed by: (a) 0.9 mmol Fe/L coagulant dose, (b) 9 mmol Fe/L coagulant dose, (c) 17.9 mmol Fe/L coagulant dose.

The images reveal that under low coagulant concentration of 0.9 mmol Fe/L, the flocs formed are of a wispy nature and are low density due to insufficient coagulant electro-dissolved into solution unable to flocculate and aggregate with colloids. At 9 mmol Fe/L concentration, flocs formed are denser and have aggregated well together forming compact structures as identified by minimal open spaces between aggregates. At the maximum coagulant dose tested of 17.9 mmol Fe/L the flocs generated are large but open structures.

These images correspond to the pollutant removal efficiencies shown in Figure 5.5 and reveal that at coagulant concentration 9 mmol Fe/L, dominant floc formation was through particle-cluster mechanism forming the densely aggregated high density structures and good removal efficiency of 90%. Whereas at 18 mmol Fe/L, floc growth was dominated by cluster-cluster aggregation producing large open structures of low density and a reduced pollutant removal efficiency of 81%.

Imagery of floc was also obtained at 0.9 and 9 mmol Fe/L coagulant additions to assess the size of flocs produced in relation to concentration. Scanning electron microscope images shown in Figure 6.7 on the following page indicate that flocs formed at the higher dosage are larger and more compactly structured than flocs formed at the lower concentration.

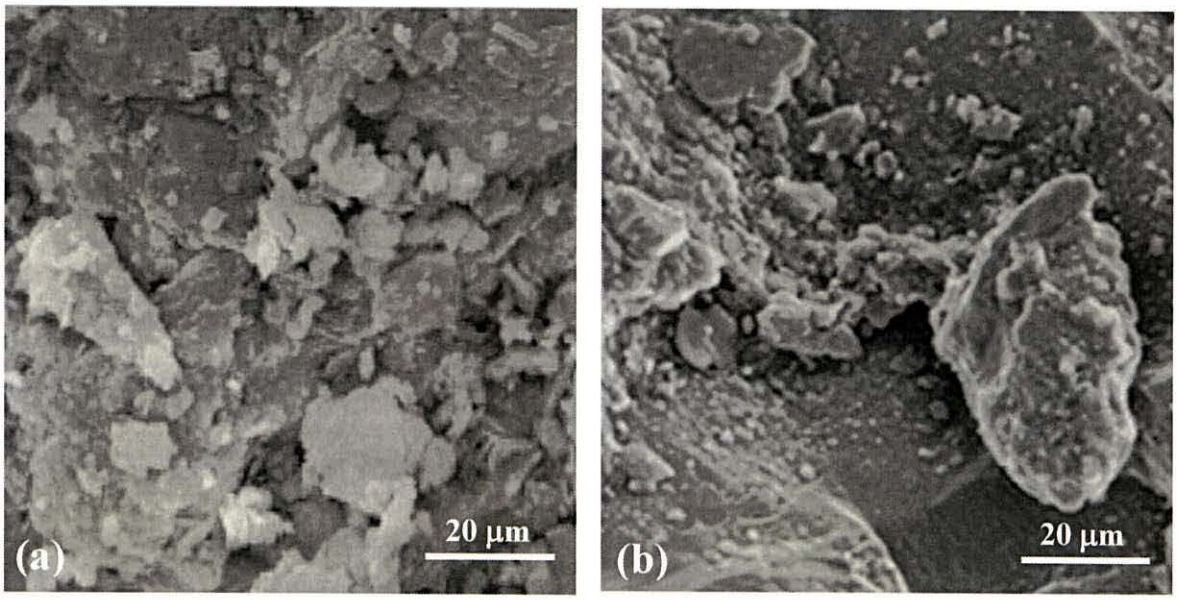

Figure 6.7. SEM images of flocs formed by: (a) 0.9 mmol Fe/L coagulant dose, (b) 9 mmol Fe/L coagulant dose.

It can be concluded therefore that at the lower coagulant concentration, destabilisation of the pollutant particles occurred through charge neutralisation mechanism *via* adsorption of small ferric hydroxide precipitates onto colloidal surfaces, whereas at the higher coagulant concentration sweep-floc conditions prevailed. This relationship of smaller size at lower coagulant concentrations is further supported by photomicrographs (at identical magnification of 20x) captured by the nano-arrayer camera shown in Figure 6.8. The nano-arrayer can assign lengths in µm to imagery and they have been included in Figure 6.8. This was a useful tool as when a floc is spherical its diameter can easily be measured. However, for irregular flocs the diameter cannot directly be measured and therefore only estimated. One approach to estimating the diameter is to measure the length that bisects the irregular floc and this is known as the Martin diameter.[323] As all flocs imaged were irregular the Martin diameter was therefore used to measure the floc sizes reported on the following page, but it should be noted that these are arbitrary figures.

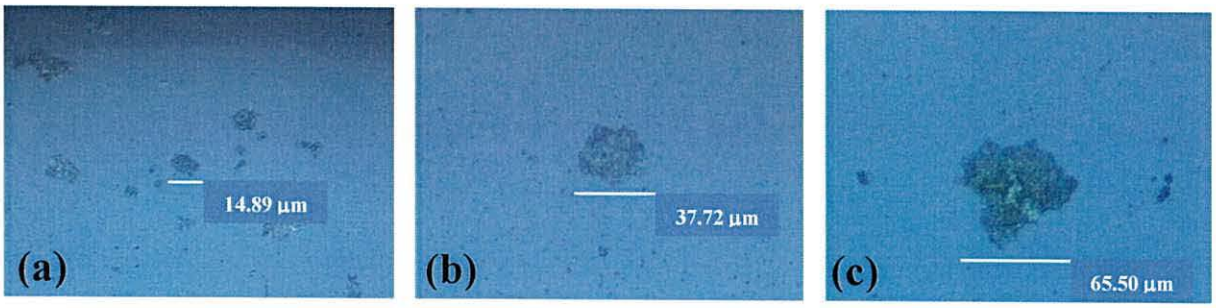

Figure 6.8. Nano-arrayer camera images of floc by: (a) 0.9 mmol Fe/L coagulant dose, (b) 9 mmol Fe/L coagulant dose, (c) 18 mmol Fe/L coagulant dose.

The photomicrographs of Figure 6.8 shows: (a) flocculant at low coagulant dose (0.9 mmol Fe/L) being angular and free of any significant aggregation; (b) at 9 mmol Fe/L, floc is larger and approximately 37 μm in length; and (c) floc formed at 18 mmol Fe/L is twice as large at approximately 65 μm in length indicating significant coalescence to form such a sized aggregate. The large floc aggregate also reveals its difference in character or texture compared to (a) and (b) appearing as much darker owing to the sweep-floc coagulation mechanism by which it grew. In (a) the flocs appear loose and fibrous whereas in (c) the floc is compact. The darker colour of (c) maybe the result of the macerated dog food suspended solids adsorbed onto the entire surface of the iron hydroxide complex.

6.5 Operational Costs

As EC requires electrical current to release metallic cations into solution, a cost is incurred both in terms of energy consumption (kW.h/m^3) and electrode consumption (kg Fe/m^3). Other associated costs are equipment maintenance and sludge disposal. For this study, an economic investigation was conducted on the energy and electrode material cost at various current densities (0.4, 0.9, 1.8, 9.4, 19 mA/cm^2). Energy consumption is already outlined in Figure 5.9 (section 5.3.1). Figure 6.9 on the following page therefore represents the total EC operational cost at various current densities by totalling energy consumption (where average price of electricity purchased by industry in the UK as of December 2014 was 0.076 GBP/kW.h), derived from Figure 5.9 and electrode cost (where cost of carbon steel plate was 0.43 GBP/kg as of December 2014).

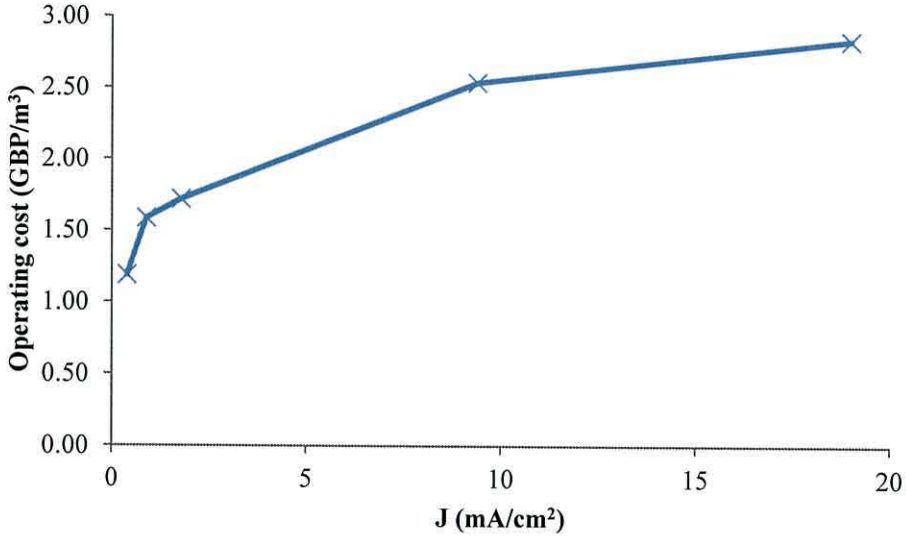

Figure 6.9. Total cost of treatment as a function of current density.

It can be seen that operational cost increased as current density did. This is due to increases in both electrical consumption and electrode material. At the optimum operating conditions of 1.8 mA/cm^2 and flow rate 0.25 L/min, the cost of treatment was 1.72 GBP/m^3.

6.6 Sludge Production

Along with the purification of treated water, sludge is generated and wet sludge volumes at the bottom of samples collected during coagulant dose trials were used to quantify the amount generated. This is summarised in Figure 6.10.

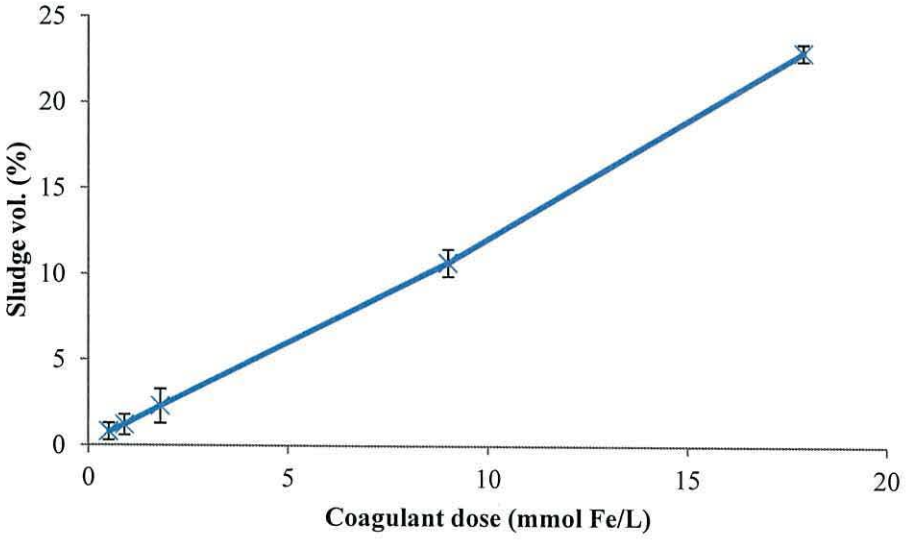

Figure 6.10. Sludge volume post-settlement as a function of coagulant dose (error bars shown are ± 1 SD).

Raw wastewater was treated at various coagulant concentrations (0.5, 0.9, 1.8, 9 and 17.9 mmol Fe/L). The amount of sludge generated in 1 L settled samples, expressed as a percentage, reveals that as coagulant dose increased from 0.5 to 17.9 mmol Fe/L, sludge volume increased linearly from 0.8% to 23%. At the optimum coagulant dose of 1.8 mmol Fe/L, the amount of sludge produced was 2.3% and after drying at 105° C for 3 hours, revealed a produced sludge mass of 1.01 kg/m^3. This figure equates to the amount of coagulant dosed (1.8 mmol Fe/L in kilograms per metre cubed is 0.1 kg/m^3) and the amount of solids removed from the effluent (91% removal efficiency from a raw solids loading of 1 g/L = 0.91 kg/m^3).

In terms of sludge disposal within the UK, as of December 2014 landfill tax was chargeable at 80 GBP/1000 kg (1 UK tonne). Therefore to incur the disposal fee, 1000 m^3 of effluent would need to be treated, generating 1010 kg of sludge that could then be finally disposed of at the charged rate.

Therefore, combining the costs of treatment and disposal, it is possible to calculate a final cost of employing EC to treat wastewater and this value is 1.80 GBP/m^3. Full cost workings for this value are shown in Appendix II.

6.7 References

318. Duan, J., Wang, J., Graham, N., Wilson, F. Coagulation of humic acid by aluminium sulphate in saline water conditions. Desalination 2002; 150 (1): 1-14.
319. Han, M. Y., Kim, W. A theoretical consideration of algae removal with clays. Microchemical Journal 2001; 68: 157-161.
320. Jefferson, B., Jarvis, P., Sharp, E., Wilson, S., Parsons, S. A. Flocs through the looking glass. Water Science and Technology 2004; 50 (12): 47-54.
321. Zhang, X., Bai, R. Adsorption behaviour of humic acid onto polypyrrolecoated nylon 6,6 granules. Journal of Materials Chemistry 2002; 12 (9): 2733-2739.
322. Deyab, M. A., Keera, S. T. Cyclic voltammetric studies of carbon steel corrosion in chloride-formation water solution and effect of some inorganic salts. Egyptian Journal of Petroleum 2012; 21: 31-36.
323. Tambo, N., Watanabe, Y. Physical characteristics of flocs-I. The floc density function and aluminium floc. Water Research 1979; 13: 409-419.

Chapter 7

Conclusions

7 Conclusions

7.1 Introduction

The final chapter in this thesis is dedicated to summarising the conclusions drawn from the data and discussions presented.

7.2 Conclusions Drawn from the Study

It has been shown that direct dosing of coagulant electrochemically cannot compete with chemical dosing in removing low concentrations of phosphate in effluent. Consequently, four important factors in influencing flocculation have been identified. Firstly, the conversion of electrochemically released Fe^{2+} ions to Fe^{3+} through increasing the dissolved oxygen content of post-treated effluent through aeration *via* agitation is necessary. Secondly, the promotion of floc nucleation rate over growth rate to generate a suspension of flocculant particles that are small in size but great in number, thus possessing overall a large active surface area for adsorption, is of great importance. Thirdly, seeding raw effluent with pre-grown flocs allows for rapid coalescence of pollutants due to coagulation based on particle size difference between flocs and discrete particles. Finally, coagulation between particles of different sizes within a polydisperse suspension proceeds faster that that between particles of the same size, since the tendency is for the very small particles to attach to larger ones.

In investigating EC parametric influences on flocculation in a high pollutant loading effluent it has been shown that the primary factor affecting flocculation is concentration of coagulant. At low concentration (0.5 – 0.9 mmol Fe/L) there is ineffective quantities of coagulum in solution to induce flocculation. At higher doses (1.8 – 17.9 mmol Fe/L) open-structured aggregates are formed but due to their low fractal nature have reduced densities and increased drag when settling. This results in poorer pollutant removal efficiencies being recorded. In order to achieve high flocculation and good settleability, a compromise between size and density is required in which smaller sized flocs with greater density are needed to both induce flocculation of pollutant species, and settle quickly without recalcitrant levels of suspended matter remaining in solution post-settlement.

Increases in pollutant loading also revealed that at constant coagulant input, active adsorption sites on floc formations are limited and high pollutant content cannot be enmeshed and successfully precipitated out.

Ohmic loss has also been shown to have a significant impact on flocculation as a result of increasing inter-electrode distance. Studies employing electrode gaps of 6 mm or more revealed that passivation of cathodes and hydroxide formation on anodic surfaces increased due to a reduction in the rate of electrophoresis of ions moving away from their source electrodes. As a result, thick boundary layers developed within the gap spacing's increasing system resistance and inhibiting the desired electrochemical reactions of anodic oxidation. This ultimately diminished the concentration of Fe^{2+} ions released into solution and impacted upon floc formation and coagulation.

Changes to current density revealed a boundary at 1.8 mA/cm^2 at which; current densities below this exhibited a removal mechanism of charge neutralisation, whilst current densities in excess exhibited sweep-floc as the desired removal mechanism. Furthermore, it was found that power consumption was related to current density and whilst there is a preference to drive down the cost of any process by reducing energy consumption, an optimum between energy used and system efficacy was alluded to.

Investigations in which varying electrolysis times at constant coagulant doses recorded no trends in flocculation performance supporting the proposition that it is coagulant concentration that is the overriding factor in determining floc formation.

Other parameters of stirrer speed and floc activation time showed that floc was dependant on shear conditions and retention time. Under agitated conditions in excess of 100 rpm it was found that irreversible floc breakage occurred leading to poor flocculation and pollutant removal efficiencies. Retaining floc beyond 5 min also revealed that floc was impacted upon and pollutant removal efficiencies were reduced due to floc conversion from ferric/ferrous hydroxide to deactivated magnetite, as a result of oxygen ingression into solution during retention (oxidation of floc to Fe_3O_4).

Finally, chemical parameters of pH and conductivity highlighted the dependence of floc on neutral pH and high conductive wastewaters in which to form and grow. An optimal pH range of 6 – 8 was found in which the predominant form of coagulant was in the desired

$Fe(OH)_3$ form. Towards the acidic range, prevalent iron was in the Fe^{2+} form and pollutant removal efficiencies were extremely low. In addition it was found that as pH dropped from 7 to 3 the percentage of Fe^{2+} increased from 46% to 92%. Increasing pH towards the alkali range saw a reversal of this trend and Fe^{2+} concentrations fell from 92% to 1% at pH 11 due to rapid increases in oxidation of Fe^{2+} to Fe^{3+} as a result of high concentrations of OH^- ions in alkali solutions. However, at higher pH (8 – 11) it was found that flocculation was affected by the conversion of $Fe(OH)_3$ to amphoteric $Fe(OH)_4^-$ that re-solubilised back into solution releasing previously absorbed pollutant particles and hence lowering pollutant removal efficiencies.

Changes in conductivity saw marginal gains in flocculation and pollutant removal efficiency but significant changes in system operation and energy consumption as cell potential decreased linearly with increases in sodium chloride concentration. Table 7.1 tabulates the conclusions drawn from this study for a quick overview (↑ = increase, ↓ = decrease):

Table 7.1 Trend summary table.

Parameter		Pollutant removal efficiency
Pollutant loading	↑	↓
Inter-electrode distance	↑	↓
Coagulant dose	↑	↑
Current density	↑	↑
Stirrer speed	↑	↓
Electrolysis time	↑	No change*
Coagulant retention	↑	↓
pH	↑	↑ up to pH 7, ↓ from 7 – 11
Conductivity	↑	↑

**Electrolysis time investigations carried out at constant coagulant dose.*

In characterising floc formed under varying parameter changes, it has been shown that ζ-potential provides an effective measurement of the charge on a particle and can be used to predict a system's stability. Increases in coagulant concentration saw increases in ζ-potential from negative values to positive values as the charge on pollutant particles was neutralised up to the isoelectric point. Further increases in coagulant dose beyond the isoelectric point saw ζ-potential continue to increase in the positive range as the overall charge of the system shifted to a positive one owing to mass increases in Fe^{3+} ion addition through increased coagulant addition. With changes in pH, ζ-potential also differed. Generally ζ-potential decreased with increasing pH due to an increase in negatively charged ions, specifically the hydroxyl ion added to increase the pH and the $Fe(OH)_4^-$ ion which was dominant above pH 9.

Imagery of floc undertaken *via* various methods revealed that coagulant addition increased floc size and density up to a critical point, thereafter floc size continued to increase but at the expense of density which did not.

Cyclic voltammetry experiments carried out under open and nitrogen purged conditions further impressed the point for the need of dissolved oxygen to be present in coagulated solutions to oxidise electro-dissolved Fe^{2+} ions to $Fe(OH)_3$.

Finally, it was found that the optimal conditions in removing suspended solids and turbidity from a synthesised raw effluent containing 1 g/L of solids loading was: 1.8 mA/cm^2 current density, 0.25 L/min flow rate, 1.8 mmol Fe/L coagulant dose, 59 sec electrolysis time, effluent pH 7.2, and 3 mm inter-electrode distance. Following jar-testing and a 30 min quiescent period, TSS removal efficiency was found to be at 91% and turbidity removal efficiency at 96%. The amount of sludge produced was 1.01 kg/m^3 and the associated cost of employing EC at these conditions was calculated at 1.80 GBP/m^3 (inclusive of treatment and disposal costs).

7.3 Future Work

Additional work may include investigating the effect of temperature on flocculation. In order to do this, various 25 L batches of raw effluent at different temperatures would be generated and either brought up or down to temperature *via* use of a water jacket circulating either chilled water or hot water derived from, for example, a ThermoHaake K10 heat-refrigerated circulator (Hakke, Germany). As all experiments ran in the previous chapters were done so at room temperature (21° C), four other temperature points would be selected: 5.5, 11, 41, 81° C. Once the batches of raw effluent achieved their selected temperature, the optimal conditions stated above would be observed. Following 30 min sedimentation time, residual turbidity and total suspended solids measurements would be taken from settled supernatant volumes of treated samples and analysed for pollutant removal efficiencies, as per the methods stated in sections 3.5.4 and 3.5.5. Potential measurements from the power supply unit would also be recorded in order to deduce any changes in energy consumption with regard to temperature variation.

The expected outcomes of the experiments would be an increase in removal efficiencies as temperature increased. This would be expected to occur owing to increased destruction of

any iron oxide film development on anodic surfaces and thus an improvement in reaction rates of all processes occurring according to the Arrhenius equation. This formula is an empirical relationship showing the temperature dependence of reaction rates. A generalisation of the Arrhenius equation is that for common chemical reactions occurring at room temperature, reaction rates double for every 10^{o} C increment. It is hypothesised therefore that increased temperature would promote metal hydroxide formation leading to greater mobility and more frequent collisions of species leading to enhanced flocculation. With regard to energy consumption and temperature, it is hypothesised that energy consumption would decrease with increasing temperature, as higher temperature gives higher conductivity and hence lower energy consumption.

However, in these investigations it would be worthy to note what would happen to EC efficacy at the highest test temperature of 81^{o} C. At high temperature, this may have an effect on the solubility of precipitates formed impacting on flocculation. This would be important to investigate and delineate in reporting any trends with regard to temperature as a process parameter. The benefits of such work would be to fill a void in the knowledge of EC as despite its existence over the last 100 years, the effect of temperature has rarely been investigated.

Another area of interest to explore would have been that of accurately measuring floc settlement rates in relation to changes in electrochemical parameters such as coagulant dose. However, due to the necessary specialised equipment needed to image capture and measure the time taken for an isolated floc aggregate to traverse a known distance, this was beyond the scope of this project. Knowing the changes (if any) to settlement rates of flocs produced at various coagulant doses would have complimented the floc images reported in section 6.4. It would be expected that larger flocs would sink faster and thus have a quicker settlement velocity than smaller floc particles.

In order to accurately determine this, a settling column filled with room temperature deionised water would be required along with a digital camera (e.g. CV M90 colour close-coupled device (CCD) from JAI UK Ltd., England) and image analysis software (e.g. Image ProPlus from Media Cybernetics, USA) to determine floc settling velocity. Settled flocs from treated samples would be removed from samples using a wide-mouthed pipette and transferred into the settling column for re-suspension within the deionised water. The

camera would be set up so that when the flocculant travelled down the column and passed the front of the camera lens, the image capturing was triggered manually to take one photograph every second for 10 s. Thus, this would allow the distance travelled by the floc to be calculated per photograph and produce a settlement velocity. The isolation and transference to a settling column filled with deionised water would negate any particle-particle interaction between the floc with other particles that may hinder settlement.

However, other points to consider would be the width of the settling column as the sides of the column would impact on settlement if the column was too narrow as drag would impede the floc. Also, during the transfer from treated sample to settling column of individual floc's, if a floc was observed to break, then it would have to be discarded and another representative floc collected.

These results however would be useful in showing whether the larger sized flocs captured in section 6.4 would have a faster settlement time than smaller flocs, or whether their larger nature allowed for drag to impede their settleability and thus slow them down. This data could also be used for the temperature parameter investigations discussed previously as it may affect floc settlement. The higher the temperature, the lower the density of the liquid would be and thus the faster sedimentation would be.

Lastly, consideration was given to investigating electrochemical parameters influencing floc formation within a batch EC reactor. In this instance, a set volume of raw effluent would be pumped into the EC vessel and current density engaged along with a calculated electrolysis time (derived from Equation 10 in section 2.2.5), to impart a known mass of coagulant. However, as most industrial water treatment practices require continuous-mode operation, it was decided that this was not suitable and was abandoned.

7.4 Final Word

Prior to this study, EC was characterised by individual case study investigations that were solely pollutant-centred and failed to further progress the technology beyond individual treatment applications. It has been found that the $Fe(OH)_n$ complexes formed electrochemically remain in solution as a gelatinous precipitate. The formed ferrous/ferric hydroxides are extremely effective in the removal of pollutants through adsorption, charge neutralization, electrostatic attraction and sweep-floc enmeshment. The most desirable

flocculant species, owing to its better coagulating character, is $Fe(OH)_3$ and is dominant in the range of pH 6 – 9 according to E-pH diagrams for Fe^{3+} chemical species and from pH investigations carried out. Electrode consumption can be estimated by Faraday's Law and the amount of flocs generated can be estimated stoichiometrically. It is hoped that the quantitative understanding produced in this study can progress EC onwards towards a more holistic approach to identifying quickly the optimal conditions (pH, coagulant concentration, etc) to treat a variety of wastewaters and provide a better scientific foundation for the advancement of this technology.

Appendix I

Main aluminium reactions occurring during electrocoagulation:

$$Al_{(s)} \rightarrow Al^{3+}_{(aq)} + 3e^- \quad \text{(anode)} \qquad \textbf{Equation 30}$$

$$2H_2O_{(l)} + 2e^- \rightarrow H_{2(g)} + 2OH^- \quad \text{(cathode)} \qquad \textbf{Equation 31}$$

Oxygen can also occur at the anode shown in Equation 3, section 2.2.4. Upon electrolytic dissolution of the anode, Al^{3+} ions undergo hydrolysis reactions generating various monomeric species in the following simplified sequence leading ultimately to the desired solid complex $Al(OH)_3$:

$$Al^{3+}_{(aq)} + H_2O_{(l)} \rightarrow Al(OH)^{2+}_{(aq)} + H^+_{(aq)} \qquad \textbf{Equation 32}$$

$$Al(OH)^{2+}_{(aq)} + H_2O_{(l)} \rightarrow Al(OH)_2{}^+_{(aq)} + H^+_{(aq)} \qquad \textbf{Equation 33}$$

$$Al(OH)_2{}^+_{(aq)} + H_2O_{(l)} \rightarrow Al(OH)_{3(s)} + H^+_{(aq)} \qquad \textbf{Equation 34}$$

In addition to the simplified sequence above; dimeric, trimeric and polynuclear hydrolysis products of Al are also formed. Hydrolysis reactions at the anode create acidic conditions at its vicinity and likewise hydrogen evolution at the cathode creates alkali conditions there. This can lead to the cathodic dissolution of alumimum cathodes, if employed, and the production of soluble $Al(OH)_4^-$:

$$Al + 4OH^- \rightarrow Al(OH)_4^- + 3e^- \qquad \textbf{Equation 35}$$

To negate this effect, a steel electrode is used instead of an aluminium one to prevent cathodic dissolution and thus preserve the lifetime of the electrodes and to avoid over-dosing of Al into solution.

Appendix II

Calculated total cost employing EC as a wastewater treatment option:

- Cost of EC generated sludge disposal, assuming 1000 m^3 of effluent is treated generating 1010 kg of sludge and therefore incurring the UK landfill tax of 80 GBP/1000 kg (1 UK tonne) = 80 GBP/1000 m^3.
- Cost of treatment (combining electrical cost and electrode material cost) of 1000 m^3 raw effluent = 1,720 GBP/1000 m^3
- Total cost of both operations (treatment and disposal):
- 80 + 1,720 = 1,800 GBP/1000 m^3
- Dividing 1,800 by 1000 = 1.80 GBP/m^3 total cost of EC operation, inclusive of treatment and disposal.